Model Scale Tunnel Fire Tests – Automatic Sprinkler

Ying Zhen Li, Haukur Ingason

BRANDFORSK project 501-091

SP Technical Research Institute of Sweden

Fire Technology

SP Report 2011:31

Model Scale Tunnel Fire Tests
Automatic Sprinkler

Ying Zhen Li, Haukur Ingason

Abstract

Model Scale Tunnel Tire Tests – Automatic Sprinklers

The study focuses on the performance of an automatic sprinkler system in a model scale tunnel with longitudinal ventilation. A total of 28 tests were carried out in a 1:15 model scale tunnel using an automatic sprinkler system with glass bulbs. The activation time of the nozzles, the maximum heat release rate, energy content and (in one case) collapse of the automatic sprinkler system were analyzed.

The results show that high ventilation and low water flow rates result in the collapse of the automatic sprinkler system in a longitudinal ventilated tunnel fire. The main reason for the collapse under the tested water flow rates was the effect of the longitudinal flow on the fire development and the hot gas flow close to the sprinklers. The fire development and the activation heat release rate of the first activated bulb are intimately related to the ventilation velocity. A short presentation of the tests conducted using the deluge system are given. Further, fire spread to the neighbouring wood crib was investigated.

Key words: model scale tests, tunnel fire, sprinkler, ventilation

SP Sveriges Tekniska Forskningsinstitut
SP Technical Research Institute of Sweden

SP Report 2011:31
ISBN 978-91-86622-62-6
ISSN 0284-5172
Borås 2011

Contents

Preface

This project was sponsored by the Swedish Fire Research Board (BRANDFORSK) and the SP Tunnel and Underground Safety Centre.

The technicians Sven-Gunnar Gustafsson, Tarmo Karjalainen and Michael Magnusson at SP Fire Technology are acknowledged for their valuable assistance during performance of the tests. They were also responsible for the construction of the test rig. Thanks also to Jonatan Hugosson and Hans Nyman, for their help during the tests.

The advisory group to the project is thanked for their contribution. The advisory group consisted of:

Arne Brodin, Faveo Projektledning
Andreas Johansson, Fire Brigade in Gothenburg
Pia Ljunggren, Trygg Hansa
Ulf Lundström, The Swedish Transport Administration
Marie Skogsberg, SKB
Sören Lundström, MSB
Emma Nordvall, Fire Brigade in Helsingborg
Conny Becker, Brandskyddslaget
Hans Nyman, Brandskyddslaget
Magnus Arvidson, SP

Summary

A total of 28 tests were carried out in a 1:15 model scale tunnel with an automatic sprinkler system or deluge system. The main focus of these tests was on the performance of the automatic sprinkler system used for a tunnel fire. The activation of the nozzles, the maximum heat release rate, the energy content and the collapse of the automatic sprinkler system were analyzed. A short discussion of the performance of a deluge system was also conducted. In addition, many fire parameters including maximum temperature beneath the ceiling, heat flux and fire spread, were investigated.

The tests show that high ventilation and low water flow rates can result in the collapse of the automatic sprinkler system in a tunnel fire. Note that the tested water flow rate for a single nozzle was 0.38 L/min, 0.46 L/min and 0.58 L/min, corresponding to 16.5 mm/min, 20 mm/min and 25 mm/min in full scale, respectively. The longitudinal ventilation plays the most important role in the collapse of a system by stimulating the fire development, i.e. the maximum heat release rate and the fire growth rate under the tested water flow rates. The different tested water flow rates did not show any obvious effect on the fire development, however, the downstream nozzles with higher water flow rate cooled the hot gases more efficiently to prevent the collapse of the system. It can be concluded that the most important parameter for an automatic sprinkler system under the tested water flow rates is the ventilation velocity rather than the water flow rate. The fire development is intimately related to the ventilation velocity, and almost independent of the water flow rate under such conditions. The maximum heat release rate in an automatic sprinkler system increases linearly with the ventilation velocity. The energy content consumed in a test increases more significantly with the ventilation velocity than the heat release rate.

The heat release rate at activation of the first nozzle (sprinkler head) increased linearly with the ventilation velocity. The location of the first activated nozzle was also mainly dependent on the ventilation velocity. The other nozzles in the measurement region were activated a short time after the activation of the first nozzle, i.e. in a range of 0 – 0.6 min.

To improve the performance of an automatic sprinkler system in a tunnel fire, special strategies were tested. It is shown that either using the Variant Ventilation Strategy or the Special Control Strategy effectively suppressed the fire development and prevented collapse of the automatic system. Both the automatic sprinkler system and the deluge system efficiently suppressed the fire spread to the neighbouring wood crib.

Note that there was no nozzle placed further than 1.6 m (4 times tunnel height) downstream of the fire source. The cooling effect was therefore underestimated in some tests. The presented data concerning the activation range and the conclusions made here are therefore conservative. In addition, the configuration of the wood cribs played an important role in extinguishment of a solid fire. Although the ventilated flow inside the tunnel and the heat release rate can be scaled properly, it is impossible to ensure that the process of extinguishment was scaled appropriately. However, it can be concluded that the discussed variables have been sufficiently well scaled and the trends shown in the analyses should be reasonable. Large scale tests are required for further verification of these results.

1 Introduction

In recent years, the interest for fire safety issues in tunnels has increased dramatically owing to numerous catastrophic tunnel fires and extensive monitoring by the media. Many new technologies, such as water sprinkler systems, have been developed and used to improve fire safety in tunnel. Much research on the extinguishment of fires using water spray has been carried out in recent decades. A short review is presented here.

Rasbash et al. [1][2] conducted a series of tests on the extinction of liquid fires. It was concluded that there are two main ways to extinguish a fire with a water spray, i.e. cooling the burning fuel and cooling the flame. The most effective of these methods of extinguishment is that water spray should reach and cool the burning fuel. In other words, the most important mechanism of extinguishment is surface cooling of the burning fuel.

Kung and Hill [3] conducted a series of experiments on extinguishment of wood crib fires by water applied directly on the top of the crib and wood pallets. The water was applied by means of a rake consisting of perforated stainless steel tubes (perforated hole diameter of 0.41mm and tube outer diameter of 6.4 mm). They presented interesting dimensionless variables which considered preburn percentage, crib height, showing dimensionless fuel consumption and total water evaporated as functions of dimensionless water flow rate.

Heskestad [4] made an interesting review of the role of water in suppression of a fire in 1980, focusing on the critical water flow rate for extinguishment of solid fires and liquid fires. It is reported that the critical water flow rate mainly lies in a range of 1.5 to 3.0 g/m^2s for extinction of wood. Further the value is as high as 200 g/m^2s for kerosene at a mass median drop size of 0.8 mm. Note that the critical water flow rate used here is defined as the water flow rate divided by the total fuel surface area, below which the fuel cannot be extinguished.

Heskestad [5][6] also gave a detailed analysis of scaling of a water spray nozzle. Further Heskestad [7] conducted a series of water spray tests using liquid pool fires, taking the nozzles are not geometrically scaled into account. He proposed an equation for pool fires to predict the critical water flow rate, which is found to be proportional to an effective nozzle diameter, and to the 0.4-power of both nozzle height and free-burn heat release rate. He also pointed out that spray-induced dilution of the flammable gas is a major factor in extinguishing fires from a gaseous discharge, and that a liquid pool fire needs higher water rates to be extinguished compared to a gas fire.

Yu et al. [8] conducted a simple analysis of spray cooling in room fires by correlating the total surface with the total heat absorbed by the water spray in a two zone model. Empirical correlations for the heat absorbed by the water spray and the convective heat loss through the room opening were established. Yu et al. [9] also made a theoretical analysis of the extinguishment of wood crib fires by cooling of the fuel surface. A fire suppression parameter was identified to correlate the fire suppression results obtained from large-scale tests conducted using two different commodities arranged in steel racks of different height. Note that they used an actual flow rate of water that impinges on the fuel, while previous researchers typically used the applied water flow rate. The actual critical water flow rate is about 6 g/m^2s for the Class II commodity and 17 to 20 g/m^2s for the plastic commodity.

Grant et Al. [10] made a full review of fire suppression by water sprays and gave a series of useful comments, including the critical water flow rate and the total volume of water required to extinguish a fire for a water spray system and a mist system.

Xin and Tamanini [11] conducted a series of fire suppression tests using representative fuels to assess the classification of commodities for sprinkler protection. They defined a critical sprinkler discharge flux as the minimum water flux delivered to the top of the fuel array capable of suppress/prevent further fire development. An equation to determine the critical flow rate was proposed. The actual sprinkler flux and the critical water flow rate were correlated with each other. Suppression correlations for tested commodities including Class 2, Class 3 and Class 4, were proposed. The results show that the estimated critical sprinkler discharge flux is 6.9 mm/min for the Class II commodity, 19.9 mm/min for the Class 3 and Class 4 commodities, and 25.6 mm/min for the plastic commodity. Although the tiers of commodities affect the critical water flow rate, the results showed that the ranking remains appropriate for various fuel array heights in the ranges tested.

To improve the fire safety in some applications, an automatic sprinkler system can be used. If a fire grows to the threshold at which the bulb is activated, the water is released to suppress the fire development immediately. Heskestad [12] proposed the controlling equation for the heat-response element, i.e. bulb, of an automatic water sprinkler. A response time index, i.e. RTI, was defined, which proves to be a constant for a given automatic sprinkler. Different classifications of bulbs were conducted according to the link temperature, from ordinary (135 - 170 ^{o}C) to ultra high (500 - 575 ^{o}C). For low-RTI sprinklers the heat loss by conduction to the sprinkler mount was included. The cooling of the bulb by water droplets in the gas stream from previously activated sprinklers was considered by Ruffino et al. [13-15]. De Ris et al. [16-17] developed a skip-resistant sprinkler with a cylindrical shield around the bulb. A series of test was conducted in a plunge tunnel apparatus in a steady state. The results show that the proper shielding of a sprinkler can significantly reduce skipping, i.e. cooling of sprinklers adjacent to an activated nozzle prevents their activation and causes the sprinkler activation to “skip” such nozzles.

There are relatively few studies on water spray systems in a tunnel fire. The differences between water spray systems in a tunnel fire and those in an enclosure fire are: the type, load and arrangement of the fuel, and the existence of a ventilated flow in a tunnel fire. Ingason [18] carried out a series of model scale tunnel fire tests with a deluge system and a water curtain system using hollow cone nozzles, in order to improve our basic understanding of water spray systems in a longitudinal tunnel flow. The water spray system used consisted of a commercially available axial-flow hollow cone nozzles. The model scale tests show that the non-dimensional ratio of HRR, excess gas temperature, fuel consumption, oxygen depletion and heat flux downstream of the fire, all correlate well to a non-dimensional water flow variable. There are also some large scale tests reported in the literatures, such as the Ofenegg tunnel tests in 1965, P.W.R.I tests in 1980, Shimizu tests in 2001 and 2nd Benelux tunnel tests in 2002 [19].

Until now, no systematic study of automatic sprinkler systems in a tunnel fire has been available. Despite this there appears to be consensus concerning the ineffectiveness of such a system due to the effects of the ventilated flow in the references cited above. This consensus is mainly related to the assessment of whether the ventilation will jeopardize the effectiveness of the system. However, how much the ventilated flow affects the performance of an automatic sprinkler system in a tunnel fire has not been quantified. Therefore there is a need to systematically investigate how the system works in various longitudinal ventilation flows.

We know that the heat from a fire plume rises vertically if there is no wind in the tunnel but in longitudinal flow, the flame and heat will be deflected and rise further downstream of the fire. The interesting question is therefore how far from the fire we obtain the

highest temperatures in the ceiling. This can have a significant effect on which sprinkler head or nozzle will activate first. Indeed, this begs the question of whether the activated sprinklers could potentially be too far away from the fire to effectively deliver water on the fire?

Another question that needs to be addressed is whether too many sprinklers might activate thereby exceeding the capacity of the system. A fully automatic sprinkler system in a tunnel is assumed here to cover the entire tunnel length without any division into different zones. In contrast, a deluge system activates one or two zones or sections, which means that the risk that the system cannot fight the fire decreases considerably. Such a system is not very sensitive to the effects of the longitudinal flow. However, when individual sprinkler bulbs activate over a large area and the system cannot deliver the amount of water needed to control the fire it will collapse. This study has, therefore, also investigated under what conditions the system might potentially exhibit such a collapse.

The work presented here is focused on answering and quantify these different concerns about the effects of the longitudinal flow on fully automatic sprinkler systems in tunnel fires. Model scale tunnel tests have been employed in this investigation as they are cost effective and can , if correctly designed, obtain important and reliable information. The results can be used to give authorities and designers more insight into the discussion of different type and activation procedures of water spray systems in tunnels.

2 Scaling theory

The widely used and well known Froude scaling technique has been applied in this project. Although it is impossible and in most cases not necessary to preserve all the terms obtained by scaling theory simultaneously, the terms that are most important and most related to the study are preserved. The thermal inertia of the involved material, turbulence intensity and radiation are not explicitly scaled, and the uncertainty due to the scaling is difficult to estimate. However, the Froude scaling has been used widely in enclosure fires and results from model scale tests seem to fit large scale results well, see references [20-25]. Since the ratio of tunnel length to tunnel height should be great enough to scale a realistic tunnel fire, it is very expensive to build a model tunnel in large scale. The scaling ratio should not be smaller than about 1:20 in order to preserve the Froude Number and to avoid producing a laminar flow in the model tunnel. Our experience of model tunnel fire tests in the scale used here (1:15) shows there is a good agreement between model scale and large scale test results on many focused issues [26-31]. Such a scale is widely used in model tunnel fire tests all over the world [32-35].

The model tunnel was built in a scale of 1:15, which means that the size of the tunnel is scaled geometrically according to this ratio. The scaling of other variables such as the heat release rate, flow rates and the water flow rate can be seen in Table 1. The scaling of the response time of the automatic sprinkler can be found in Appendix A.

Table 1 A list of scaling correlations for the model tunnel.

Type of unit	Scaling model*	Eq. number
Heat Release Rate (HRR) (kW)	$\frac{Q_F}{Q_M} = (\frac{L_F}{L_M})^{5/2}$	Eq. (1)
Volume flow (m^3/s)	$\frac{\dot{V}_F}{\dot{V}_M} = (\frac{L_F}{L_M})^{5/2}$	Eq. (2)
Velocity (m/s)	$\frac{V_F}{V_M} = (\frac{L_F}{L_M})^{1/2}$	Eq. (3)
Time (s)	$\frac{t_F}{t_M} = (\frac{L_F}{L_M})^{1/2}$	Eq. (4)
Energy (kJ)	$\frac{E_F}{E_M} = (\frac{L_F}{L_M})^{3}$	Eq. (5)
Mass (kg)	$\frac{M_F}{M_M} = (\frac{L_F}{L_M})^{3}$	Eq. (6)
Temperature (K)	$T_F = T_M$	Eq. (7)
Water flow rate (L/min)	$\frac{\dot{q}_{w,F}}{\dot{q}_{w,M}} = (\frac{L_F}{L_M})^{5/2}$	Eq. (8)
Water density (mm/min)	$\frac{\dot{q}''_{w,F}}{\dot{q}''_{w,M}} = (\frac{L_F}{L_M})^{1/2}$	Eq. (9)
Pressure difference (Pa)	$\frac{P_F}{P_M} = \frac{L_F}{L_M}$	Eq. (10)

Water droplet (μm)	$\frac{d_F}{d_M} = (\frac{L_F}{L_M})^{1/2}$	Eq. (11)
Response time Index ($m^{1/2}s^{1/2}$)	$\frac{\mathrm{RTI}_M}{\mathrm{RTI}_F} = (\frac{l_M}{l_F})^{3/4}$	Eq. (12)

*Assume the ratio of heat of combustion $\Delta H_{c,M} / \Delta H_{c,F} = 1$. L is the length scale. Index M is related to the model scale and index F to full scale (L_M=1 and L_F=15 in our case).

3 Experimental Setup

A total of 28 tests were carried out in a 1:15 scale model tunnel. Both an automatic sprinkler system and a deluge system were tested. The fire spread between wood cribs with a free distance of 1.05 m (15.75 m in large scale) was also tested. Further, the effect of different ventilation velocities and water flow rates on the activation of nozzles, heat release rate, fire growth rate, gas temperature, heat radiation and fire spread was investigated.

Longitudinal ventilation was established using an electrical axial fan attached to the entrance of the model tunnel, see Figure 1. The fan itself was 0.375 m long with an inner diameter of 0.315 m. Average longitudinal velocities of 0.5 m/s, 1 m/s, 1.5 m/s and 2 m/s, obtained by adjusting a frequency regulator, were used in the test series. According to Equation (3), the corresponding large-scale velocities were 2 m/s, 4 m/s, 6 m/s and 8 m/s. To smooth the air flow from the fan, a net consisting of smooth pipes with lengths of 450 mm and diameter of 45 mm was attached to the fan, and a steel net was also installed at the entry of the tunnel.

Figure 1 A photo of the 1:15 model scale tunnel using automatic sprinkler system. A fan was attached to the tunnel entrance and windows were placed along one side in order to observe the smoke flow and the flame volume.

The tunnel itself was 10 m long, 0.6 m wide and 0.4 m high, see Figure 1. The corresponding large-scale dimensions were 150 m long, 9 m wide and 6 m high, respectively. During the tests the smoke flow produced was removed by the central laboratory ventilation system connected to the end of the model tunnel. In order to eliminate the effect of central ventilation system on the model tunnel ventilation, a cubic box made of Promatect H boards was installed between them, as shown in Figure 2. The cubic box was closed except the bottom which was directly connected to the ambient air.

The model, including the floor, ceiling and one of the side walls, was constructed using non-combustible, 15 mm thick Promatect H boards, while the front side of the tunnel was covered with a fire resistant window glaze, mounted in steel frames. The thickness of the glaze was 5 mm. The manufacture of the Promatect H boards provides the following technical data: the density of the boards is 870 kg/m^3, the heat capacity is 1130 J/(kg·K) and heat conduction is 0.175 W/(m·K).

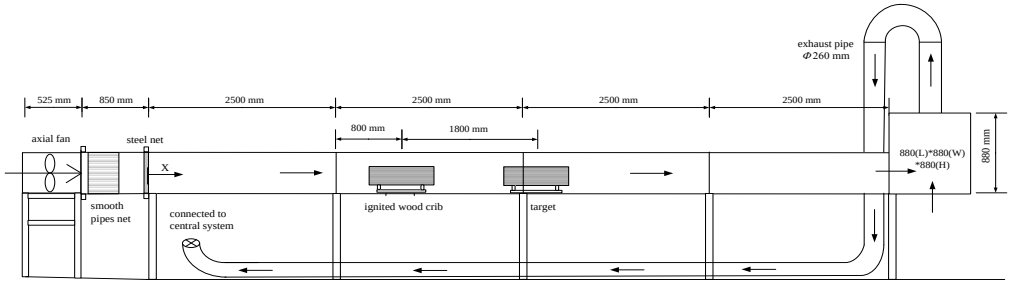

Figure 2 A schematic drawing of the model tunnel using longitudinal flow.

3.1 The fire load

The fire load consisted of wood cribs (pine), as shown in Figure 3. More detailed information about the wood cribs for each test is given in Table 2 to Table 4.

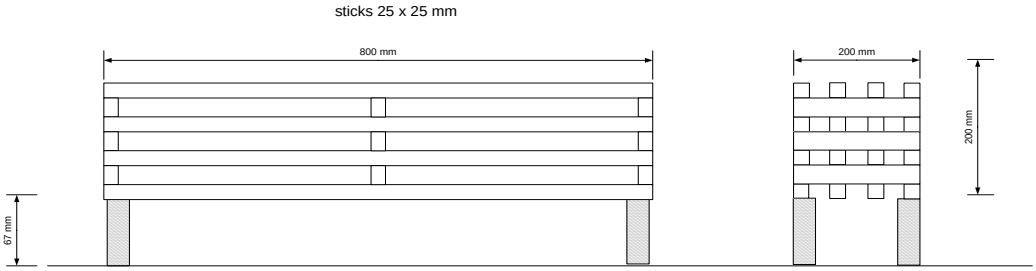

Figure 3 Detailed drawing of the wood crib.

The total the weight of wood crib was about 4.4 kg. The free distance between each horizontal stick was 0.033 m and the total fuel surface area of a wood crib was estimated to be 1.37 m^2. The estimated heat release rate was about 200 MW in large scale.

The crib porosity, *P*, was about 2.0 mm for wood crib. This means that the wood cribs should not show any type of under-ventilated tendencies during a test [36]. This is important in order to compare a fuel that is not under-ventilated during ambient conditions.

3.2 Instrumentation

Various measurements were conducted during each test. Figure 4 shows the layout and identification of instruments in the series of tests. The first wood crib was placed on a weighing platform (W), consisting of scales attached by four steel rods to a free floating dried Promatect H board measuring 1.0 m long, 0.45 m wide and 0.015 m thick. In the case when more than one wood cribs was used in the tests, only the first wood crib was weighed. The weighing platform was connected to a data logging system recording the weight loss every second. The centre of the weighing platform was 3.3 m from the tunnel entrance (x=0) and the accuracy of the weighing platform was +/- 0.1 g.

The temperature was measured with welded 0.25 mm type K thermocouples (T). The location of the thermocouples is shown in Figure 4. Most of the thermocouples were placed along the ceiling at a distance of 0.04 m from the ceiling. A set of thermocouple was placed 4.65 m (pile A in Figure 4) and 8.75 m from the inlet opening (pile B in Figure 4), respectively. The thermocouples in each set were placed in the centre of the tunnel and 0.04 m, 0.12 m, 0.20 m, 0.28 m and 0.36 m, respectively, above the floor.

Four plate thermometers [37-38] (P24, P25, P26 and P27) were placed at the floor level during the tests. The locations of the plate thermometers were 2.3 m, 4.65 m, 6.25 m and 8.75 m from the tunnel inlet at x=0. The incident heat fluxes are calculated by the following equation:

$$[q''_{inc}]^{i+1} = \frac{\varepsilon_{PT}\sigma[T_{PT}^4]^i + (h_{PT} + K_{cond})([T_{PT}^4]^i - T_g) + C_{heat,\beta=1/3}\dfrac{[T_{PT}]^{i+1} - [T_{PT}]^i}{t^{i+1} - t^i}}{\varepsilon_{PT}} \qquad (13)$$

where the conduction correction factor K_{cond} = 8.43 W/m^2·K, and the lumped heat capacity coefficient $C_{heat,\ \beta\ =1/3}$ = 4202 J/m^2·K, the surface emissivity of Plate thermometer ε_{PT} =0.8.

Two bi-directional probes [39] (B22 and B23) were placed at the centreline of the tunnel 1.3 m and 8.7 m, respectively, from the inlet. The pressure difference was measured with a pressure transducer with a measuring range of +/- 30 Pa. Another bi-directional probe was installed in the centre of the exhaust duct at the floor level and 3.75 m horizontally away from the tunnel inlet.

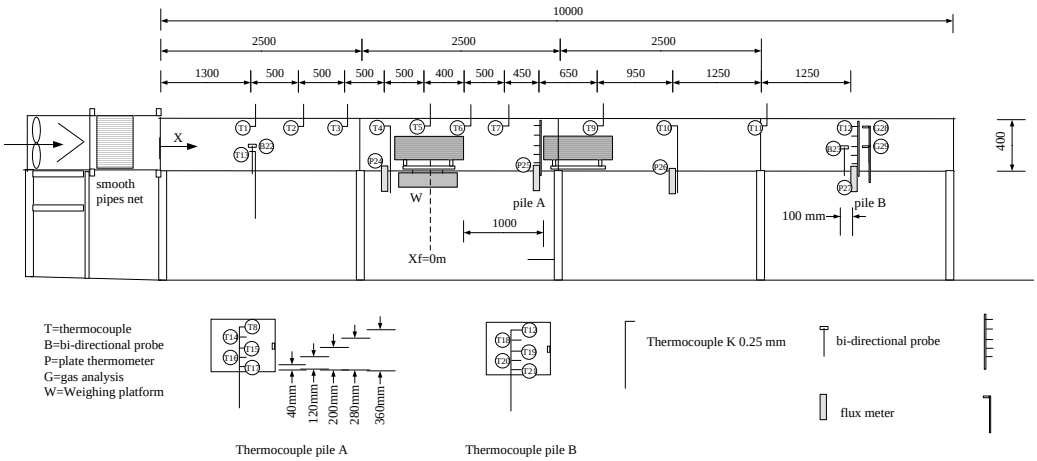

Figure 4 The layout and identification of instruments in the series of tests (dimensions in mm).

The gas concentrations 8.8 m from the entrance (at pile B, i.e. G28, G29), including O_2, CO_2 and CO, were sampled by two probes consisting of open copper tubes (Ø 6 mm). They were located at two different heights, 0.2 m and 0.35 m above the floor. However, O2 at the centre line (G29) was not measured. The gas concentrations in the centre of the exhaust duct at the floor level and 3.7 m horizontally away from the tunnel inlet were also measured. Oxygen was measured with an M&C Type PMA 10 (0 – 21 %) and the CO (0 – 3 %) and CO2 (0 – 10%) were measured with CO/CO2 Siemens Ultramat 22P. In Figure 4 the number of and identification of the probes used is presented.

3.3 Water spray system

A drawing of the water spray system using 9 couples of nozzles can be seen in Figure 5 and Figure 6. Eighteen nozzles were installed in the second section of the model tunnel, 35 mm below the ceiling. The interval between two neighbouring nozzles is always 0.3 m. A pressurized water tank was used to supply the water. Two pressure transducers (0 – 10 bar) were installed in the water supply pipe adjacent to the tank and nozzles, respectively. A valve was also installed close to the tank to adjust the pressure. According to the analysis in Appendix B, the water flow rate is dependent on the pressure close to the

nozzle. In the tests the pressure was kept at a constant level to assure the flow rate of each nozzle was the same. The total water flow rate in the main water supply pipe was measured with a Krone flowmeter with a measuring range of 0 – 200 L/min.

Figure 5 A photo of the water supply system for the automatic water sprinklers

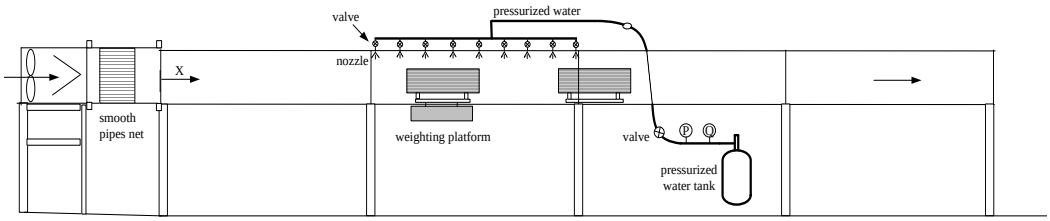

Figure 6 A sketch of the water spray system using 18 nozzles.

Figure 7 shows the bird-eye view drawing of the water spray system. Two nozzles placed in a cross-section were connected together by a pipe with a valve to control whether these two nozzles were both opened or closed.

In the tests with the automatic sprinkler system, the bulbs were placed 35 mm below the ceiling and special activation equipment was used to activate the nozzles after the corresponding bulbs were broken (activated). Due to the symmetrical arrangement of the nozzles and in order to simplify the test setup, bulbs were only placed on one side. Each bulb was installed beside the corresponding nozzle. Due to the convenience of the arrangement, there was a small distance between the nozzle and the corresponding bulb, see Figure 7. Both the horizontal and vertical distances between the nozzle and the bulb were 30 mm. The special activation equipment send a signal and then opened the automatic value which was placed in the pipe close to the nozzle, immediately after the corresponding bulb was activated.

In the tests with the deluge system, all automatic valves were open which means that there were no bulbs mounted in the activation assembly. The total water flow rate was controlled by the valve adjacent to the tank. The activation time of the nozzles was set to 75 s after ignition. The reason for this fixed activation time will be discussed later. As shown in Figure 7, each nozzle covered one tunnel section with 0.3 m × 0.3 m area. The water density, which will be discussed later, is defined as the average water flux in this specific section.

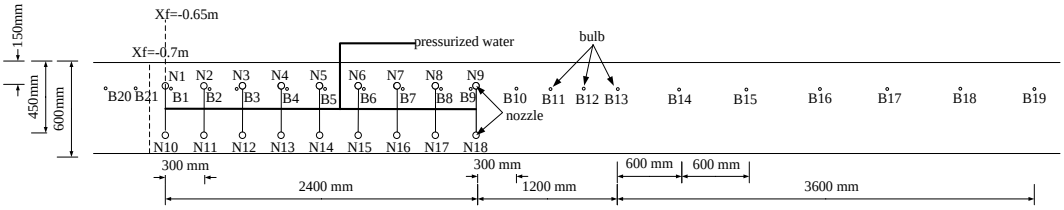

Figure 7 A bird-eye view sketch of the water spray system .

The nozzles used in the tests were of the type Lechler full Cone Spray 460.368.17.CA.00.0, see Figure 8. This nozzle creates a very fine uniform full cone spray, which means that the fine water droplets should be uniformly distributed within the cone area. The narrowest nozzle passage diameter was 0.7 mm (10.5mm in large scale). The spray angle was 120 ^{o} and the spray diameter at a pressure of 2 bar was 680 mm at a distance of 200 m below the nozzle and 1220 mm at a distance of 500 mm. The tested water flow rate of a single nozzle was 0.38 L/min, 0.46 L/min and 0.58 L/min, corresponding to 16.5 mm/min, 20 mm/min and 25 mm/min at full scale, respectively, according to Eq. (9).

The bulbs used in the tests were F1.5×16 with RTI of 14 and a diameter of 16 mm and a length of 16 mm, produced by Job Thermo Bulbs. The RTI of the bulbs was scaled according to Equation (A9), see Appendix A. The corresponding RTI is 107 in large scale, using Equation (A9). Two types of bulbs with the same geometry and different link temperature of 68 ^{o}C and 141 ^{o}C, respectively, were used to analyze the effect of response time on the performance of the automatic sprinkler system.

Figure 8 Nozzle used in the model scale tests (Lechler full Cone Spray series 460) .

The weighing platform (W), thermocouples, pressure transducers, gas analysers, flux meters, flow meter, and activation equipments were all connected to IMP 5000 KE Solotron loggers. The data was recorded on a laptop computer at a rate of approximately one scan per second.

4 Test procedure

The wood cribs used in each test were dried overnight in a furnace at 60 ℃ (<5% moisture). Before the tests, the weight of each wood crib was measured. In addition, the moisture of the first wood crib was measured with MC-300w Humitest wood moisture meter with a measuring range of 0 – 80 % H_2O. The first wood crib was placed on the weighing platform at a height of 50 mm above the tunnel floor. A cube of fibreboard measuring 0.03 m, 0.03 m and 0.024 m and soaked in heptane was placed at the same level as the bottom of the wood cribs and on the upstream edge of the wood crib, as shown in Figure 9. The cube was filled with 9 ml heptane in the tests, with the exception of those tests with an initial longitudinal velocity of 8 m/s, in which double the amount of heptane was used for ignition of the wood crib. For each test, the logging system was initiated two minutes prior to ignition of the fibreboard cube. After each test, the remains of the wood cribs or char was dried overnight and measured to determine the net weight loss during a fire test.

Figure 9 A photo showing a growing fire. The ignition source consisted of a fibreboard cube placed at the same level as the bottom of the wood crib and at the upstream edge of the wood crib. Another wood crib was placed downstream in order to investigate the risk for fire spread.

Two wood cribs were arranged in the tunnel fire tests, see Figure 10, to investigate the risk for fire spread. In most tests, the free distance between two wood cribs was 1.05 m (15.75 m in large scale). A drawing of the location of the two wood cribs is shown in Figure 10.

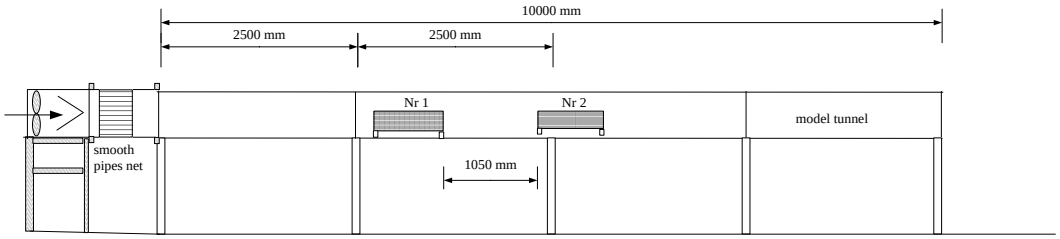

Figure 10 Locations of the two wood cribs arranged in test series.

A total of 28 fire tests were carried out in the model tunnel, including 21 tests with automatic sprinkler system (Test 1 – Test 21), 3 tests with deluge system (Test 22 – Test 24) and 4 free-burn tests (Test 25 – Test 28). Further, a series of nozzle tests were also

carried out. In Test 1 – Test 24, the geometry of the second wood crib is the same. In Test 25 – Test 28 the wood crib is half the size of that in the other tests.

4.1 Automatic sprinkler system

In Table 2, detailed information on the tests with automatic sprinkler system is presented. The effect of ventilation velocity, water flow rate, and link activation temperature were considered in the tests. In addition, fire spread to a wood crib downstream with the same type was also tested.

In some tests, i.e. Test 5, 6, 10, 11, 17 and 19, the ventilation velocity inside the tunnel was decreased from a higher value, i.e. 2 m/s or 1.5 m/s, to 0.5 m/s to optimize the performance of the automatic sprinkler system. These values correspond to 8 m/s, 6 m/s and 2 m/s, respectively, in full scale. This measure was called the Variant Ventilation Strategy. In most of other tests a constant ventilation velocity was used, which was called Constant Ventilation Strategy.

The normal control strategy is to activate the nozzle if the bulb beside the nozzle is activated. In test 21 a Special Control Strategy was used to optimize the performance of the automatic sprinkler system. The Special Control Strategy involved that a nozzle be activated if the bulb installed 0.6 m downstream of the nozzle was activated. For example, Nozzle N1 was activated if Bulb B3 was activated, see Figure 7.

Table 2 Summary of tunnel fire tests with automatic sprinkler system

Test Nr	V	q_w	T_L	1st wood crib			
				Initial moisture	Initial Weight	Left weight	Net weight loss
	m/s	L/min	°C	%	G	g	g
1	0.5	0.58	141	7.0	5010	4896	114
2	0.5	0.38	141	7.0	4980	4140	840
3	1.0	0.38	141	6.1	4920	4124	796
4	1.5	0.38	141	6.6	5388	2197	3191
5	1.5-0.5	0.38	141	6.1	4942	4325	617
6	2.0-0.5	0.38	141	5.9	5188	4464	724
7	0.5	0.46	141	7.3	4598	4525	73
8	1.0	0.46	141	7.0	5260	4785	475
9	1.5	0.46	141	6.5	4855	2069	2786
10	1.5-0.5	0.46	141	6.3	4669	4354	315
11	2.0-0.5	0.46	141	7.0	5117	4625	492
12	1.0	0.58	141	7.3	4997	4649	348
13	1.5	0.58	141	5.7	5336	3135	2201
14	0.5	0.46	68	7.0	4944	4904	40
15	1.0	0.46	68	6.0	4976	4725	251
16	1.5	0.46	68	7.0	5022	3707	1315
17	1.5-0.5	0.46	68	6.7	4867	4486	381
18	0.5	0.38	141	7.0	4970	4612	358
19	2.0-0.5	0.58	141	6.0	5016	4257	759
20	2.0	0.58	141	7.0	4713	2142	2571
21	2.0	0.58	141	4.5	4157	3928	229

*there was some problem with the bulb which was not activated during the test.

4.2 Deluge system

Table 3 gives a summary of tunnel fire tests conducted using the deluge system. The main parameters taken into account here is the ventilation velocity. The ignition time of 75 s corresponds to 4.8 min in large scale. This activation time was chosen based on Ingason's work [18]. In addition, averaging the first activation time of the bulbs in the tests with automatic sprinkler system gives a value of about 78 s, which corresponds well to the designed value and therefore makes the comparison between these two systems reasonable.

Table 3 Summary of tunnel fire tests with deluge system

Test no	V	q_w	Activation time	1st wood crib			
				Initial moisture	Initial weight	Left weight	Net weight loss
	m/s	L/min	s	%	G	g	G
22	0.5	0.38	75	6.0	4665	4601	64
23	1.0	0.38	75	5.5	4517	4374	143
24	1.5	0.38	75	5.4	4540	4413	127

4.3 Free burn

Free burning tunnel fire tests were also carried out for comparison with the water spray tests. Table 4 gives a summary of these free burn tests. Different ventilation velocities were used during the tests. This series was conducted after all water spray tests had been finished in order to avoid fire damage to the model tunnel.

During the tests, the 2nd wood crib is only half the size of the 1st one. In tests 25-27, the 2nd wood crib was charred, however, fire spread did not occur. Note that the free distance between two wood cribs was 1.05 m. Therefore, in Test 28, the free distance between the two wood cribs was decreased to a distance of 0.6 m. This allowed a clear fire spread between the first and the second wood cribs. The fact that the fire did not spread in most of the water spray tests, is of course a disappointment, but the main conclusions of the test series remain unchanged. In Test 28, where the fire spread, only the total left weight of 1st and 2nd wood crib were measured after the test.

Table 4 Summary of free burn tests in the model tunnel

Test no	V	Initial Moisture (1st)	Weight of 1st / 2nd wood crib			Arrangement of wood cribs	Free distance between wood cribs
			Initial	Left	Net loss		
	m/s	%	g	g	g		M
25	0.5	7.0	4747/2429	662/2322	4085/107	1+1/2*	1.05
26	1.0	7.0	4321/2503	204/2433	4117/70	1+1/2	1.05
27	1.5	7.0	4856/2424	318/2424	4538/0	1+1/2	1.05
28	0.5	7.0	4977/2424	1098**	6303**	1+1/2	0.6

*2nd wood crib is half of the 1st one. **total mass of 1st and 2nd wood cribs (unfortunately they were mixed together).

It can be seen in Table 2 and Table 4 that the initial moisture of the wood crib is in the range of 5.0 % to 7.0 %.

5 Test results

All the detailed test results for each test are given in Appendix D. The chapter contains a presentation of selected numerical results and the methodology used for the graphical presentation in Appendix D. The heat release rate was measured both by measuring the weight loss and using oxygen consumption calorimetry. Note that only the weight loss of the first wood crib was measured during the tests.

5.1 Heat release rate

The heat release rate was determined using two different measurement techniques: using the fuel weight loss and using oxygen consumption calorimetry, see Appendix C. Once a nozzle close to the fire was activated, the heat release rate based using the mass loss method, i.e. the "mass" curve in Appendix D, was no longer reliable, and only the oxygen consumption technique was used to estimate the heat release rate. During the tests, the gas concentrations were measured in two stations - 5.5 m downstream of the fire source and in the duct. In addition, the longitudinal ventilation velocity was measured both upstream and downstream of the fire. Therefore based on the measurement of gas concentration and gas flow in the duct and inside the tunnel, three heat release rate curves, i.e. "duct", "upstream" and "downstream", could be obtained, as shown in the Appendix D. The duct curve was estimated based on the gas concentration and gas flow measured in the extraction duct. The upstream curve was estimated based on the gas concentration measured downstream and gas flow measured upstream. The downstream curve was estimated based on the gas concentration and gas flow measured upstream. In some tests, some smoke leaked out of the box at the end of the tunnel. This implies that the upstream and downstream curves are more reliable. However, only small differences are found between these four curves in most cases. It can be seen clearly in the free-burn tests, i.e. Tests 25-28, that the estimated heat release rate using the oxygen consumption method shows a small lag during the decay period. In some tests, i.e. Test 25, the platform was destroyed and touched the floor at the beginning of the decay period therefore data after this time is not shown in the figures.

5.2 Gas temperatures

Test results related to the measured gas temperatures are shown in Table 5. The maximum ceiling temperature at distance X_f from the centreline of the fire source is shown in columns four to fifteen. The values listed here are the maximum values measured by the thermocouple during one test. The identification and location of these thermocouples can be found in Figure 4.

5.3 Total heat flux

The total heat fluxes were registered using plate thermometers at floor level and different locations from the fire (identified as S24, S25, S26 and S27 in Figure 4.). In the last four columns of Table 5, the heat fluxes measured with plate thermometers, i.e. Max flux 1 to Max flux 4, are given. Note that the values given in Table 5 represent the maximum total heat fluxes measured.

5.4 Activation time of bulbs

The activation times for the bulbs in an automatic sprinkler system are listed in Table 6. In tests 1 - 3, the bulbs downstream (Bulbs B14 to B19) were not installed, therefore the furthest bulb that might have been activated is not known. However, in other tests, all the bulbs, B1-B21 were replaced.

Table 5 Test results relevant to temperature and heat flux.

Test Nr	Q_{max}	$Q_{a,1}$	$T_{1,max}$	$T_{2,max}$	$T_{3,max}$	$T_{4,max}$	$T_{5,max}$	$T_{6,max}$	$T_{7,max}$	$T_{8,max}$	$T_{9,max}$	$T_{10,max}$	$T_{11,max}$	$T_{12,max}$	*Max flux 1*	*Max flux 2*	*Max flux 3*	*Max flux 4*
	kW	kW	°C	°C	°C	°C	°C	°C	°C	°C	°C	°C	°C	°C	kW/m^2	kW/m^2	kW/m^2	kW/m^2
X_f (m)			-2m	-1.5m	-1m	-0.5m	0m	0.4m	0.9m	1.35m	2.2m	2.95m	4.2m	5.45m	-1m	1.35m	2.95m	5.45m
1	15.5	10.7	21.1	21.2	21.9	76.6	161.1	153.8	136.0	113.1	97.2	81.4	67.6	57.5	-*	-	-	-
2	62.9		144.0	184.8	233.3	379.8	641.2	940.7	353.5	303.2	206.7	184.8	148.3	122.9	1.25	1.86	0.85	0.66
3	119.5	20.9	21.5	21.7	24.0	34.5	921.5	527.6	411.8	304.6	271.4	232.4	204.5	179.8	0.84	2.3	1.23	0.90
4	119.8	18.8	22.1	22.3	26.8	46.7	561.7	777.6	381.5	238.2	250.7	236.2	215.3	187.1	1.45	1.71	0.97	0.95
5	58.5	19.1	275.4	332.4	376.7	699.9	936.4	749.2	398.7	290.0	237.6	204.8	155.9	141.3	2.41	3.75	0.82	0.66
6	94.9	26.1	150.9	201.7	248.4	354.7	872.3	842.6	446.5	317.0	291.3	248.0	199.9	184.6	1.29	5.27	1.19	0.88
7	10.9	7.6	19.7	19.8	20.3	65.5	127.1	159.8	118.7	84.6	86.1	60.8	50.6	45.9	-	-	-	-
8	79.2	24.5	20.3	20.6	24.6	42.6	698.0	390.2	312.9	240.7	172.3	148.0	130.0	120.0	0.90	3.36	0.74	0.67
9	128.1	24.9	21.9	22.0	26.9	47.3	563.0	793.4	338.9	212.4	203.1	199.4	184.1	169.8	1.34	1.81	0.99	0.94
10	84.0	22.6	125.9	173.9	225.2	317.4	861.5	394.0	324.5	252.3	220.2	181.4	145.3	133.1	1.15	4.06	0.81	0.72
11	87.9	35.7	139.4	186.0	240.9	328.9	882.2	846.4	419.7	295.3	260.5	215.6	170.7	158.5	1.12	5.16	1.06	0.77
12	77.0	13.3	19.9	20.3	23.7	37.4	679.8	244.1	207.4	186.9	165.1	131.7	111.6	109.0	0.84	3.20	0.72	0.64
13	109.6	26.5	22.2	22.5	27.4	52.0	543.2	481.0	227.0	153.5	148.8	151.2	129.4	117.7	0.99	1.73	0.75	0.81
14	6.7	5.5	21.5	21.6	22.0	24.0	80.7	89.2	79.6	63.5	61.4	51.4	42.2	40.4	-	-	-	-
15	46.3	6.4	22.2	22.4	24.1	32.0	568.3	178.8	171.2	156.0	103.1	93.4	76.7	76.0	0.66	2.30	0.55	0.51
16	137.0	11.8	22.2	22.4	26.4	41.9	471.8	783.9	398.8	226.8	236.5	221.5	195.5	175.0	1.06	1.91	1.04	1.01
17	41.2	15.6	53.2	92.2	120.3	153.3	852.0	369.1	260.6	170.6	145.7	115.5	86.4	80.2	0.67	3.44	-	-
18	18.4	9.4	19.6	19.7	21.9	70.5	166.1	166.8	137.1	110.4	111.8	88.7	72.4	64.9	-	-	-	-
19	108.6	36	80.0	107.8	128.3	178.5	900.9	553.4	278.3	231.9	200.8	187.1	139.3	125.8	0.99	4.20	0.99	0.84
20	199.5	37.1	22.4	22.7	26.1	40.7	380.4	767.2	607.3	87.3	49.5	186.6	171.3	158.8	0.94	2.98	1.10	1.31
21	64.6	32.1	20.9	20.9	21.7	23.1	96.8	410.6	180.0	87.8	52.5	82.3	96.9	88.7	0.62	0.66	0.57	0.77
22	19.6	17.8	51.4	95.0	127.6	171.8	508.4	352.7	267.5	205.0	192.7	146.4	104.9	87.7	0.77	1.38	0.50	0.53

23	38.3	36.4	21.3	21.4	23.2	29.4	493.8	329.5	288.7	224.5	227.9	195.6	150.9	138.2	0.61	2.36	0.63	0.65
24	34.7	21.2	21.7	21.7	22.3	24.0	121.2	199.7	125.1	52.9	55.7	104.4	80.9	69.4	-	-	-	-
25	211.7		250.4	303.5	388.5	634.2	1063.7	818.4	701.6	529.0	454.2	368.5	285.9	253.8	4.38	15.99	3.69	1.96
26	244.9		33.3	42.0	63.4	143.2	809.1	1085.3	781.4	537.2	481.8	428.6	342.7	321.6	2.56	23.15	6.55	3.47
27	244.9		29.4	34.4	50.6	97.1	545.2	1042.0	915.5	427.0	449.9	398.3	333.1	309.7	2.25	25.33	6.05	2.89
28	430.1 (269.3)**		35.8	47.0	74.6	142.5	870.8	1090.4	893.8	865.0	916.4	632.9	475.4	420.9	3.03	9.89	26.05	9.83

The main test results related to the heat release rate, gas temperature and heat flux are given. The test number is given in the first column. The second and third column show the maximum heat release rate, Q_{max}, and the heat release rate at the activation time of the first activate bulb, $Q_{a,1}$, respectively. In the calculations, a combustion efficiency of χ =0.9 and the heat of combustion of 16.7 MJ/kg obtained from previous tests [26][36] were applied. Columns four to fifteen show the measured maximum gas temperatures beneath the ceiling. Columns sixteen to nineteen show the measure maximum heat flux. An asterix (*) indicates a value less than 0.5kW/m^2. A double asterix (**) indicates that the total heat release rate is 430.1 kW and the heat release rate of the first wood crib is 269.3 kW.

Table 6 The activation time of the bulbs in the tests with automatic sprinkler system.

Test Nr	Activation time t_a (min)													
	B1	B2	B3	B4	B5	B6	B7	B8	B9	B10	B11	B12	B13	B14-B19
X_f (m)	-0.75	-0.43	-0.17	0.21	0.53	0.83	1.13	1.43	1.73	2.03	2.33	2.63	2.93	3.53-6.53
1			1.04											
2		1.85	*	2.35	1.31	*	*	1.78	1.88					
3			2.79	1.72	1.51	1.51	1.41	1.48	1.51	1.73	1.93	1.83	2.08	unknown[a]
4				1.56	1.64	1.78	1.83	1.83	1.83	1.89	1.98	2.05	2.21	all gone[b]
5		1.66	1.58	*	1.39	1.48	1.53	1.57	1.6	1.6	1.61	1.63	1.65	3 left[c]
6		1.68	1.5	1.35	1.21	1.13	1.18	1.3	1.36	1.36	1.33	1.35	1.38	all gone
7			0.59											
8			1.24	0.96	1.06	1.18	1.13	1.06	1.08	1.51				
9				1.59	1.51	1.69	1.83	1.79	1.79	1.83	2.02	*	2.25	all gone
10		2.01	1.76	1.29	1.16	1.38	1.48	1.46	1.48	1.51	1.63	1.65	1.71	3left
11		1.85	1.63	1.61	1.25	1.25	1.34	1.48	1.51	1.54	1.52	1.54	1.57	2left
12			1.98	1.21	1.41	1.45	1.73	1.83	1.92					
13			6.31	2.12	2.11	2.29	2.4	2.35	2.35	2.33	3.39	5.48		
14			0.56											
15			1.5	0.68	0.96	1.15	1.06	1.05	1.39	1.42	1.5	1.54	1.64	3left
16			2.75	1.43	1.21	1.28	1.52	1.63	1.63	1.62	1.61	1.62	1.61	all gone
17		1.95	1.7	1.51	1.33	1.39	1.6	1.6	1.62	1.61	1.61	1.63	1.65	1left
18			0.94	2.04										
19			2.19	1.68	1.47	1.42	1.46	1.78	1.88	1.97	2.06	2.11		4left
20				1.8	1.35	1.31	1.35	1.62	*	*	1.75	1.7	1.68	1left
21			0.98											

[*] there was some problem with the bulb which was not activated during the test. [**]the large-scale value. Blank means no activation.
[a] no addictive bulb was placed in this range during this test. [b] all the bulbs were broken during the test. [c] three bulbs furthest away from the fire left after the test.

5.5 Fire spread

In the tests with an automatic sprinkler system or a deluge system, no fire spread occurred and the second wood crib was not charred in any test. In most of the free-burn tests, i.e. Test 25, Test 26 and Test 27, the second wood crib was clearly charred, however not burnt. Note that in tests 1-27 the free distance between two wood cribs was 1.05 m, corresponding to 15.75 m in large scale, which seems too far to allow flame spread for such a fire. Therefore in Test 28, the free distance was adjusted to be 0.6 m, corresponding to 9 m in large scale, and the second wood crib was totally burnt out after the test.

6 Discussion of results

The main focus of these tests has been the performance of an automatic sprinkler system in a tunnel fire. The activation of the nozzles, the maximum heat release rate, energy content and the potential for collapse of an automatic sprinkler system were analyzed based on a large amount of data obtained from the tests presented in Section 6.1 to 6.6. A short investigation of performance of a deluge system was also conducted. In addition, many fire dynamic parameters including maximum temperature beneath the ceiling, heat flux and fire spread were investigated.

6.1 Activation of the first activated bulb

The activation of a bulb is closely related to its RTI, gas temperature and velocity around the bulb as shown in Equation (A1), see Appendix A. Although the controlling equation is well understood, the activation time and the activation conditions for a bulb cannot be predicted simply due to the transient thermal conditions produced close to the blub in a tunnel fire.

6.1.1 Activation condition of the first activated bulb

The activation of the first bulb plays an important role in the performance of an automatic sprinkler system in a tunnel fire. The first bulb to activate is normally capable of suppressing the fire spread in the growth period since it is location close to the fire source. In the following we analysis the activation conditions for the first activated bulb.

Figure 11 and Figure 12 show the activation heat release rates (AHRR) of the first activated bulb, Q_{a1}, as a function of the ventilation velocity with a link temperature of 141 ^{o}C and 68 ^{o}C. respectively. It can be seen that there is a strong correlation between these parameters. The activation heat release rate increases linearly with the ventilation velocity. This is as expected since the higher ventilation cools the gas, which in turn increases the AHRR necessary to fulfil the activation conditions for the bulb. In addition, the linear correlation between the AHRR and the longitudinal ventilation velocity shows that the activation ceiling temperature is almost a constant according to the equations proposed by Li and Ingason [29]. The reason may be that the ceiling gas temperature plays a much more important role than the gas velocity in the activation of the bulbs in a tunnel situation. If we assume that 1/4 of the wood crib was burning at the upstream edge of the wood crib at this time, since the heat release rate is very low compared to the maximum heat release rate in the corresponding free-burn test, the calculated activation temperature according to the equations proposed by Li and Ingason [29] is about 206 ^{o}C and 109 ^{o}C for a link temperature of 141 ^{o}C and 68 ^{o}C respectively. This corresponds to an excess activation temperature is 65 ^{o}C and 41 ^{o}C higher than a link temperature of 141 ^{o}C and 68 ^{o}C, respectively.

Comparing Figure 11 and Figure 12 shows clearly that the AHRR of the first bulb with a link temperature of 68 ^{o}C is approximately half that of the bulb with a link temperature of 141 ^{o}C, i.e. close to the ratio between the two link temperatures.

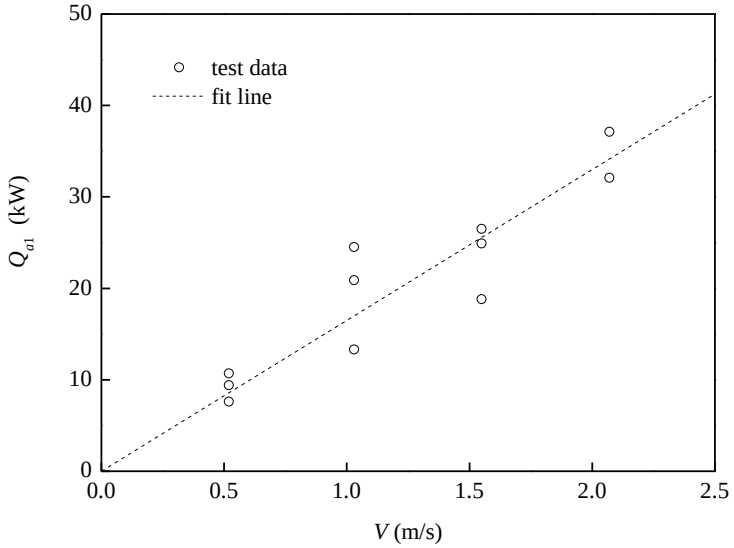

Figure 11 The activation heat release rate of the first bulb in the tests with automatic sprinkler system (T_L=141 ^oC).

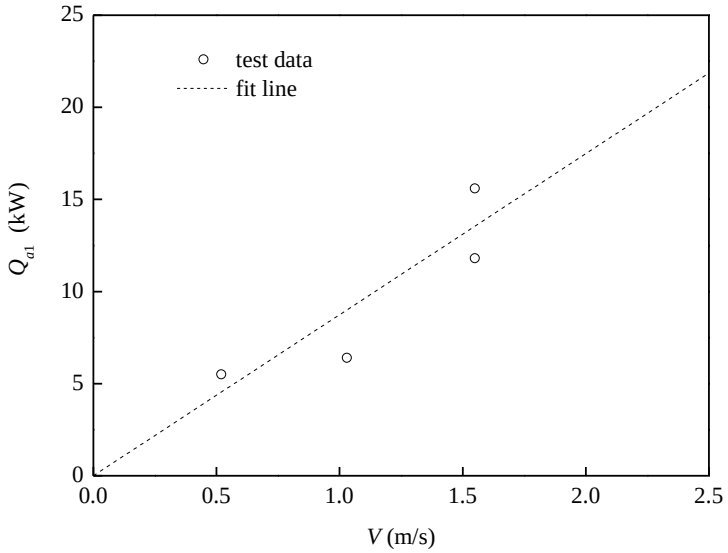

Figure 12 The activation heat release rate of the first bulb in the tests with automatic sprinkler system (T_L=68 ^oC).

Figure 13 and Figure 14 show the activation temperatures of the first bulb, T_{a1}, in the tests with automatic sprinkler system with a link temperature of 141 ^{o}C and 68 ^{o}C respectively. It is shown that the activation temperature of the first bulb with a link temperature of 141 ^{o}C and 68 ^{o}C mainly lie in a range of 110 ^{o}C – 230 ^{o}C and 70 ^{o}C – 110 ^{o}C respectively. Note that the predicted values of 206 ^{o}C and 109 ^{o}C based on the activation heat release rate lie within these ranges. However, some data seems counterintuitive since the activation temperature of the first bulb should always be higher than the corresponding link temperature. The reason for the discrepancy found in some of the experiments on the bulb with a link temperature of 141 ^{o}C may be that the data presented here is the transient temperature data registered by the thermocouples which may be lower than that experienced by the bulb.

It is shown clearly in Figure 13 and Figure 14 that the activation temperature of the first bulb with a link temperature of 68 ^{o}C is much lower than that with a link temperature of 141 ^{o}C. The two figures also show a trend towards a slightly increased activation temperature of the first bulb slowly with the ventilation velocity. The reason could also be due to the transient registered data.

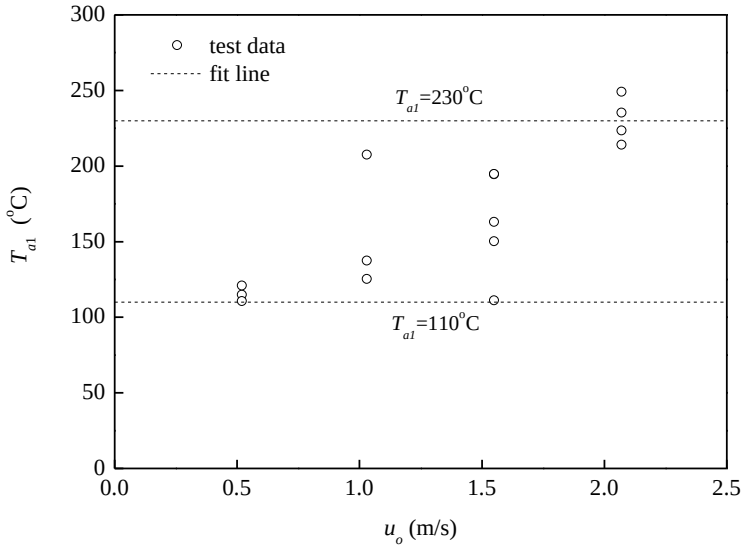

Figure 13 The activation temperature of the first bulb in the tests with automatic sprinkler system (T_L=141 ^{o}C).

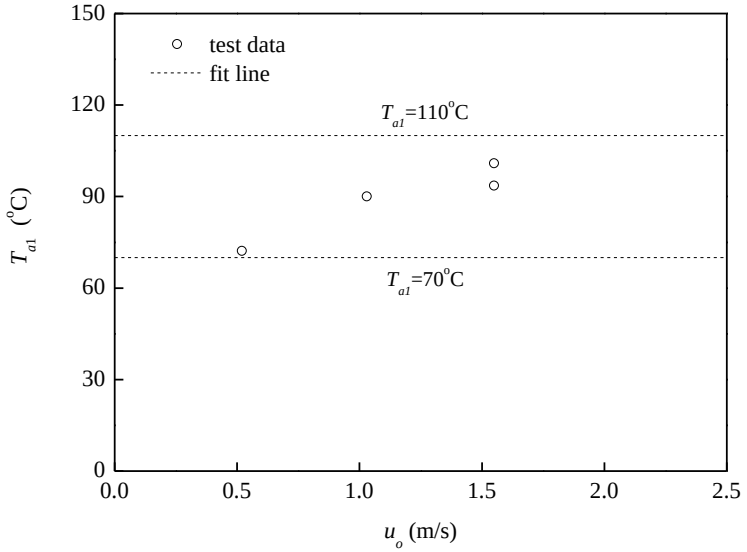

Figure 14 The activation temperature of the first bulb in the tests with automatic sprinkler system (T_L=68 ^{o}C).

6.1.2 Activation time of the first activated bulb

Figure 15 shows the activation time of the first activated bulb. It can be seen that the activation of the bulb increases with the link temperature. This is due to the higher AHRR for a higher link temperature. In addition, it is known that the fire growth rate is intimately related to the ventilation velocity.

It is also shown in Figure 15 that the activation time of the first activated bulb increases with the ventilation velocity below 1.5 m/s and decreases above this value. However, the activation time of the bulb is directly related to the fire development, which is directly related to the ventilation velocity and the ignition source. The ignition source has little influence on the fire development during the linear growth period, however, it can significantly affect the fire development in the ignition phase, usually at a level of 30 to 60 seconds in our tests. A higher ventilation velocity results in a lower fire development at the ignition stage if the same ignition source is used. In the tests with longitudinal ventilation velocities of 2 m/s (8m/s in large scale), the 9 ml heptane ignition source could not ignite the wood crib due to the high ventilation, therefore 18 ml heptane source was used in these tests. This can explain why the activation time of the bulb decreases when the ventilation velocity is above 1.5 m/s.

If we assume that the fire is developed during the beginning of the linear growth period, i.e. a heat release rate of about 15kW in our tests, the activation time should be the same since the AHRR is proportional to the ventilation velocity and in the linear growth period the fire growth rate increases linearly with the ventilation velocity. Therefore the trend seen in Figure 15 is probably more dependent on the effect of ventilation in the ignition period than in the fire growth period.

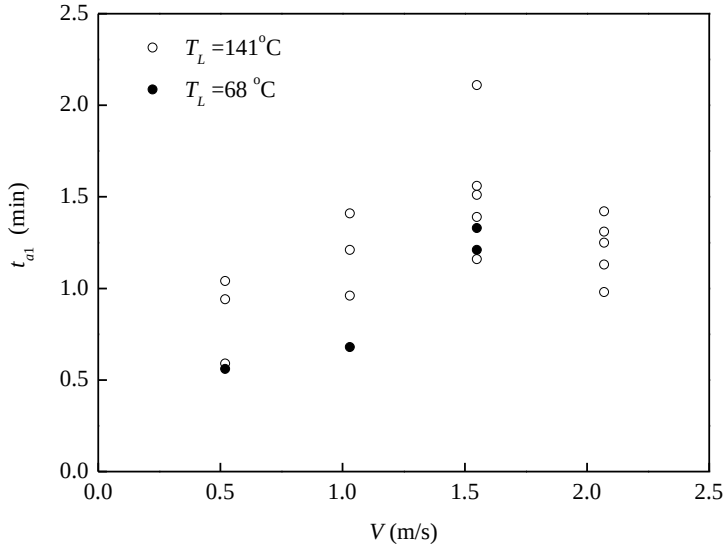

Figure 15 The activation time of the first bulb in the tests with automatic sprinkler system.

6.1.3 Location of the first activated bulb

The location of the first bulb is difficult to be predicted. The parameters involved in include gas temperature and gas velocity, or more explicitly expressed, heat release rate and ventilation velocity.

Table 7 shows the location of the first activated bulb in the tests with an automatic sprinkler system. L_a is the distance between the fire source centre and the location of the first activated bulb. At a velocity of 0.52 m/s, the third bulb (N3) was that first activated and its location was -0.17 m. Note that the actual fire source centre at the time was not the real fire source centre (X_f=0 m) since the ignition source was placed at the upstream edge of the wood crib and only the upstream part of the wood crib was burning at the first activation time.

The location of the first activated bulb was about 0.21 m at a velocity of 1.03 m/s, 0.53 m at 1.55 m/s and 0.83 m at 2.07 m/s. Clearly, the location of the first activated bulb increases with longitudinal ventilation velocity. The location of the first activated bulb is also related to the AHRR, although the AHRR can also be expressed as a function of the ventilation velocity. This may be the reason why there seems to be a strong correlation between the location of the first activated bulb and the ventilation velocity. In addition, the link temperature should also have an influence on the location of the first activated bulb since the AHRR is different for different link temperatures. However, the results show no clear difference related to the different link temperatures.

Table 7 Summary of the location of the first activated bulb in tests with automatic sprinkler system.

u_o	L_a						
m/s	*M*						
0.52	-0.17	-0.17	-0.17	-0.17			
1.03	1.13	0.21	0.21	0.21			
1.55	0.21	0.53	0.53	0.53	0.53	0.53	0.53
2.07	0.83	0.53	0.83	0.83	0.53		

According to previous research, the flame angle, φ, defined based on the position of the maximum temperature can be expressed as follows:

$$\sin\varphi = \frac{H_{ef}}{L_{traj}} = \begin{cases} 1, & V' \le 0.19 \\ (5.26V')^{-3/5}, & V' > 0.19 \,\&\, Q^* \le 0.15 \\ 0.25(b_{fo}V^{*3}/H)^{-1/5} & V' > 0.19 \,\&\, Q^* > 0.15 \end{cases} \qquad (14)$$

The dimensionless parameters in Equation (14) are defined as:

dimensionless heat release rate: $Q^* = \dfrac{Q}{\rho_o c_p T_o g^{1/2} H^{5/2}}$

dimensionless longitudinal velocity: $V^* = \dfrac{V}{\sqrt{gH}}$,

dimensionless modified Richardson number: $\mathrm{Ri}' = \dfrac{gQ}{\rho_o c_p T_o V^3 H}$

dimensionless ventilation velocity: $V' = \frac{V}{w^*} = V/(\frac{gQ}{b_{fo}\rho_o c_p T_o})^{1/3}$

where b_{fo} is the equivalent radius of the fire source, c_p is the heat capacity, H is the tunnel height, H_{ef} is the effective tunnel height (tunnel height above the fire source bottom), g is the gravitational acceleration, Q is the total heat release rate, L_{traj} is the trajectory length, T_o is the ambient temperature and ρ_o is the ambient density, .

The position of maximum temperature beneath the ceiling away from the centre of the fire source can be expressed as:

$$L_{MT} = H_{ef} \cot(\arcsin \varphi) \qquad (15)$$

Equation (14) and Equation (15) suggest that the position of the maximum temperature is independent of heat release rate if the dimensionless heat release rate is greater than 0.15.

As shown in the controlling equation of the activation of the bulb, i.e. Equation (A1), the activation of the bulb is much more dependent on the ceiling temperature than the gas flow velocity. This means that the position of the maximum temperature beneath the ceiling should be close to the location of the first activated bulb. For simplicity, it is assumed here that the location of the first activated bulb is the position of the maximum temperature at the activation time.

Figure 16 shows a comparison of the measured location of the first activated bulb and the predicted value using Equation (14) and Equation (15). At the beginning of the fire development the fire centre does not lie in the wood crib centre, but a distance upstream of the wood crib centre. According to the observation during the tests and the data of heat release rate, it is assumed that 1/4 part of the wood crib is burning at the time of activation of the first bulb. Therefore is necessary to add 0.3 m to the values in Table 7 to correct for this difference in the fire position and improve the comparison. It is shown in Figure 16 that there is a good agreement between the measured value and the predicted value. Interesting is that the location of the first activated blub seems to be closely related to the velocity, independent of the heat release rate, as observed in Table 7. This phenomenon correlates well with Equation (14) and Equation (15). As the heat release rate is over 17 kW (Q^*>0.15), the position of the maximum temperature is independent of the heat release rate and only depends on the ventilation velocity.

An outlier, far away from the measured-predicted time equivalency line, is also shown in Figure 16. The reason for this outlier was explained previously, i.e. in this test with a ventilation velocity of 1 m/s many bulbs close to the fire were activated simultaneously. In any case, the generally good agreement between the measured and predicted values further verifies Equation (14) and Equation (15), and proves the assumption that the activation of the bulb is much more dependent on the ceiling temperature than the gas flow velocity.

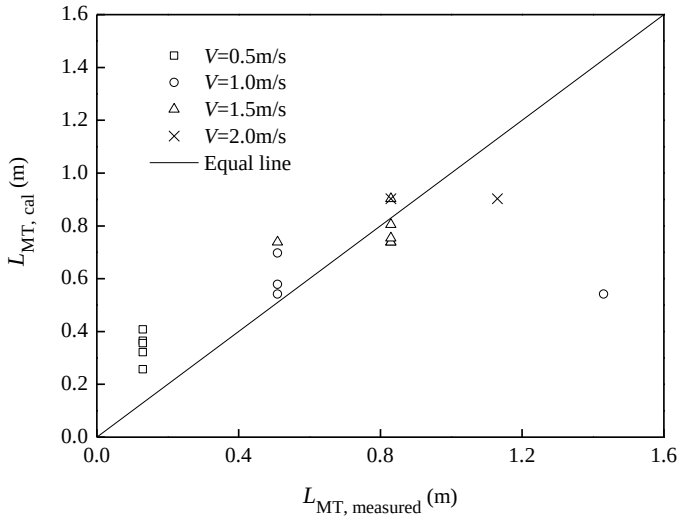

Figure 16 Comparison of the measured location of the first activated bulb and the predicted value using Equation (14) and Equation (15)

6.2 Activation of the bulbs

6.2.1 Activation condition of the bulbs

Figure 17 shows the activation temperature of different nozzles in tests using Constant Ventilation Strategy with a link temperature of 141 ^{o}C. It is shown that the activation temperatures of these nozzles placed more than 0.5 m away from the fire source centre mainly lies in a range of 100 ^{o}C - 200 ^{o}C. Note that the lower value is below the link temperature, probably due to the fact that these temperatures correspond to the transient measurement of gas temperatures made by thermocouples. It is also shown in Figure 17 that the activation temperature of nozzles placed in the vicinity of the fire seems much higher than others, in a range of 350 ^{o}C - 500 ^{o}C. These tests data correspond to the tests with ventilation velocity higher than 1 m/s. There are two reasons for the high values. Firstly, under these ventilation conditions there is no back-layering upstream and the flame is inclined towards the downstream direction. This means that during the beginning of the fire development the flames exist on the downstream edge of the wood crib. As the fire continues to develop and flames spread to the upstream edge of the wood crib. In this case the flames exist on the upstream edge of the wood crib, which makes the upper gas temperature increase immediately even without back-layering. Secondly, most of the temperature data in Figure 17 comes from linear extrapolation of the neighboring values. This can also induces a large error due to sharp temperature gradients in this region.

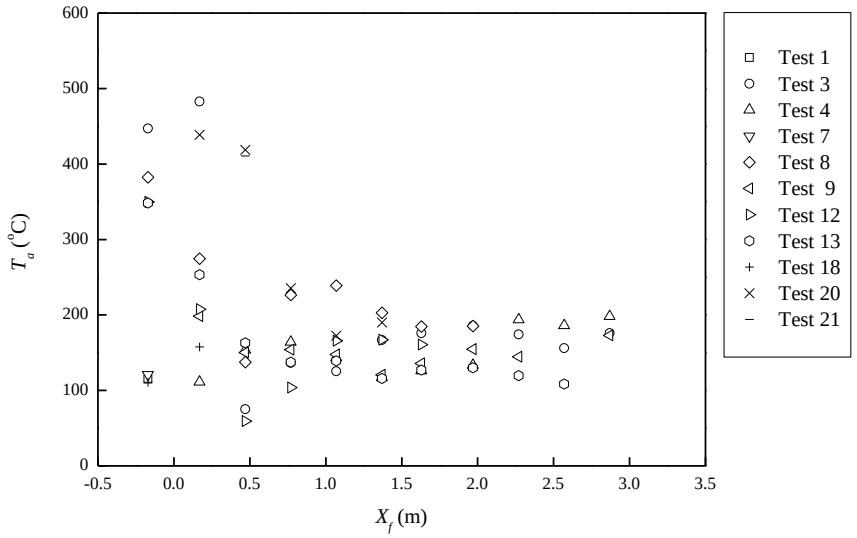

Figure 17 The activation temperature of nozzles in tests using Constant Ventilation Strategy (T_L=141 °C)

Figure 18 shows the activation temperature of different nozzles in tests using Variant Ventilation Strategy with a link temperature of 141 °C. It is shown that the activation temperatures of these nozzles placed more than 0.5 m away from the fire source centre mainly lie in a range of 140 °C - 200 °C. In addition, the activation temperature of nozzles in the vicinity of the fire seems to be much higher than others. This may be due to the same phenomenon discussed earlier. Note that the activation temperatures of nozzles in the vicinity of the fire were even higher than the values in Figure 18. The reason is that in tests using Variant Ventilation Strategy, there is no back-layering at a high ventilation velocity, however, the back-layering appears after the ventilation velocity is changed to 0.5 m/s.

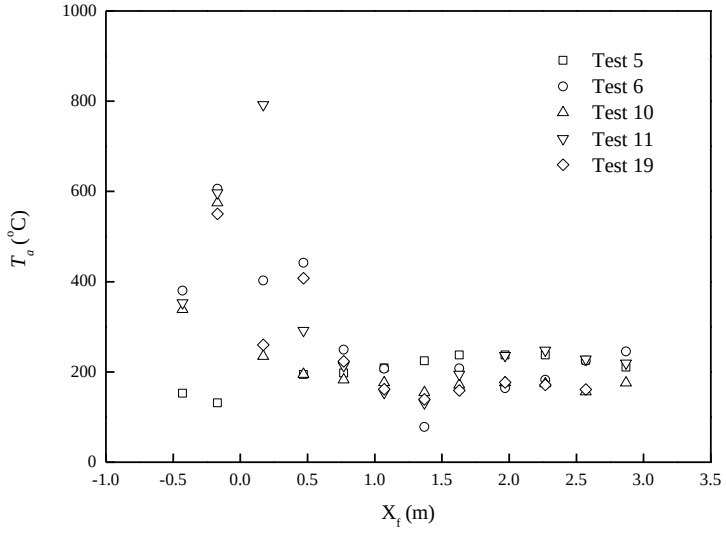

Figure 18 The activation temperature of nozzles in tests using Variant Ventilation Strategy (T_L=141 °C)

6.2.2 Activation sequence and time of the bulbs

Figure 19 show the activation time of the bulbs in the tests with an automatic sprinkler system with a link temperature of 141 °C. It is shown that most of the nozzles with a link

temperature of 141 ^{o}C were activated in a relative short period. The activation time of the nozzles mainly lies in the range of 1 min to 2 min, corresponding to about 4 min to 8 min in large scale. However, at the ends of the activation range, i.e. the range of activated nozzles, in some cases, the activation of these nozzles may need much more time than others, see Figure 19.

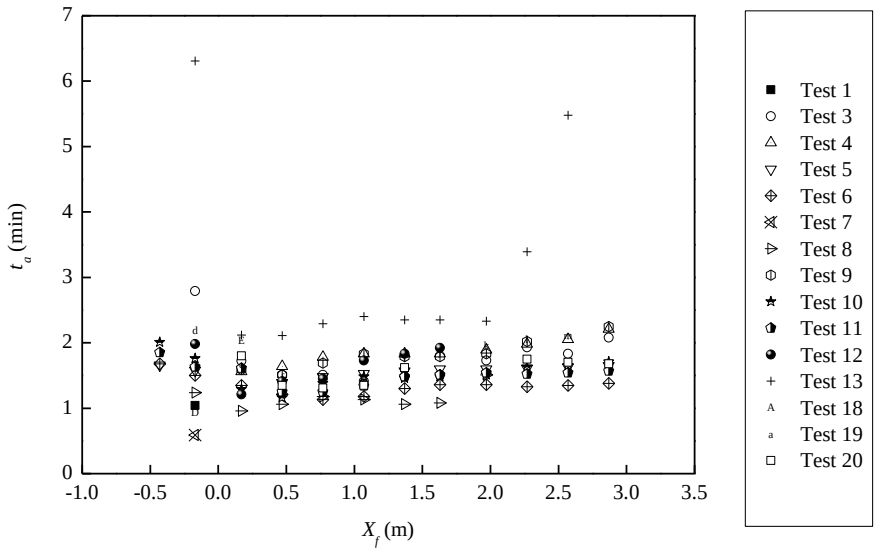

Figure 19 The activation time of the bulbs in the tests with automatic sprinkler system (T_L=141 ^{o}C).

Figure 20 show the activation time of the bulbs in the tests with an automatic sprinkler system with a link temperature of 68 ^{o}C. It shows that most of the nozzles with a link temperature of 68 ^{o}C were activated in a relative short period of time. The activation time of the nozzles mainly lies in a range of 1 min to 1.5 min, corresponding to about 4 to 6 min in large scale. However, at the ends of the activation range, i.e. the range of activated nozzles, the activation of these nozzles may also be delayed, as observed in Figure 20.

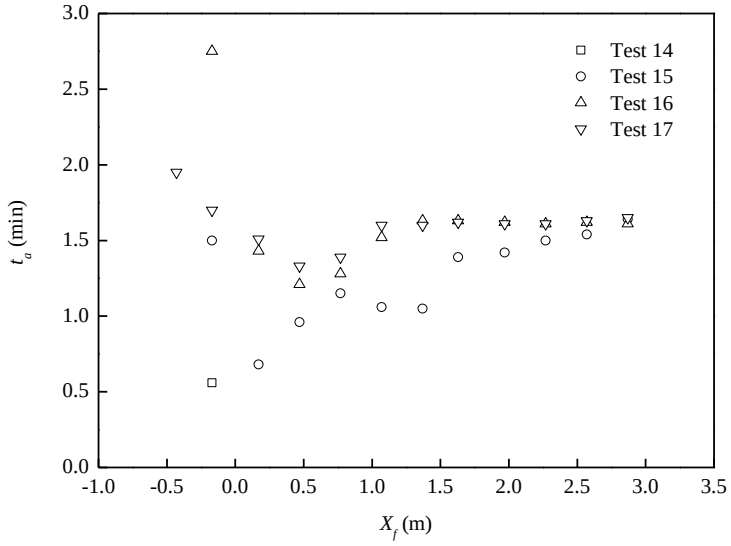

Figure 20 The activation time of the bulbs in the tests with automatic sprinkler system (T_L=68 ^{o}C).

From the analysis of activation time of the first activated bulb, it is shown that the ventilation has an important influence on the activation time as it affects the ignition time. Therefore a time difference, $\Delta t = t_a - t_{a1}$, is used here to re-analyze the results. Figure 21 shows the activation time difference of the bulbs with a link temperature of 141 ^{o}C. It is clear that the activation time after the activation of the first nozzle mainly lies in a range of 0 – 0.6 min in the measured region. This means the majority of nozzles will be activated a short time after the first activation.

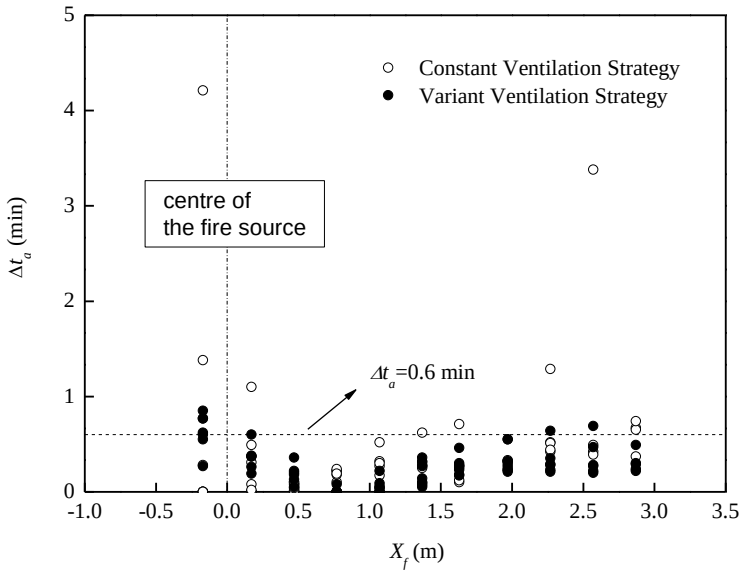

Figure 21 The activation time difference of the bulbs in the tests with automatic sprinkler system (T_L=141 ^{o}C).

It is also shown in Figure 21 that there is no significant difference between the activation time for nozzles downstream of the fire source centre for different ventilation strategies. This may be due to the fact that the nozzles in the downstream region were activated during the period of changing the velocity from a high value to 0.5 m/s. However, in each test using Variant Ventilation Strategy some nozzles upstream were activated in a short period. In the tests using the Variant Ventilation Strategy some nozzles upstream may have been activated due to flame spread to the upstream edge of the wood crib, but more time was required to activate these nozzles under the same initial ventilation conditions.

6.3 Heat release rate and energy content

6.3.1 Maximum heat release rate

Only one or two nozzles, including the first activated nozzle, were activated during a test with a longitudinal ventilation velocity of 0.5 m/s. Under higher ventilation at least several nozzles, including the first activated nozzle and the nozzles placed in the vicinity of the first wood crib, were activated, and the nozzles upstream of the first activated were usually not activated or activated after a relatively long time. This means that the first activated nozzle and the nozzles downstream of the first activated nozzle play the most important roles in the fire development in a tunnel with an automatic sprinkler system.

According to the analysis in 6.1.3, it is known that the location of the first activated bulb is closely related to the ventilation velocity and almost independent of the heat release

rate. In addition, the maximum heat release rate in such scenarios is dependent on the burning surface area, which directly relies on the location of the first activated nozzle. As a consequence, the maximum heat release rate is intimately related to the ventilation velocity.

Figure 22 shows the maximum heat release rate in an automatic sprinkler test with a link temperature of 141°C using Constant Ventilation Strategy. A dimensionless maximum heat release rate, $Q_{max}/Q_{max,freeburn}$, is used to normalize the results. Since no free burn tests with a ventilation velocity of 2.0 m/s were carried out and the fire is fuel-controlled, the maximum heat release rate under these ventilation conditions is assumed to be equivalent to that with a ventilation velocity of 1.5 m/s which is a conservative assumption. In practice the fires in free burn tests are fuel controlled. This implies that the maximum heat release rates are almost the same under different ventilation.

In Figure 22 the maximum heat release rate increases linearly with the ventilation velocity when the dimensionless longitudinal velocity is in the range of 0.2 to 1.0. This means that the maximum heat release rate in an automatic sprinkler test is almost independent of the water flow rate. This verifies the former analysis. It should be kept in mind that the water flow rates, i.e. 0.38 L/min, 0.46 L/min and 0.58 L/min, are at a high level so that the fire can be extinguished immediately if applied in a deluge system. This is shown in data from the deluge system tests with a water flow rate of 0.38 L/min. For an automatic sprinkler system, the water flow rate should not be too low since the system may collapse. Under such conditions, only part of the nozzles will have an influence on the fire development through cooling of the flame and burning surfaces, depending on the ventilation velocity. Most of other nozzles simply cool the hot gases downstream to prevent the collapse of the system. This indicates the ventilation velocity rather than the water flow rate is the most important parameters for an automatic sprinkler system used in a tunnel fire. However, this requires that the water flow rate applied in such a system is sufficiently high.

According to former research [29], when the ventilation velocity is very low the effect of ventilation on the fire plume can be ignored. This means that the ventilation has no influence on the heat release rate under such conditions. This critical value can be estimated using the ceiling temperature calculation and the activation temperature analyzed earlier (206°C for a link temperature of 141°C). The correlation in Figure 22 can be expressed as:

$$\frac{Q_{max}}{Q_{max,freeburn}} = \begin{cases} 0.011, & V' \le 0.19 \\ -0.10 + 0.82V^*, & V' > 0.19 \end{cases} \qquad (16)$$

In Equation (16), Q_{max} is the maximum heat releaser rate in a test with an automatic sprinkler system, $Q_{max,freeburn}$ is the maximum heat release rate in a free-burn tests in the tunnel without water spray system. V^* and V' are the dimensionless longitudinal velocity and dimensionless ventilation velocity, respectively, defined in Equation (14).

A correlation coefficient of 0.9554 was found for Equation (16). According to Equation (16), the dimensionless longitudinal velocity at which the water spray has no influence on the maximum heat release rate can be estimated to be 1.3. It should be kept in mind that the ventilation may produce a cooling effect at such a high ventilation velocity although this phenomenon was not observed in our tests. In addition, one should note that high-momentum nozzles were used for the automatic sprinkler system. If a water mist system were used, the dimensionless maximum heat release rate should be greater due to the stronger deflection effect of ventilation on the movement of small droplets.

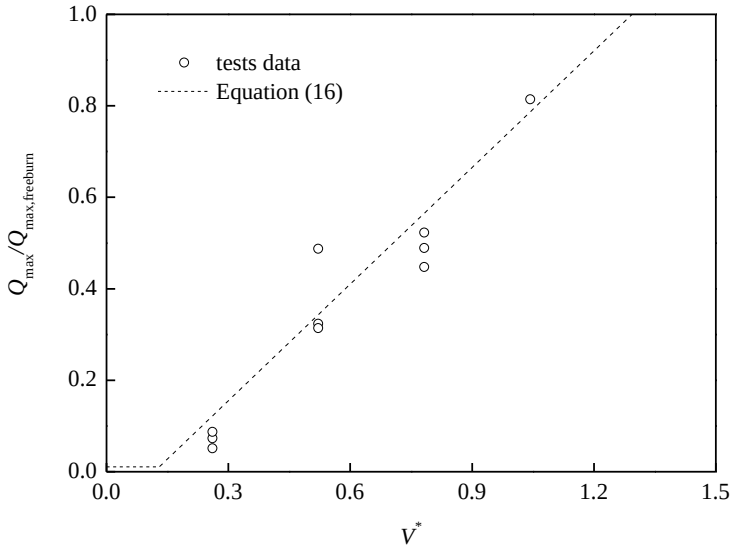

Figure 22 The dimensionless maximum heat release rate in a test with an automatic sprinkler system as a function of the dimensionless longitudinal velocity (Constant Ventilation Strategy, T_L=141^{o}C).

The maximum heat release rates in an automatic sprinkler test with a link temperature of 68 ^{o}C using Constant Ventilation Strategy show the same trend as in Figure 22. However, the correlation was slightly lower than that with a link temperature of 141 ^{o}C. The reason is the faster response of the nozzles with a link temperature of 68 ^{o}C. The maximum heat release rates in an automatic sprinkler test using Variant Ventilation Strategy were significantly lower than that using Constant Ventilation Strategy since the fire could be efficiently suppressed after the ventilation velocity was lowered to 0.5 m/s.

6.3.2 Energy content

The energy content consumed in a test is the integral of the transient heat release rate during the entire test. Therefore there should be a similar trend with regard to the dimensionless longitudinal velocity.

Figure 23 shows the maximum heat release rate in an automatic sprinkler test with a link temperature of 141^{o}C using Constant Ventilation Strategy. A dimensionless energy content consumed in a test, E_{loss}/E_t, has been used to normalize the results. It is shown in Figure 23 that the energy content consumed in a test increases significantly with the dimensionless longitudinal velocity.

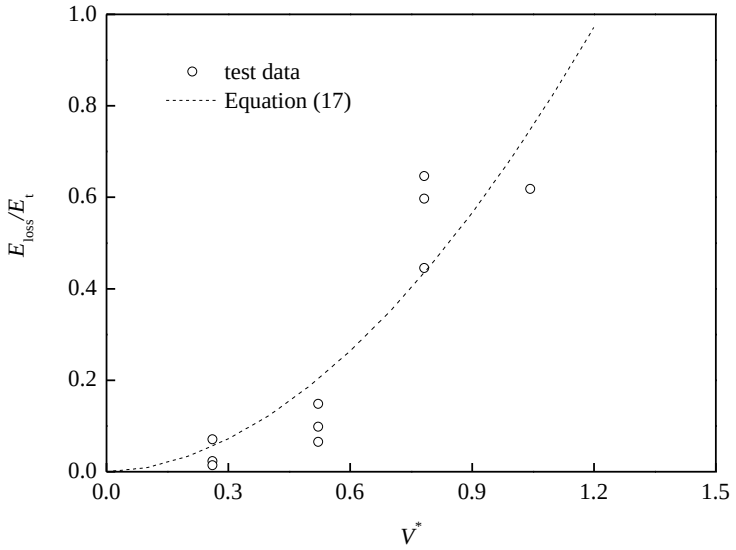

Figure 23 The dimensionless energy content consumed in a test with an automatic sprinkler system as a function of the dimensionless longitudinal velocity (Constant Ventilation Strategy, T_L=141^{o}C).

The correlation in Figure 23 can be expressed as:

$$\frac{E_{loss}}{E_t} = 0.69V^{*1.88} \qquad (17)$$

where E_{loss} is the energy content of the wood crib consumed in a test, and E_t is the initial energy content of the wood crib. This ratio is equivalent to the ratio of mass loss and initial total mass of the wood crib in a test.

A correlation coefficient of 0.9004 was found for Equation (17). Based on Equation (17), the dimensionless longitudinal velocity at which the water spray has no influence on the maximum heat release rate can be estimated to be 1.22. This value correlates well with the former value estimated using Equation (16).

Some effort was made to include the water flow in Equation (17) with a reduction in the correlation. This verifies the consistency in the analysis of the maximum heat release rate and the energy content.

6.4 Collapse of an automatic sprinkler system

For an automatic sprinkler system installed in a tunnel, the key issue is whether this type of system will collapse or not for certain conditions. If too many nozzles are activated, the automatic sprinkler system cannot work properly, which is designated as a system collapse.

Until now there is no valid definition of the collapse of an automatic sprinkler system installed in a tunnel. The main reason is partly that there are so few automatic water sprinkler systems installed worldwide. The numbers of activated nozzles should not be

larger than for a deluge system. Otherwise there is no advantages of installing an automatic sprinkler system in a tunnel rather than a deluge system. In a deluge system installed in a tunnel, one section normally covers a region of about 30 m – 50 m. In some special cases, i.e. when a fire occurs between two sections, all nozzles in the neighboring two sections will be opened. This means that the maximum possible activated nozzles lie in a range of 60 m – 100 m. This value can be used as a reference to determine whether an automatic sprinkler system employed in a tunnel will collapse or not. Therefore the collapse of an automatic sprinkler system installed in a tunnel is defined as an automatic sprinkler system where the activation range is equal or more than 100 m in large scale. In our tests, the furthest bulb was placed 6.5 m downstream of the fire source, which corresponds to 98 m in large scale. Normally the bulbs upstream were not activated. Therefore the furthest bulb at the end of the tunnel is used as a mark of the collapse of an automatic sprinkler system in the tests. This is a conservative definition as there were no nozzles with water close to the bulbs further than 1.6 m downstream of the fire source centre. If that would have been the case, probably less bulbs would have activated.

In an automatic sprinkler system in a tunnel, the fire suppression can be divided into two stages: direct fire suppression and downstream cooling. In the preliminary stage, few nozzles in the vicinity of the fire source are activated at a short time after ignition to efficiently suppress the fire development and cool the hot gases above the fire. In the second stage many nozzles downstream of the fire source are activated to cool the hot gases inside the tunnel. In some cases, a few of the upstream nozzles were also activated after a long time. The direct fire suppression plays the most important role in the suppression or collapse of an automatic sprinkler system in the tunnel.

The main parameters involved in the collapse of an automatic sprinkler system in a tunnel are the ventilation, the water flow rate, the link temperature and the type and arrangement of the fuel. The type and arrangement of the fuel have an influence on the fire growth rate in a ventilated flow, which is directly related to the response time of the bulb. However, a HGV fire mainly consists of solid fuels, i.e. furniture (mainly wood) and plastic, and the wood crib can be used as a typical fuel. Therefore the type and arrangement of the fuel was not analyzed here. Instead the longitudinal ventilation velocity, water flow rate and link temperature were in focus in the tests presented here.

6.4.1 Effect of ventilation

Figure 24 shows the effect of longitudinal ventilation velocity on the range of activated nozzles with different water flow rates. A collapse line, corresponding to a distance of about 100 m at large scale, is also included. A data point lying on this line indicates that the automatic sprinkler system has collapsed. The data point with a water flow rate of 0.38 L/min and ventilation velocity of 1 m/s is estimated by the activation temperature of 206 ^{o}C obtained in Section 6.1.

In Figure 24 it can be observed that the activation range increases significantly with the ventilation velocity. This means that an automatic sprinkler system collapse more readily at a higher ventilation velocity.

Increasing longitudinal ventilation velocity results in a greater deflection. Therefore the position of the maximum temperature moves further downstream. On the other hand, the forced ventilated flow deflects the water spray in the downstream direction. Therefore at a high ventilation velocity, the nozzles above the fire cannot be activated immediately. In other words, the first activated nozzle and the activation range move further downstream as the velocity increases.

According to the analysis of the maximum heat release rate in Section 6.3 (Figure 22), it is known that the maximum heat release rate increases linearly with the ventilation velocity as the dimensionless longitudinal velocity is greater than 0.13 (the dimensionless ventilation velocity is greater than 0.19). This indicates that a higher heat release rate in a high ventilation results in a higher gas temperature. Both the high gas temperature and the high ventilation enhance the heat transfer to the bulbs. As a consequence, the activation range moves further downstream, which results in the collapse of an automatic sprinkler system.

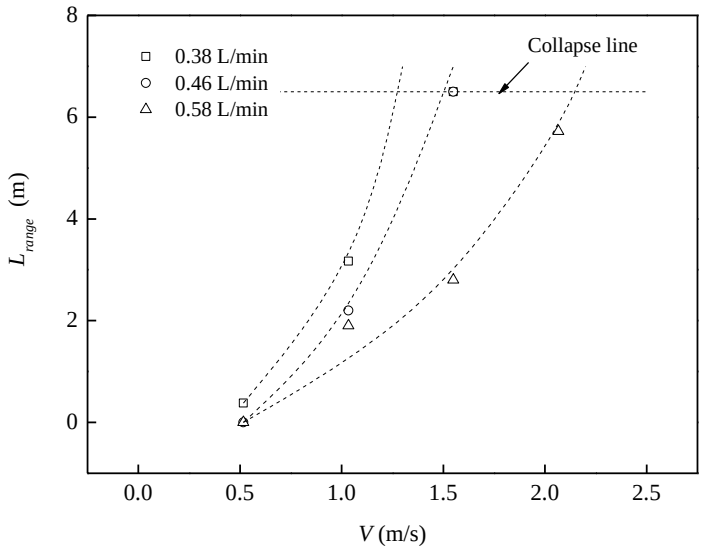

Figure 24 The effect of ventilation velocity on the activation range (T_L=141 ^oC).

6.4.2 Effect of water flow rate

Figure 25 shows the effect of the water flow rate on the activation range in an automatic sprinkler system with a link temperature of 141 ^oC. It clearly shows that the activation range decreases significantly with the water flow rate, especially at higher ventilation.

There may be two reasons for this decrease in the activation range with increasing water flow rate. One is, more efficient suppression of fire development due to activated nozzles close to the fire. The water droplets absorb a large amount of heat from the fire and hot gases, which decreases the heat gain on the burning surface and results in a lower burning rate. The other is, more efficient cooling of hot gases due to activated sprinklers on the downstream side.

However, according to the analysis of the maximum heat release rate in Section 6.2, the tested water flow rates are at such a high level that the fire could be extinguished immediately in a deluge system. Therefore the maximum heat release rate is only dependent on the ventilation velocity under the tested water flow rates. This means that there is no significant difference in the effect of water flow rates at the tested level on the fire development in the tests. In other words, the difference in the effect of water flow rate on the collapse of a system in these tests mainly results from the different effect of cooling the hot gases downstream of the fire.

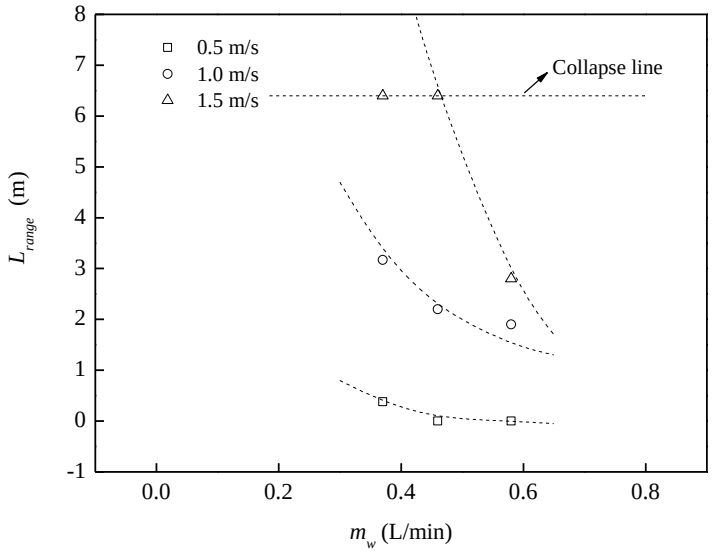

Figure 25 The effect of water flow rate on the activation range (T_L=141 ^oC).

6.4.3 Effect of link temperature

Two types of bulbs with the same RTI and different link temperatures, 68°C and 141°C, were used in the tests. The water flow rate was 0.46 mm/min in tests with a link temperature of 68 °C. Comparing the activation range with different link temperatures and under different ventilation conditions shows that nozzle N3 was activated first and the fire was suppressed immediately when the ventilation velocity was 0.5 m/s. The activation range was found to be 2.2 m and 4.9 m, respectively, for a link temperature of 141 °C and 68 °C when the ventilation velocity was 1.0 m/s. All the bulbs were activated for both link temperatures when the ventilation velocity was 1.5 m/s. When the Variant Ventilation Strategy was applied, the activation range for a link temperature of 141 °C and 68 °C is 5.16 m and 6.36 m, respectively. As a consequence, the system with a link temperature of 68°C was activated more rapidly and thereby suppressed the fire more efficiently. However, it was much easier to obtain a system collapse under high ventilation conditions for the lower link temperature. Therefore the bulb with a link temperature of 68 °C is not recommended for applications in a tunnel. Based on these results the bulb with a link temperature of 141 °C should be a better choice.

6.4.4 Determination of collapse of an automatic spray system

For application of these results to real cases, several dimensionless parameters are defined here:

dimensionless water flow rate: $q_w^* = \dfrac{q_w''}{\sqrt{W}}$

dimensionless activation range: $L'_{range} = \dfrac{L_{range}}{H}$

where W is tunnel width (m), H is tunnel height (m), q_w'' is the water density (mm/min), L_{range} is the activation range (m).

A 3D plot of the dimensionless activation range as a function of the dimensionless longitudinal ventilation velocity and the dimensionless water flow rate is shown in Figure 26. The dimensionless longitudinal velocity is according to Equation (14). It is shown in Figure 26 that the ventilation velocity and the water flow rate have an insignificant influence on the activation range for low ventilation velocities and high water flow rates. However, the water flow rate plays a much more important role in the activation range under higher ventilation velocities and lower water flow rates.

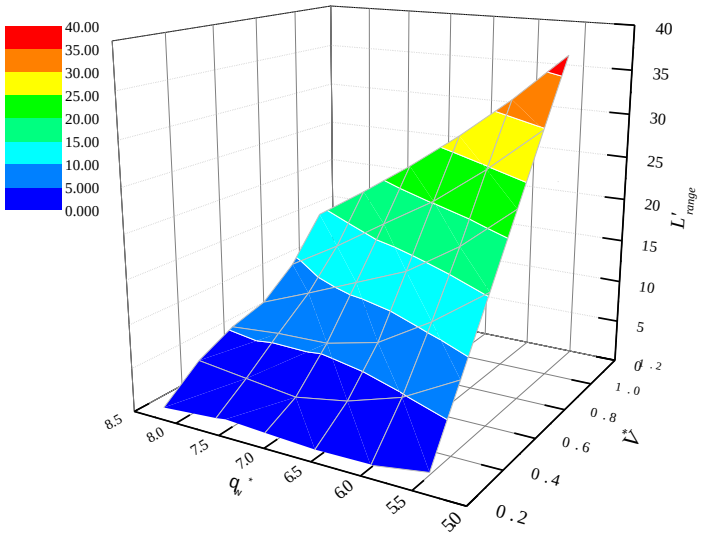

Figure 26 A 3D plot of the dimensionless activation range as a function of the dimensionless longitudinal ventilation velocity and the dimensionless water flow rate (T_L=141 ^oC).

To better illustrate the results, a figure consisting of contour lines is shown in Figure 27. It is clearly shown that the water flow rate has little influence on the activation range when the dimensionless longitudinal velocity is lower than 0.5. However, both the ventilation velocity and the water flow rate play important roles in the activation range under higher ventilation conditions.

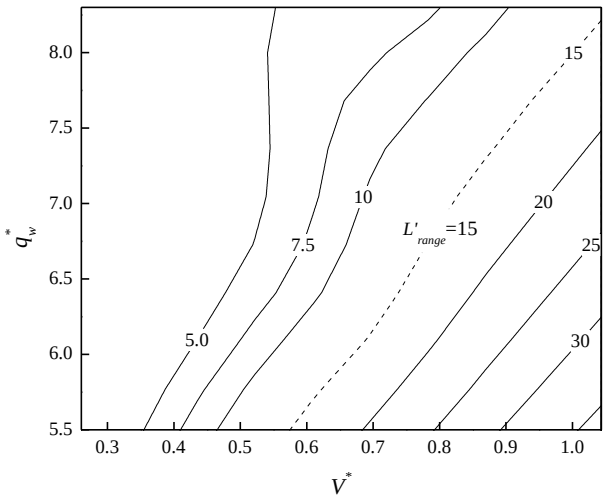

Figure 27 Determination of collapse of an automatic sprinkler system (T_L=141 ^oC).

As discussed previously, the collapse of an automatic sprinkler system can be recognized when the dimensionless activation range is over about 15. The collapse line of $L'_{range} = 15$, as shown in Figure 27, can be approximately expressed as:

$$q''^{*}_{w} = 5.8V^{*} + 2.2 \qquad (18)$$

Equation (18) is valid when the dimensionless water flow rate is in the range of 5.5 to 8.3. From Equation (18), it is shown that under high ventilation conditions, the water flow rate must be increased linearly with the ventilation velocity to prevent collapse of an automatic sprinkler system in a tunnel fire. When using Eq. (18), it should be noted that the unit of the water density q''_w is mm/min but others metric unit.

It should be pointed out that no nozzle was installed further than 1.6 m (4 times tunnel height) downstream of the fire source. Therefore the data presented and the conclusion made here are conservative and only valid within the tested range.

6.5 Variant ventilation strategy

In some tests the ventilation velocity inside the tunnel was decreased from a higher value, i.e. 2 m/s or 1.5 m/s, to 0.5 m/s to optimize the performance of the automatic sprinkler system. This methodology has been called the Variant Ventilation Strategy.

In Table 6 the activation time is compared for the two different ventilations strategies employed. After the first bulb was activated, the other nozzles were activated in a shorter period in tests using Variant Ventilation Strategy and resulted in a more efficient in fire suppression than when a Constant Ventilation Strategy was used.

Comparing the range of activate nozzles with a link temperature of 141 ^{o}C shows a narrower range in tests using Variant Ventilation Strategy. When the ventilation velocity was 6 m/s, all the bulbs were activated in tests using a Constant Ventilation Strategy and a water flow rate of 0.38 L/min or 0.46 L/min, while the activation range was 5.16 m in tests using a Variant Ventilation Strategy. Under the same initial ventilation velocities, the activation range was 5.72 m for the Constant Ventilation Strategy and 4.3 m for the Variant Ventilation Strategy.

Comparing the range of activate nozzles with a link temperature of 68 ^{o}C also shows a narrower range in tests using the Variant Ventilation Strategy. All the bulbs were activated in tests using the Constant Ventilation Strategy, while all but the final bulb were activated using the Variant Ventilation Strategy.

Thus, the Variant Ventilation Strategy can effectively suppress the collapse of an automatic system in a tunnel fire.

Comparing the heat release rate and the ceiling temperature in Table 5, it is seen that using the Variant Ventilation Strategy can effectively reduce the maximum heat release rate, however, the maximum gas temperatures obtained were slightly higher than those measured when using the Constant Ventilation Strategy. This indicates that a decreased ventilation velocity induces a higher ceiling temperature, despite the fact that the fire development is suppressed efficiently and the maximum heat release rate is lower.

6.6 Special control strategy

The Normal Control Strategy is to activate a nozzle if the bulb close to the nozzle is activated. In a tunnel fire, the strong forced ventilation significantly deflects the fire plume, which induces a distance of about one to two times the tunnel height for the position of the maximum ceiling temperature, and also deflects water droplet towards the downstream. In test 21 a Special Control Strategy was used to optimize the performance of the automatic sprinkler system. The Special Control Strategy entailed the activation of a nozzle if the bulb installed 0.6 m downstream of the nozzle is activated. For example, Nozzle N1 was forced to activate if Bulb B3 is automatically activated, see Figure 7.

Note that the only difference between Test 20 and Test 21 was the control strategy for nozzles. In Test 20 the nozzles, i.e. N4 – N18, were activated in a period of 1.3 min to 1.8 min after ignition, while only N3 was activated in Test 21 using the Special Control Strategy. The maximum heat release rate was 199.5 kW and 64.6 kW, and the maximum ceiling gas temperature was 767 ^{o}C and 411 ^{o}C, in Test 20 and Test 21 respectively. It can be seen that using the Special Control Strategy for nozzles can efficiently suppress the fire development, reduces the gas temperature and suppress the collapse of an automatic sprinkler system in a tunnel fire.

A Special Control Strategy could also be to activate a nozzle if the bulb installed 0.3 m downstream of the nozzle is activated. This should also be effective in an automatic sprinkler system. Note that the ventilation velocity in Test 21 is 2 m/s, corresponding to 8 m/s in large scale.

The main uncertainty associated with such Special Control Strategies is whether such systems will work if the ventilation velocity is very low. If we assume that the ventilation velocity is zero in a tunnel with an automatic sprinkler system using the Special Control Strategy (0.6 m). Therefore the fire is symmetrical to the fire source. At the beginning the bulb above the fire is activated. At this point the nozzle 0.6 m on the left-hand side will be activated at the same time according to the Special Control Strategy. However, the activated nozzle may be too far away from the fire and cannot suppress the fire growth. Therefore the fire continues to develop until both bulbs 0.3 m away from the fire are activated. The broken bulbs will activate the nozzles 0.3 m and 0.9 m on the left-hand side. The fire may be suppressed, or it will continue to develop until both bulbs 0.6 m away from the fire are activated. The broken bulbs will activate the nozzle right above the fire and 1.2 m on the left-hand side. At this point the fire should be suppressed, or all the nozzles close to the fire will be activated, just like a deluge system. Therefore the Special Control Strategy should still work even when the ventilation velocity inside the tunnel is very low or very high, although it has not been verified. Large-scale tunnel fire tests are required for further verification.

6.7 Deluge system

In Tests 22 to 24, the deluge system was tested. The water flux was 0.38 L/min (15 L/min in large scale). The main parameter considered was the ventilation velocity. The effect of ventilation on the water spray can be ignored due to the entire movement of the water spray. However, the ventilation has an influence on the fire development by increasing the fire growth rate.

According to Table 5, the maximum heat release rates were 19.6 kW, 38.3 kW and 34.7 kW in Test 22, 23 and 24, respectively. The maximum heat release rate in Test 24 with a ventilation velocity of 1.5 m/s was lower than in Test 23 with a ventilation velocity

of 1.0 m/s. The reason is that the higher ventilation suppressed the fire development at the ignition stage, while the activation time in these tests was of the same, 75 s (4.84 min in large scale).

In each test the fire was suppressed efficiently after the deluge system was activated. This means a water flux of 0.38 L/min is great enough to extinguish such a tunnel fire.

6.8 Fire spread

In the tests with the automatic water sprinkler system and the deluge system, the free distance between the two wood cribs was 1.05 m, corresponding to 15.75 m in large scale. After each test the second wood crib was inspected and not found to be charred. This means the automatic water sprinkler system and the deluge system using the tested water flux were able to prevent the fire spread between vehicles with such a free distance. This can also be concluded from the ceiling temperature above the upstream edge of the second wood crib (T8). According to previous research on the fire spread, the ceiling temperature above the upstream edge of the wood crib should be higher than a value of about 600 ^{o}C [26]. In Test 1 to 27, the measured maximum temperatures by the thermocouple T8 was in a range of 84.6 – 304.6 ^{o}C, much lower than 600 ^{o}C. This may explain why the water spray was readily able to suppress the fire spread.

In free-burn tests 25 to 27, the free distance between the two wood cribs was 1.05 m. After each test the second wood crib was inspected. The top surfaces of the second wood crib in Test 25 and 26 were charred obviously but not in Test 27. This may show some effect of ventilation on the flame length, since in Test 27 the ventilation velocity was 1.5 m/s higher than others, although our former research tells us that there is only a limited effect of ventilation on the flame length in a large tunnel fire. The ceiling temperature above the edge of the second wood crib was in the range of 427 ^{o}C to 529 ^{o}C, i.e. less than 600 ^{o}C. Since in tests 25 to 27 no fire spread was observed, the free distance between the first two wood cribs was adjusted to be 0.6 m, corresponding to 9 m in large scale, in Test 28. In about 3 minutes after ignition in Test 28, the second wood crib began to burn from the top to the bottom. The ceiling temperature above the second wood crib was in a range of 500 ^{o}C (registered at T8) to 800 ^{o}C (registered at T7).

The results confirm the condition for the fire spread to the second wood crib that the ceiling temperature above the second wood crib should be higher than about 600 ^{o}C to promote ignition.

6.9 Practical application

High ventilation enhances the fire development, thus potentially results in collapse of an automatic sprinkler system. An automatic sprinkler system should be used in a tunnel with a low ventilation velocity or natural ventilation.

Therefore, it is recommended that an automatic sprinkler system can be used in a tunnel with transverse ventilation system or a bi-directional tunnel since the longitudinal ventilation velocity is relatively low in these tunnels.

In contrast an automatic sprinkler system is not recommended for use in a longitudinally ventilated tunnel with a high longitudinal ventilation velocity, unless either the Variant Ventilation Strategy or the Special Control Strategy are applied in the tunnel system.

7 Conclusions

A total of 28 tests were carried out in a 1:15 model scale tunnel with an automatic sprinkler system. The main focus of these tests was the performance of an automatic sprinkler system in a tunnel fire under different ventilation conditions. The activation of the nozzles, the maximum heat release rate, energy content and the collapse of an automatic sprinkler system were analyzed.

In an automatic sprinkler system in a tunnel, the fire suppression can be divided into two modes: fire suppression through surface and gas cooling and downstream gas cooling. In the preliminary stage of a fire, few nozzles in the vicinity of the fire source are activated a short time after ignition to efficiently suppress the fire development and cool the hot gases above the fire. The nozzles activated at this stage play the most important role in the fire development. In the second stage many nozzles downstream of the fire are activated to cool down the hot gases inside the tunnel. However, in some cases with low velocities, some of the upstream nozzles were also activated after a long time due to slower flame spread towards the upstream edge of the wood crib.

High ventilation and low water flow rates can result in the collapse of an automatic sprinkler system in a tunnel fire. Note that the tested water flow rate for a single nozzle was 0.38 L/min, 0.46 L/min and 0.58 L/min, corresponding to 16.5 mm/min, 20 mm/min and 25 mm/min at full scale, respectively. The results show that the longitudinal ventilation plays the most important role in the collapse of a system by stimulating the fire development, i.e. the maximum heat release rate and the fire growth rate under the tested water flow rates. The different tested water flow rates do not show any obvious effect on the fire development, although, the downstream nozzles with higher water flow rate cool the hot gases more efficiently to prevent the collapse of the system. It can be concluded that the most important parameter for an automatic sprinkler system under the tested water flow rates in a tunnel fire was the ventilation velocity rather than the water flow rate. The fire development was intimately related to the ventilation velocity, and almost independent of the water flow rate under such conditions. The maximum heat release rate in an automatic sprinkler system was found to increase linearly with the ventilation velocity. The energy content consumed in a test was found to increase more significantly with the ventilation velocity than the heat release rate.

The activation heat release rate (AHRR) of the first activated nozzle was found to increase linearly with the ventilation velocity. Similarly, the location of the first activated nozzle relied mainly on the ventilation velocity and could be predicted using Equations (14) and (15). The other nozzles in the measured region were activated in a short time, i.e. in a range of 0 – 0.6 min, after the first nozzle was activated.

To improve the performance of an automatic sprinkler system in a tunnel fire, special strategies were tested. It is shown that either using the Variant Ventilation Strategy or the Special Control Strategy effectively suppressed the fire development and prevented the collapse of an automatic system in a tunnel fire.

Both the automatic sprinkler system and the deluge system were found to efficiently suppress the fire spread to the neighbouring wood crib.

Note that no nozzle was placed further than 1.6 m (4 times tunnel height) downstream of the fire source. The cooling effects were therefore underestimated in some of the tests. The presented data concerning the activation range and the conclusions drawn here are therefore conservative. In addition, the configuration of the wood cribs was found to play an important role in the extinguishment of a solid fire.

One should also note that while the ventilated flow inside the tunnel, the fire power and the fuel can be scaled adequately, it is difficult to ensure that the process of extinguishment was scaled equally well. However, it can be postulated that the discussed variables have been scaled appropriately and the trends shown in the analyses corroborate the scaling methodology used. In any case, large scale tests are required for further verification of these results.

8 References

1. Rasbash D.J., *The extinction of fires by water sprays*, Fire Research Abstracts and Reviews, 1962, 4, 28.
2. Rasbash D.J., Rogowski Z.W. and Stark G.W.V., Mechanisms of extinction of liquid fires with water sprays. Combustion and Flame, 1960, 4, 223.
3. Kung H.C., Hill J.P., Extinction of wood crib and pallet fires, Combust and Flame 1975, 24, 305 – 317.
4. Heskestad G. The role of water in suppression of fire: a review. Journal of Fire & Flammability, 11, 254-262.
5. Heskestad G. Preliminary technical report-model study. Factory Mutual Research. Norwood, Massa-chusetts, 1972.
6. Heskestad G. Scaling the interaction of water sprays and flames. Fire Safety Journal. 2002, 37, 535-548.
7. Heskestad G. Extinction of gas and liquid pool fires with water sprays. Fire Safety Journal. 2003, 38, 301-317.
8. Yu H.Z., Kung H.C., Han Z.X., Spray cooling in room fires. Technical Report. Factory Mutual Research. Norwood, Massa-chusetts, 1986.
9. Yu H.Z., Lee J.L., and Kung H.C., Suppression of Rack-Storage Fires by Water. In: Proceedings of the Fourth International Symposium, International Association For Fire Safety Science, 1994, pp. 901–912.
10. Grant G., Brenton J., Drysdale D., Fire suppression by water sprays, Prog. Energy Combust. Sci., 2000. 26, 79–130.
11. Xin Y.B., Tamanini F., Assessment of commodity classification for sprinkler protection using representative fuels. In: Proceedings of the ninth International Symposium, International Association For Fire Safety Science, 1994, pp. 901–912.
12. Heskestad G., Quantification of thermal responsiveness of automatic sprinklers including conduction effects. Fire Safety Journal, 1988, 14, 113-125.
13. Ruffino P. and Di Marzo M., Temperature and Volumetric Fraction Measurements in a Hot Gas Laden with Water Droplets. Journal of Heat Transfer, 2003, 125(2), 356–364
14. Ruffino P. and Di Marzo M., The Effect of Evaporative Cooling on the Activation Time of Fire Sprinklers. In: Proceedings of the Seventh International Symposium, pages 481–492. International Association for Fire Safety Science, 2002. 75
15. Gavelli F., Ruffino P., Anderson G., and Di Marzo M., Effect of Minute Water Droplets on a Simulated Sprinkler Link Thermal Response. NIST GCR 99-776, National Institute of Standards and Technology, Gaithersburg, Maryland, July 1999.
16. De Ris J.L., Ditch B., Yu H.Z., The skip-resistant sprinkler concept – theoretical evaluation. Journal of Fire Protection Engineering, 2009, 19, 275-289.
17. Ditch B., De Ris J.L., Yu H.Z., The skip-resistant sprinkler concept – An experimental evaluation. Journal of Fire Protection Engineering, 2009, 19, 291-308.
18. Ingason H., Model scale tunnel tests with water spray, Fire Safety Journal, 2008, 43, 512-528.
19. Ingason H. Fire testing in road and railway tunnels. In: Flammability testing of materials used in construction, transport and mining (Apte V. B., Editor), Woodhead Publishing and CRC Press. 2006, pp. 231-274.
20. Heskestad G., Modeling of Enclosure Fires, In: Proceedings of the Fourteenth Symposium on Combustion, The Combustion Institute, Pennsylvania, 1972, pp.1021-1030.

21. Quintiere J. G., Scaling Applications in Fire Research, Fire Safety Journal, 1989, 15, 3-29.
22. Heskestad G., Physical Modeling of Fire, Journal of Fire & Flammability, 1975, 6, 253-273.
23. Heskestad G. Scaling the interaction of water sprays and flames, Fire Safety Journal, 2002, 37, 535-548.
24. Heskestad G. Extinction of gas and liquid pool fires with water spray. 2003, 38, 301-317
25. Yu H.Z., Zhou X.Y., Ditch B.D., Experimental validation of Froude-modeling-based physical scaling of water mist cooling of enclosure fires. In: Proceedings of the ninth international sysposium, the International Assocation for Fire Safety Science, 2008, pp. 553-564.
26. Ingason H., Li Y.Z., Model scale tunnel fire tests with longitudinal ventilation. Fire Safety Journal, 2010, 45(6-8): 371-384.
27. Li Y.Z., Lei B., and Ingason H., Study of critical velocity and backlayering length in longitudinally ventilated tunnel fires, Fire Safety Journal, 2010, 45(6-8): 361-370.
28. Ingason H., Li Y.Z., Model scale tunnel fire tests with extraction ventilation. Journal of Fire Protection Engineering, 2011, 21(1): 5-36.
29. Li Y.Z., Lei B., Ingason H., The maximum temperature of buoyancy-driven smoke flow beneath the ceiling in tunnel fires, Fire Safety Journal, 2011, 46: 204-210.
30. Li Y.Z., Ingason H., Maximum ceiling temperature in a tunnel fire, SP Swedish National Testing and Research Institute SP Report 2010:51, Borås, Sweden, 2010.
31. Li Y.Z., Ingason H., The maximum ceiling temperature in a large tunnel fire. Fire Safety Journal, 2011. (Submitted)
32. Saito N., Yamada T., Sekizawa A., Yanai E., Watanabe Y., Miyazaki S., Experimental Study on Fire Behavior in a Wind Tunnel with a Reduced Scale Model, In: Second International Conference on Safety in Road and Rail Tunnels, Granada, Spain, 1995, 3-6 April, pp. 303-310,
33. Vantelon, J. P., Guelzim, A., Quach, D., Son, D., K., Gabay, D., and Dallest, D., Investigation of Fire-Induced Smoke Movement in Tunnels and Stations: An Application to the Paris Metro, In: Proceedings of the third international symposium, pp. 907-918, Edinburg, 1991.
34. Vauquelin, O. and Mégret, O., Smoke extraction experiments in case of fire in a tunnel. Fire Safety Journal, 2002, 37, 525-533.
35. Vauquelin, O. and Telle, D., Definition and experimental evaluation of the smoke "confinement velocity" in tunnel fires. Fire Safety Journal, 2005. 40, 320-330.
36. Ingason H., Model scale tunnel fire tests with longitudinal ventilation, SP Swedish National Testing and Research Institute, SP REPORT 2005:49, Borås, Sweden, 2005.
37. Wickström, U., The Plate Thermometer - A simple Instrument for Reaching Harmonized Fire Resistance Rests, SP Swedish National Testing and Research Institute SP Report 1989:03, Borås, Sweden, 1989.
38. Häggkvist, A., The plate thermometer as a mean of calculating incident heat radiation - a practical and theoretical study, Master thesis, Luleå University of Technology, 2009.
39. McCaffrey B.J., Heskestad G., Brief Communications: A Robust Bidirectional Low-Velocity Probe for Flame and Fire Application. Combustion and Flame, 1976, 26, 125-127.
40. Janssens M., Parker W.J., Oxygen Consumption Calorimetry, in: Heat Release in Fires (V. Babrauskas and T.J. Grayson, Editors), 1995, E & FN Spon: London, UK. pp. 31-59.

41. Ingason, H., Fire Dynamics in Tunnels, in: The Handbook of Tunnel Fire Safety (R.O. Carvel and A.N. Beard, Editors). Thomas Telford Publishing, London. 2005, pp. 231-266.
42. Newman, J.S., Experimental Evaluation of Fire-Induced Stratification, Combustion and Flame, 1984, 57, 33-39.
43. Ingason H., Correlation between temperatures and oxygen measurements in a tunnel flow, Fire Safety Journal, 2007, 42:75-80.
44. Hermann S., Boundary-layer theory (6th edition). McGraw hill. New York. 1987. p. 596-600.

Appendix A Response time of the sprinkler

Normally an automatic water sprinkler is activated after a bulb installed in the sprinkler breaks up. The bulb (element) is a cylinder with a diameter of 1.5 mm to 5 mm, which can be assumed to be thermally thin. This means that the element inside is isothermal. The governing equation for heat balance of the element can be expressed as [12-15]:

$$\frac{dT_e}{dt} = RTI^{-1}u^{1/2}(T_g - T_e) - C \cdot RTI^{-1}(T_e - T_m) - C_2 \cdot RTI^{-1}\beta u \qquad (A1)$$

where C-Factor, *C*, and Response Time Index of the bulb, RTI, is respectively defined as:

$$C = \frac{C'RTI}{mc_b}, \qquad \mathrm{RTI} = \frac{mc_b}{hA}u^{1/2}$$

Here T_e is the link temperature, T_g is the gas temperature close to the element, T_m is the temperature of the sprinkler mount (assumed ambient), and β is the volume fraction of (liquid) water in the gas stream. The RTI and C-Factor are determined experimentally. The constant C_2 has been empirically determined by DiMarzo et al. to be 6×10^6 K/(m/s)$^{1/2}$ [13-15], and its value is relatively constant for different types of sprinklers. Note that C_2 is a constant but C is not.

Equation (A1) are normalized with a characteristic temperature, T_o, and a characteristic time, t_o. Therefore it can be transformed into:

$$\frac{d\hat{T}_e}{d\hat{t}} = RTI^{-1}u^{1/2}t_o(\hat{T}_g - \hat{T}_e) - C \cdot RTI^{-1}t_o(\hat{T}_e - \hat{T}_m) - C_2 \cdot RTI^{-1}ut_o\beta T_o^{-1} \qquad (A2)$$

Assuming that *T* and β are the same in both scales and ignore the hollow zone when calculating mass of the element, the following dimensionless terms that should be preserved are:

$$\mathrm{SP1} = RTI^{-1}u^{1/2}t_o = \frac{hAt_o}{mc_b} = \frac{t_o}{\tau} \qquad (A3)$$

$$\mathrm{SP2} = \frac{t_o}{mc_b} \qquad (A4)$$

$$\mathrm{SP3} = RTI^{-1}ut_o \qquad (A5)$$

The three terms SP1, SP2 and SP3 correspond to the three terms on the right-hand side of Eq. (A2), respectively. This means that SP1, SP2 and SP3corresponds to the convective heat transfer term, the heat conduction loss term, and the term that accounts for the cooling of the link by water droplets in the gas flow from upstream activated sprinklers.

According to SP1, RTI should be scaled as:

$$\frac{\mathrm{RTI}_M}{\mathrm{RTI}_F} = \left(\frac{l_M}{l_F}\right)^{3/4} \qquad (A6)$$

According to SP2, RTI should be scaled as:

$$\frac{\mathrm{RTI}_M}{\mathrm{RTI}_F} = (\frac{l_M}{l_F})^{-1} \qquad (A7)$$

According to SP3, RTI should be scaled as:

$$\frac{\mathrm{RTI}_M}{\mathrm{RTI}_F} = (\frac{l_M}{l_F})^{1} \qquad (A8)$$

Comparing Equation (A6), Equation (A7) and Equation (A8) shows a self-contradiction between them. Note that the scales are close to each other according to SP1 and SP3, and the heat transfer dominates the heat balance of the element. Here SP2 is ignored and SP1 is conserved only. In a conclusion, RTI should be scaled as:

$$\frac{\mathrm{RTI}_M}{\mathrm{RTI}_F} = (\frac{l_M}{l_F})^{3/4} \qquad (A9)$$

It is normally impossible to get a very small automatic nozzle. Here two methods are considered to scale RTI. Firstly, we can use a small cylinder with a specific material and diameter which fulfills the condition discussed later. Note that a typical sensing element can be seen as a circular cylinder. Due to the Reynold Number in a range of 40 to 4000, the convective heat transfer coefficient can be approximately expressed as:

$$h = \frac{\lambda Nu}{d} = \frac{\lambda}{d} C_k \,\mathrm{Pr}^{1/3}\,\mathrm{Re}^{1/2} = C_k \,\mathrm{Pr}^{1/3} \frac{\lambda}{d} (\frac{ud}{v})^{1/2} = C_k \,\mathrm{Pr}^{1/3} \frac{\lambda}{v^{1/2}} \frac{u^{1/2}}{d^{1/2}} \qquad (A10)$$

Therefore

$$\mathrm{RTI} = \frac{mc_b u^{1/2}}{hA} = \frac{v^{1/2}}{4C_k \,\mathrm{Pr}^{1/3}\,\lambda} \rho_b c_b d_b^{3/2} \qquad (A11)$$

Combining Equation (A9) and Equation (A11) gets:

$$\frac{\rho_M d_M^{3/2} c_{b,M}}{\rho_F d_F^{3/2} c_{b,F}} = (\frac{l_M}{l_F})^{3/4} \qquad (A12)$$

If a small cylinder can fulfill the above condition, the RTI of the element is scaled properly. The problem is that the element in model scale is generally so small that makes it impossible to produce it.

Another way of scaling RTI is using a commercial bulb with a small RTI. In the series of tests, this method was used. Two bulbs with a RTI of 14, corresponding to 107 in full scale were used in the tests, according to Eq. (A9).

Appendix B Flow distribution of sprinkler system

A water spray system consists of water supply system or a water tank, pump, pipe and nozzles. A diagram of distribution of water flow rate in a system with two nozzles is shown in Figure B1.

The controlling Equation for the water flow can be expressed:

$$\Delta P = SQ_w^2 \qquad (B1)$$

For one nozzle opened, Equation (24) can be expressed as:

$$\Delta P_1 = S_1 Q_{w,1}^2 \qquad (B2)$$

Whereas for several nozzles (N) opened, Equation (24) can be expressed as:

$$\Delta P_N = S_N Q_{w,N}^2 \qquad (B3)$$

where ΔP is the pressure loss, S is the total flow resistance and Q_w is the total water flow rate, the subscript "1" indicates a system with one nozzle opened, and "N" means a system with N nozzles opened ($N \geq 1$).

Note that dominating pressure loss in the pipe occurs close to the nozzle, the ratio of flow resistance for one nozzle system and several nozzles system can be expressed:

$$\frac{S_1}{S_N} = N^2 \qquad (B4)$$

where N is equal to or greater than 1.

The impulse of a pump decreases with the increasing water flow rate, as shown in Figure B1. Therefore

$$\Delta P_1 \geq \Delta P_N \qquad (B5)$$

Combing Equations (B2) to (B5) gives:

$$\frac{Q_{w,N}}{Q_{w,1}} \leq N \quad \text{or} \quad \frac{Q_{w,N}}{N} \leq Q_{w,1} \qquad (B6)$$

This means that the flow rate per nozzle is lower in a system with several nozzles opened than one nozzle due to the decrease of impulse of the pump. The difference in the flow rate per nozzle is intimately related to the pump performance curve.

If the pump performance curve in Figure B1 tends to be parallel to the horizontal line, or the tank used in model scale tests was large enough or a special measure was used, the supplied pressure could be approximately kept as a constant, as shown in Figure B2. Equation (B6) can be transformed into:

$$\frac{Q_{w,N}}{N} \approx Q_{w,1} \qquad (B7)$$

This means that the water flow rate per nozzle in a system with several nozzles opened is the same as one nozzle system. Therefore the water flow rate of each nozzle can be estimated if the total water flow rate is known. In the model scale tests, a large tank, in which the pressure was kept as a constant according to the pressure transducer and the valves, was used in the model scale tests.

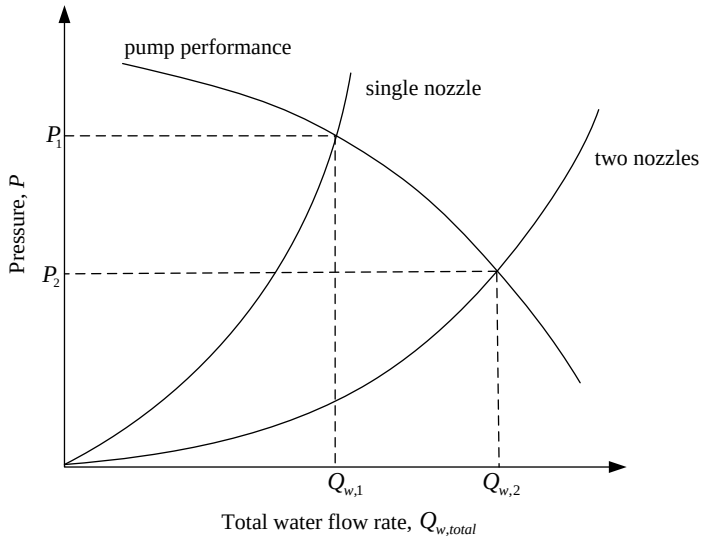

Figure B1 A diagram of distribution of water flow rate in a system with two nozzles.

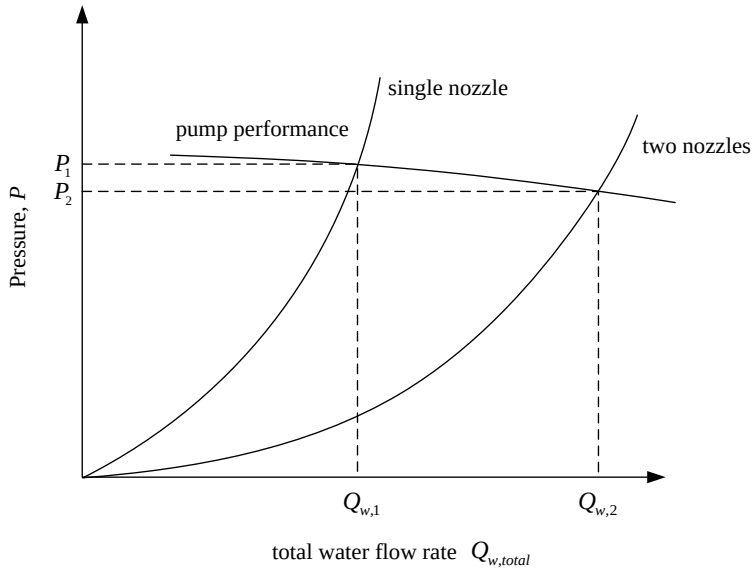

Figure B2 A diagram of distribution of pipe water flow rate in a system with two nozzles (operating pressure close to constant).

Appendix C Determination of heat release rate

Two methods were used to calculate the heat release rate in the tests: by measuring the fuel mass loss rate and by oxygen consumption technique [40-41].

The heat release rate, Q (kW), which is directly proportional to the fuel mass loss rate, $\dot{m}_f$ (kg/s), can be calculated using the following equation:

$$Q = \dot{m}_f \chi H_T \qquad (C1)$$

where H_T is the net heat of complete combustion (kJ/kg). The fuel mass loss rate, $\dot{m}_f$, is determined by the weight loss. In fires the combustion of fuel vapours is never complete, and thus the effective heat of combustion (H_c) is always less than the net heat of complete combustion (H_T). Further, χ, is the ratio of the effective heat of combustion to net heat of complete combustion, i.e., $\chi = H_c / H_T$.

The actual heat release rate, Q (kW), at a measuring point can be obtained by the use of the following equation (without correction due to CO production) using oxygen consumption calorimetry [40-41].

$$Q = 14330 \dot{m}_a \left(\frac{X_{0,O_2}(1 - X_{CO_2}) - X_{O_2}(1 - X_{0,CO_2})}{1 - X_{O_2} - X_{CO_2}} \right) \qquad (C2)$$

where X_{0,O_2} is the volume fraction of oxygen in the incoming air (ambient) or 0.2095 and X_{0,CO_2} is the volume fraction of carbon dioxide measured in the incoming air or $X_{0,CO_2} \approx 0.00033$. X_{O_2} and X_{CO_2} are the average volume fractions of oxygen and carbon dioxide downstream of the fire or in the extraction duct.

If X_{CO_2} has not been measured equation (C2) can be used by assuming X_{CO_2} =0. This will simplify equation (C2) and usually the error will not be greater that 10 % for most fuel controlled fires. In the derivation of equation (C2) it is assumed that $\dot{m}_a = \rho_o VA$ and that 13100 kJ/kg is released per kg of oxygen consumed. It is also assumed that the relative humidity (RH) of incoming air is 50%, the ambient temperature is 15°C, CO_2 in incoming air is 330 ppm (0.033 %) and the molecular weight of air, M_a, is 0.02895 kg/mol and 0.032 kg/mol for oxygen (M_{O2}). Further, ρ_a is the ambient air density, u is the ventilation velocity upstream the fire in m/s and A is the cross-sectional area of the tunnel in m^2 at the same location as the ventilation velocity is measured.

Due to the similarity of vertical distribution between gas concentration and gas temperature in a tunnel fire, the average gas concentration inside tunnel can be calculated by [42][43]:

$$\Delta X_{avg,i} = \Delta X_i \frac{\Delta T_{avg}}{\Delta T} \qquad (C3)$$

where the ith average gas concentration $\Delta X_{avg,i}$ ($\Delta X_{avg,i} = X_{avg,i} - X_{0,i}$), the ith gas concentration ΔX_i ($\Delta X_i = X_i - X_{0,i}$) at a given height, the average gas temperature in one cross-section ΔT_{avg} and the excess gas temperature ΔT at a given height. Note that ΔX_i and ΔT should be measured at the same height. The validity of this equation in ventilated tunnel fires has been investigated by Ingason [43].

The total air mass flow rate, $\dot{m}$, inside the tunnel (and in the exhaust duct) can be determined both on the upstream ($\dot{m}_{us}$) and downstream side ($\dot{m}_{ds}$), based on the measured centre line velocity, u_c. The general equation for the air mass flow rate is:

$$\dot{m} = \zeta \frac{T_0 \rho_0}{T} u_c A \qquad (C4)$$

Actually the average ventilation velocity can be expressed as $V = \xi u_c$ in most cases for the temperature at the measurement point equals to the ambient temperature. The theoretically determined mass flow correction factor (ratio of mean to maximum velocity), ζ, is dependent on the temperature and velocity over the cross-section of the the exhaust duct or the tunnel. In the calculations of the air mass flow rates, a theoretical value of ζ =0.817 was used [44].

The gas velocity was determined with aid of the measured pressure difference, Δp, for each bi-directional probe [39] and the corresponding gas temperature. The diameter of the probes, D, used was 16 mm and the probe length, L, was 32 mm. The velocity was obtained from the following equation:

$$u_c = \frac{1}{k} \sqrt{\frac{2 \Delta p T}{\rho_0 T_0}} \qquad (C5)$$

where k was a calibration coefficient equal to 1.08. The ambient values used in equation (C5) were T_0 = 293 K and ρ_0 =1.2 kg/m^3.

Appendix D Test Results – Automatic Sprinkler

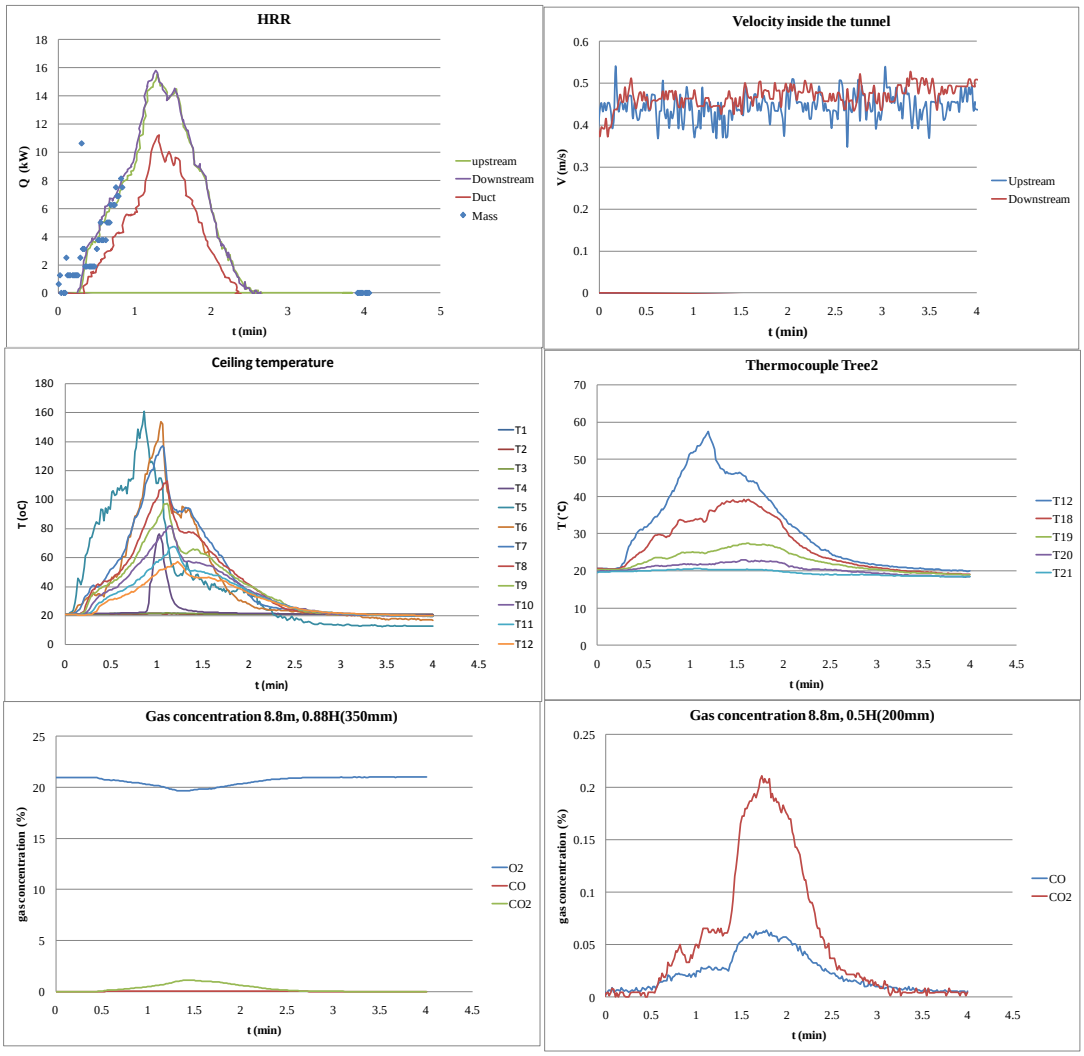

Figure D1 Measured heat release rate, velocity, temperature and gas concentrations in Test 1.

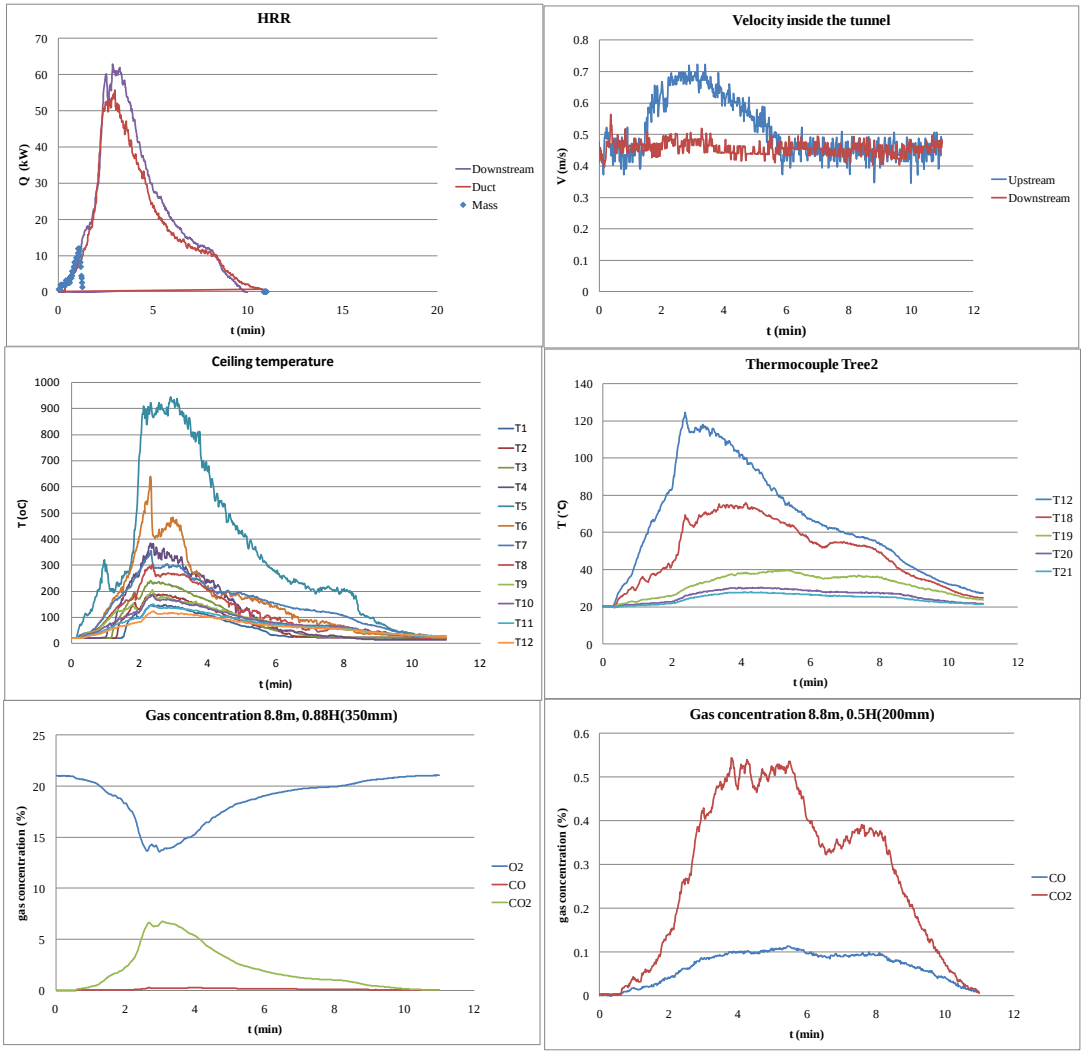

Figure D2 Measured heat release rate, velocity, temperature and gas concentrations in Test 2.

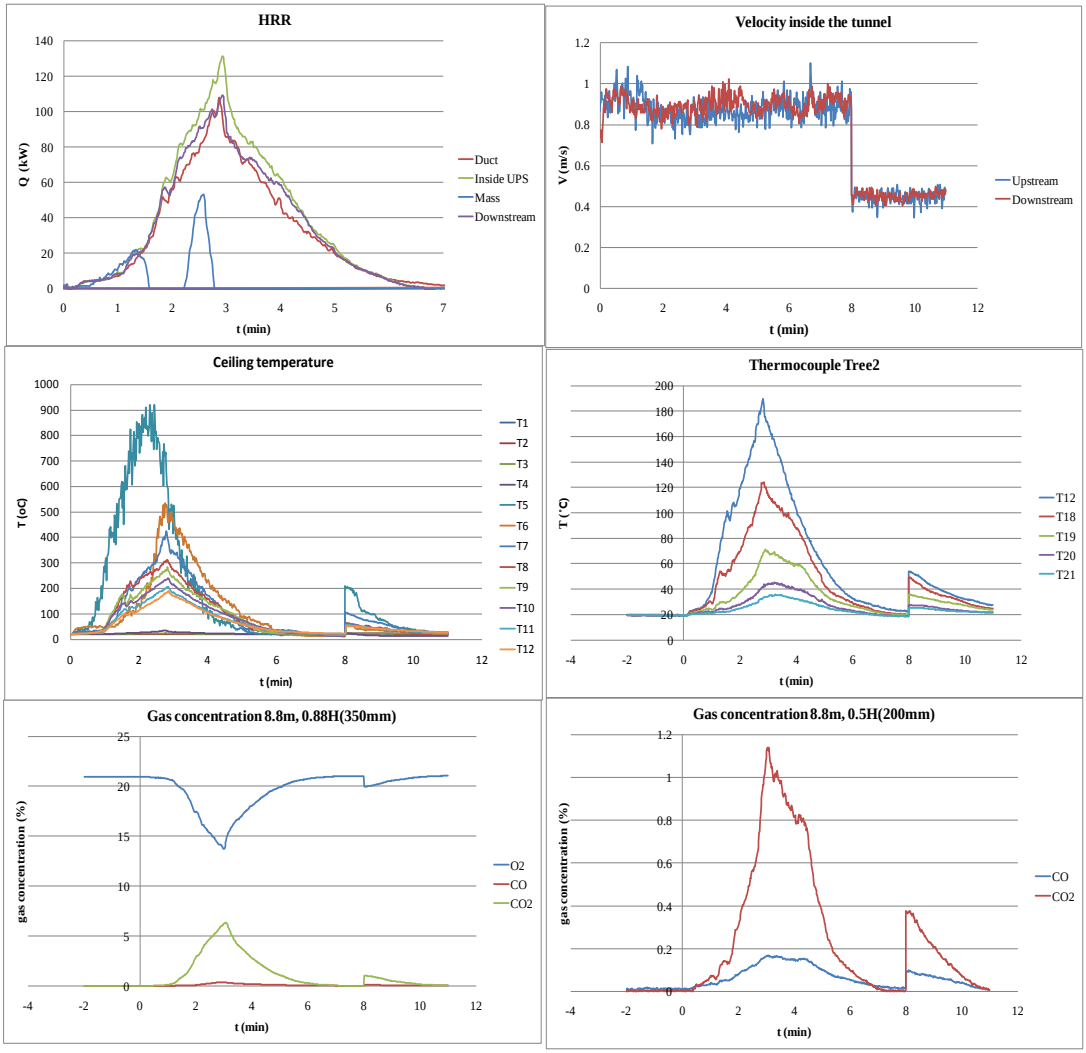

Figure D3 Measured heat release rate, velocity, temperature and gas concentrations in Test 3.

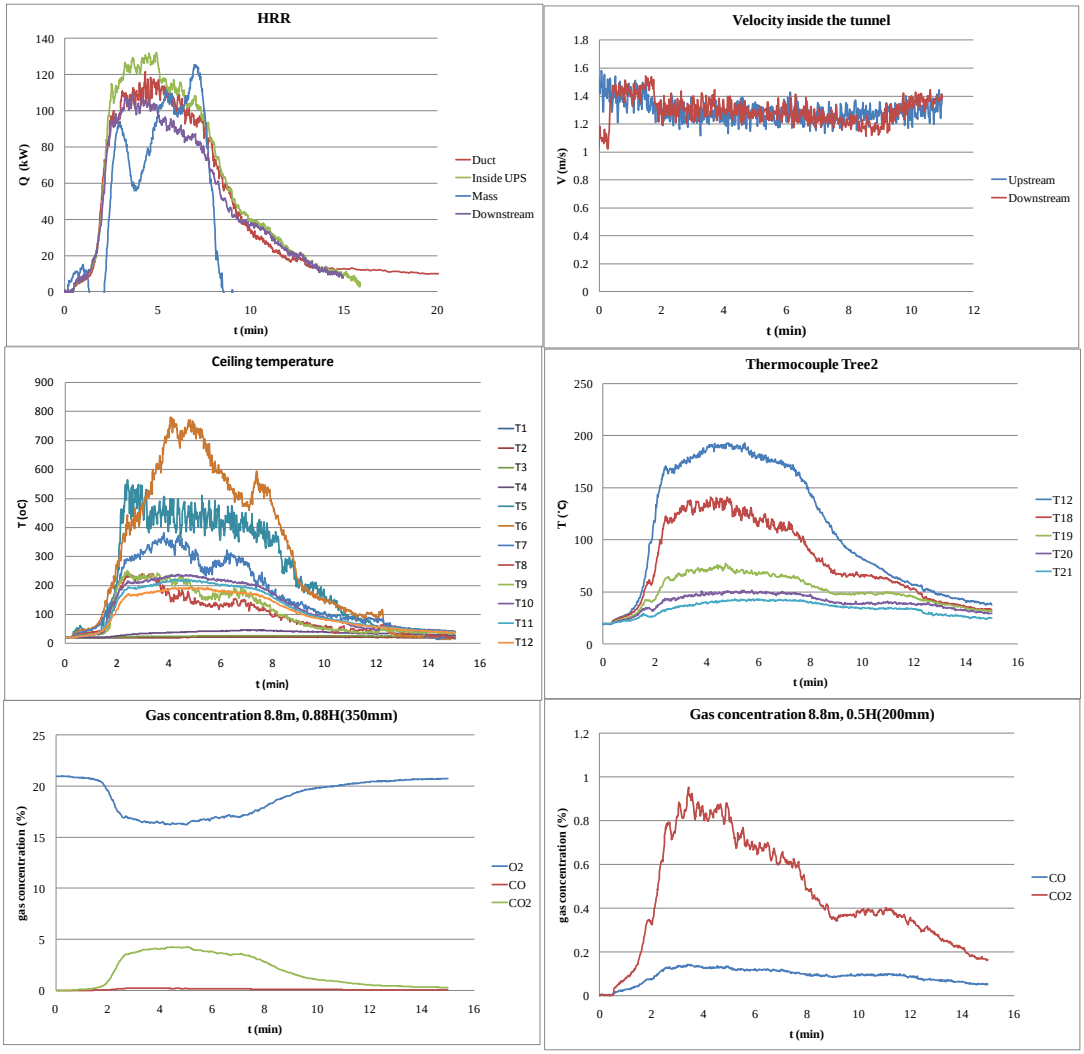

Figure D4 Measured heat release rate, velocity, temperature and gas concentrations in Test 4.

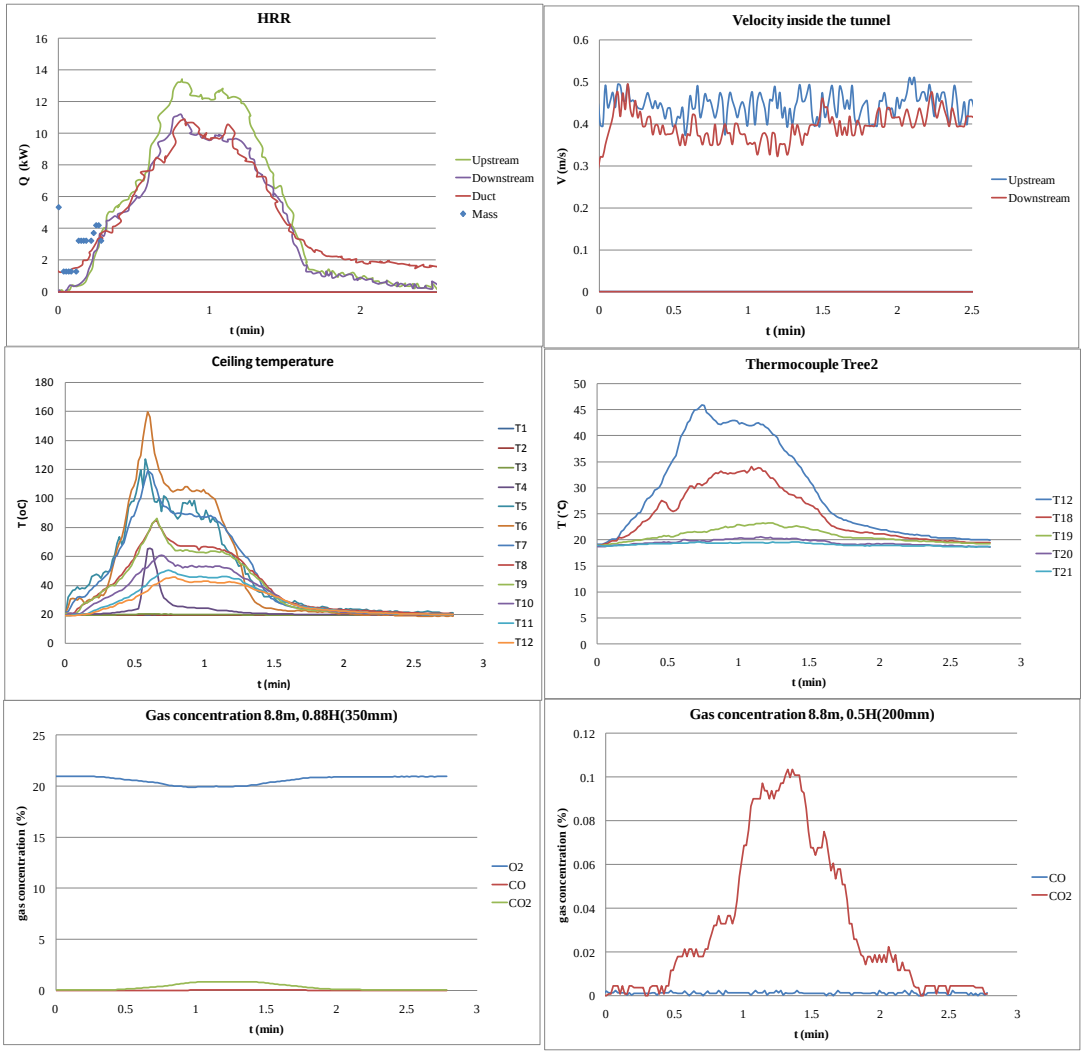

Figure D5 Measured heat release rate, velocity, temperature and gas concentrations in Test 5.

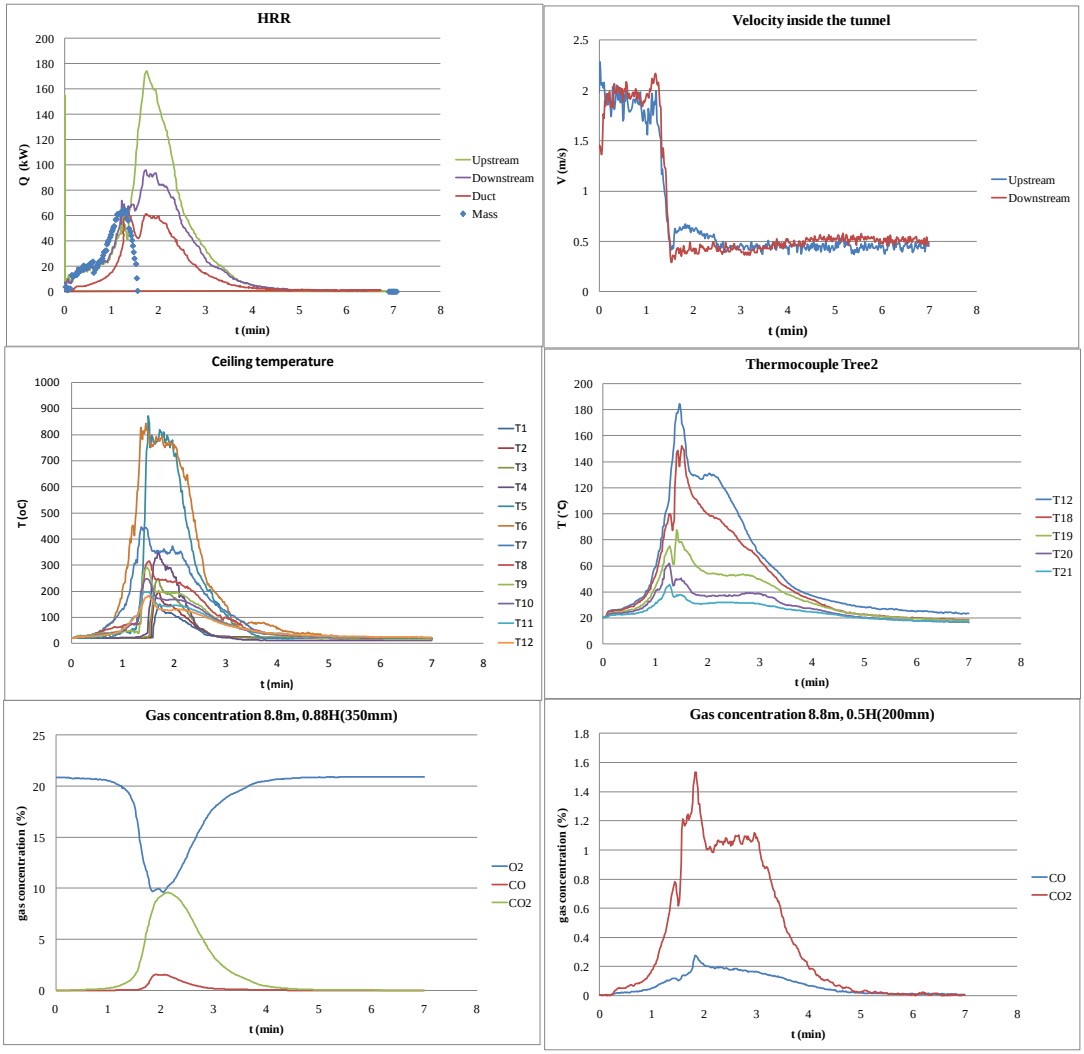

Figure D6 Measured heat release rate, velocity, temperature and gas concentrations in Test 6.

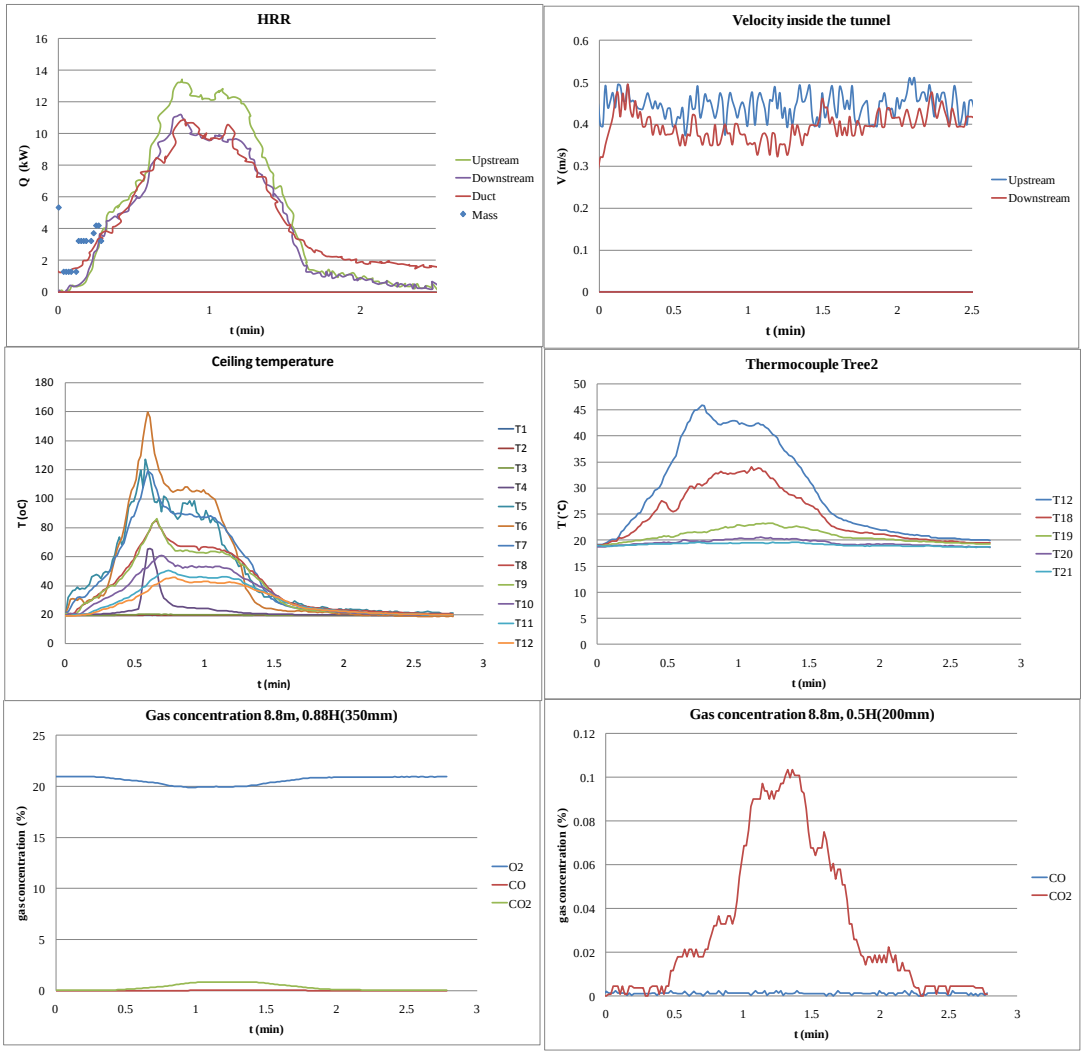

Figure D7 Measured heat release rate, velocity, temperature and gas concentrations in Test 7.

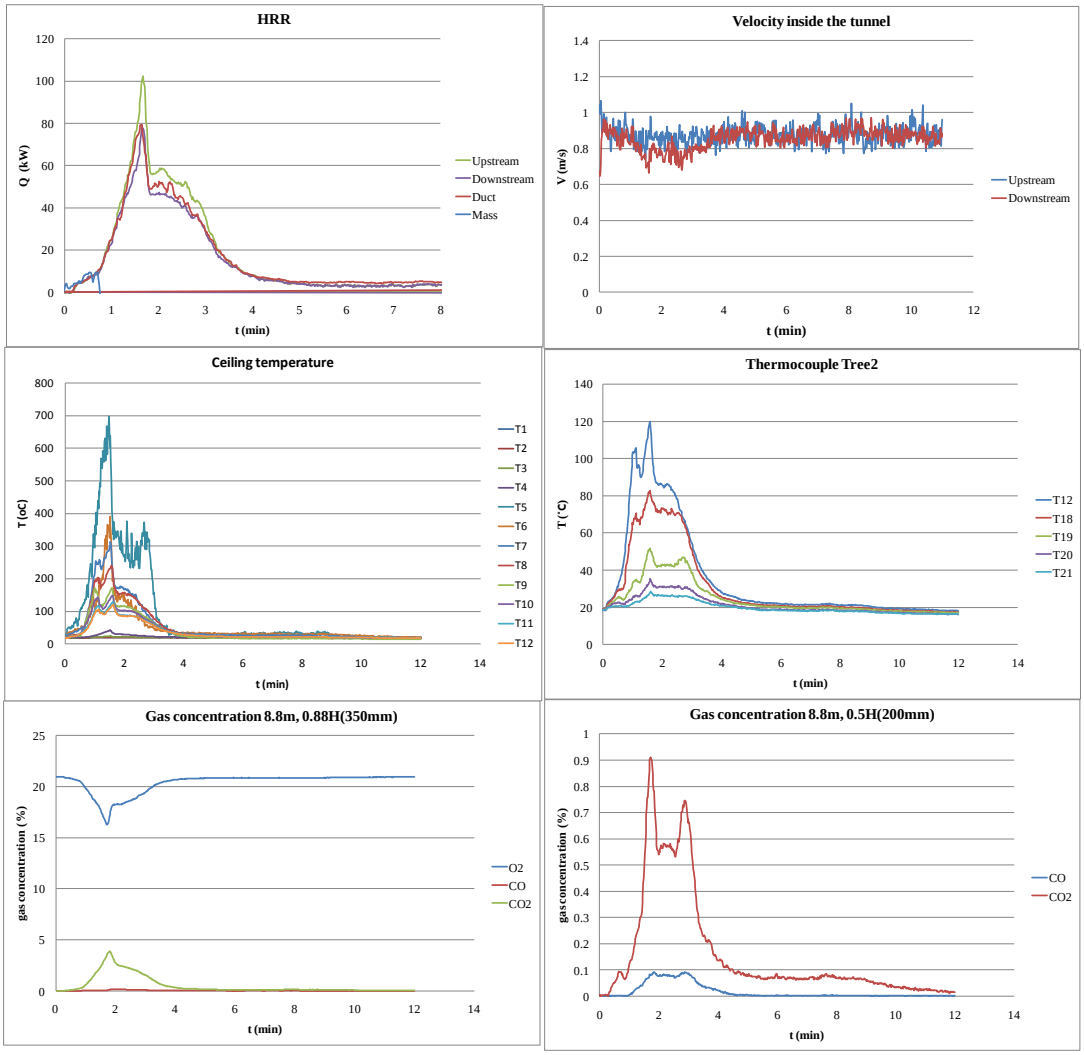

Figure D8 Measured heat release rate, velocity, temperature and gas concentrations in Test 8.

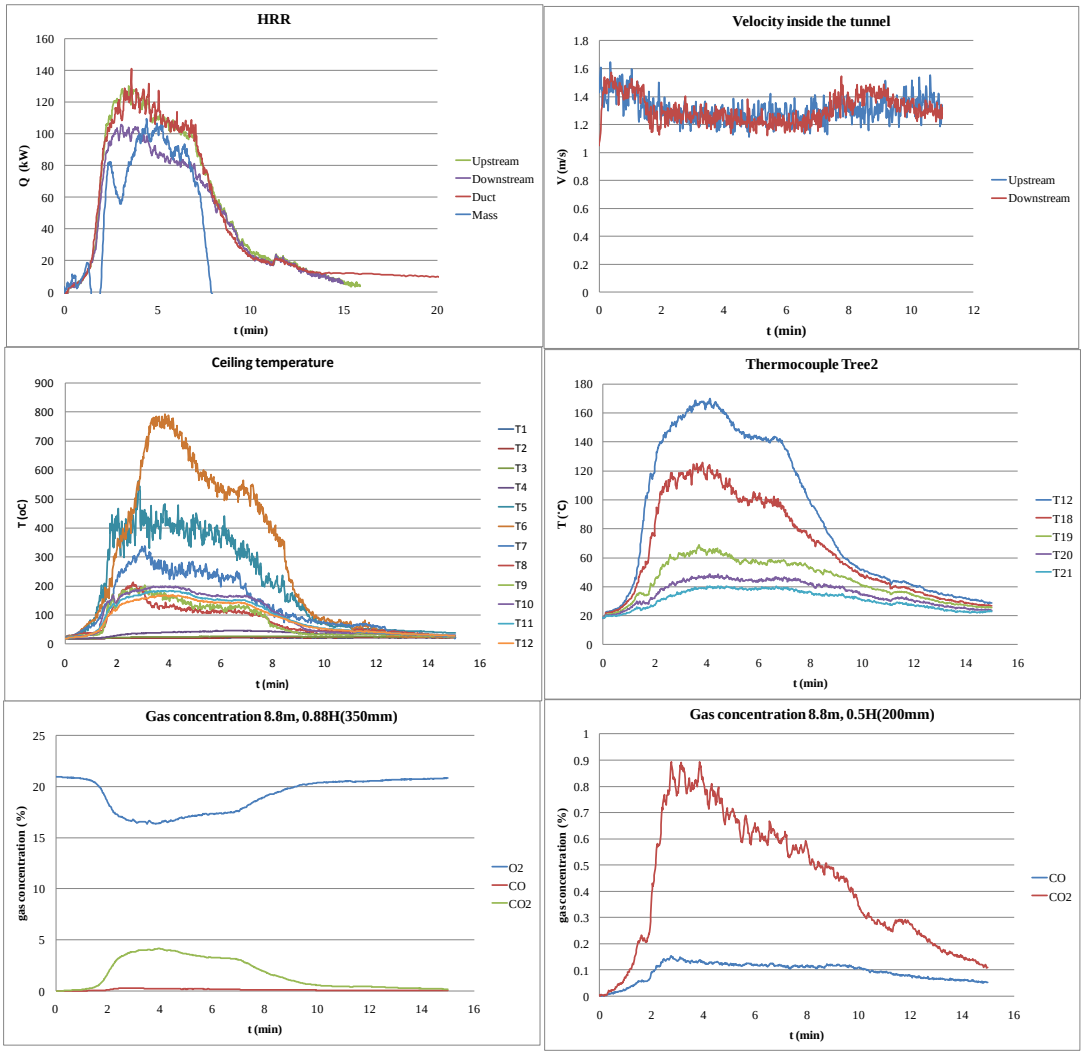

Figure D9 Measured heat release rate, velocity, temperature and gas concentrations in Test 9.

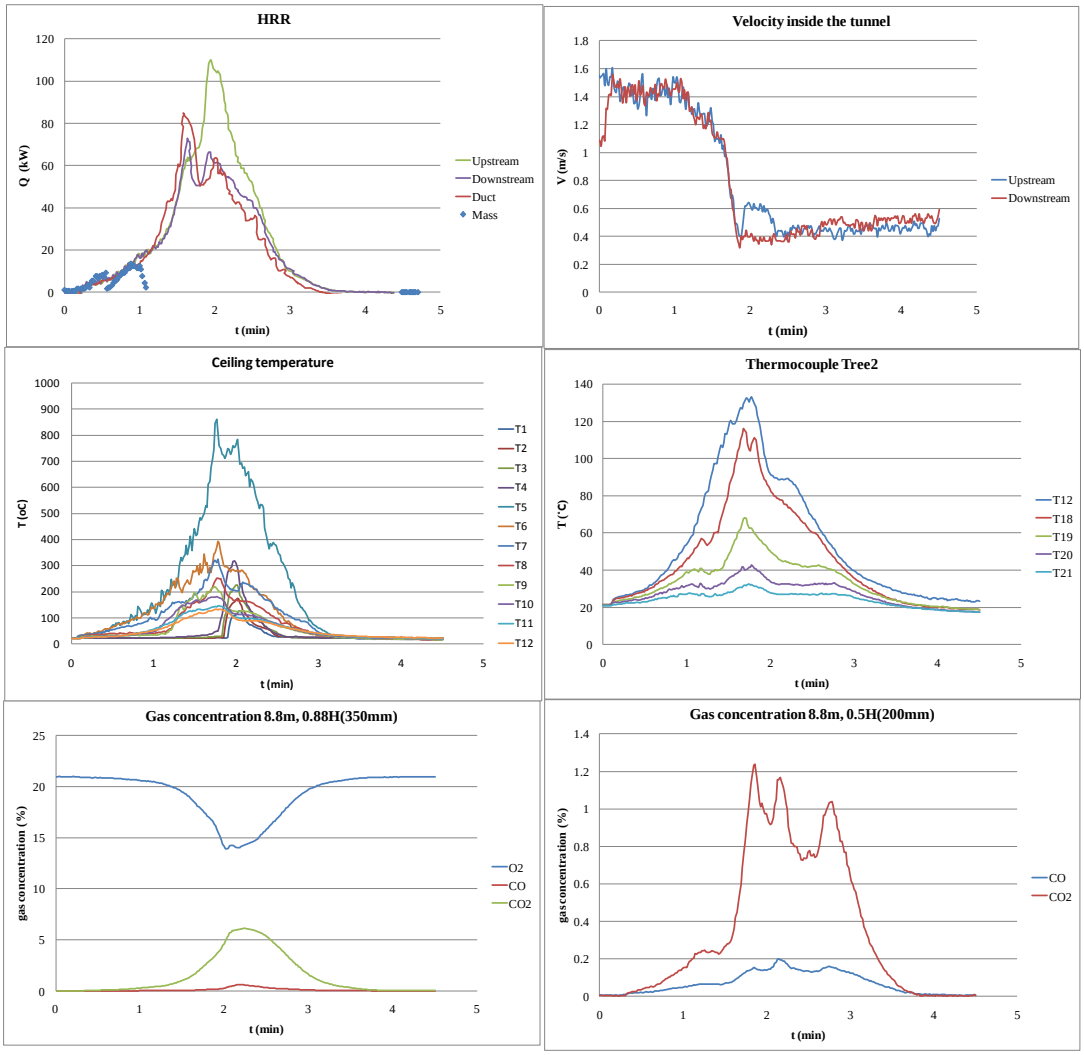

Figure D10 Measured heat release rate, velocity, temperature and gas concentrations in Test 10.

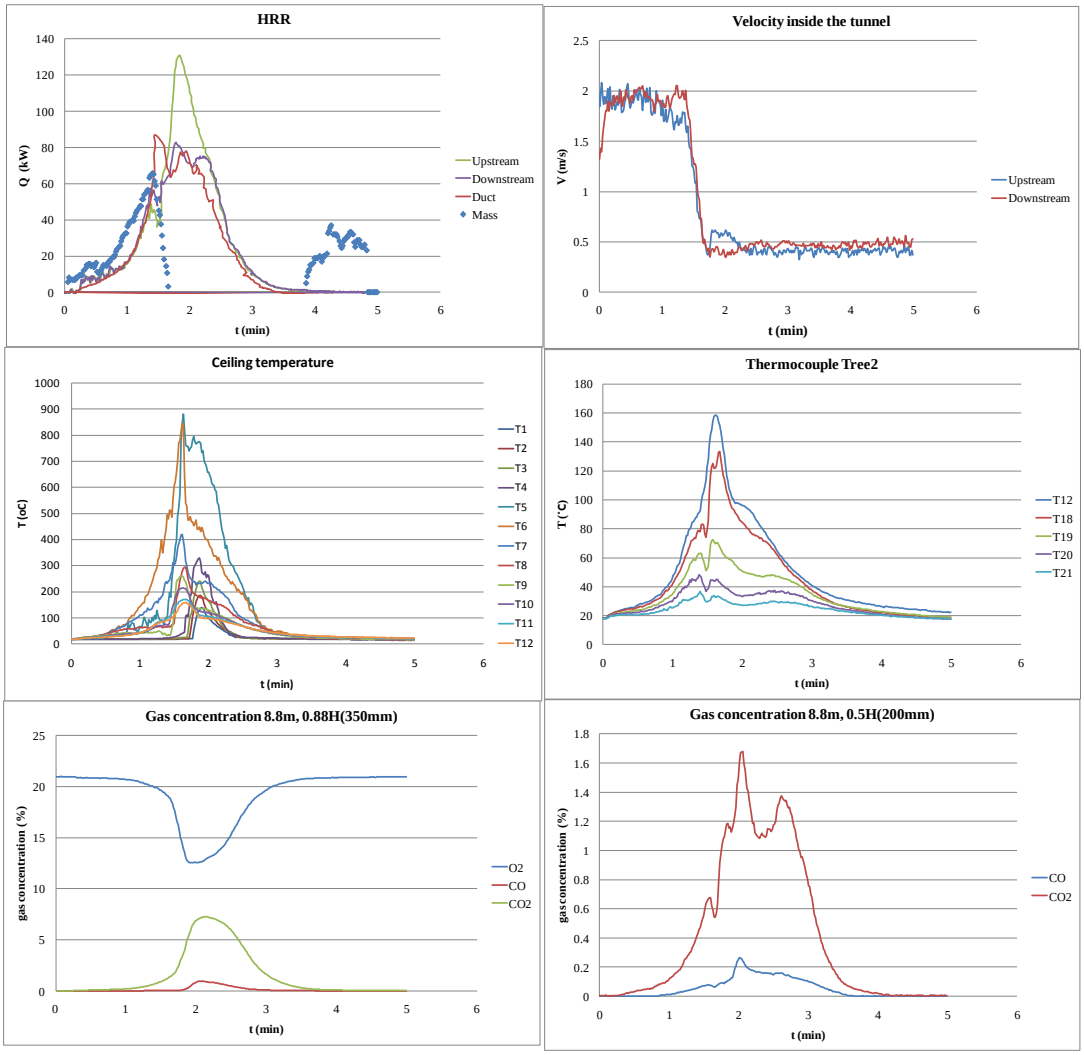

Figure D11 Measured heat release rate, velocity, temperature and gas concentrations in Test 11.

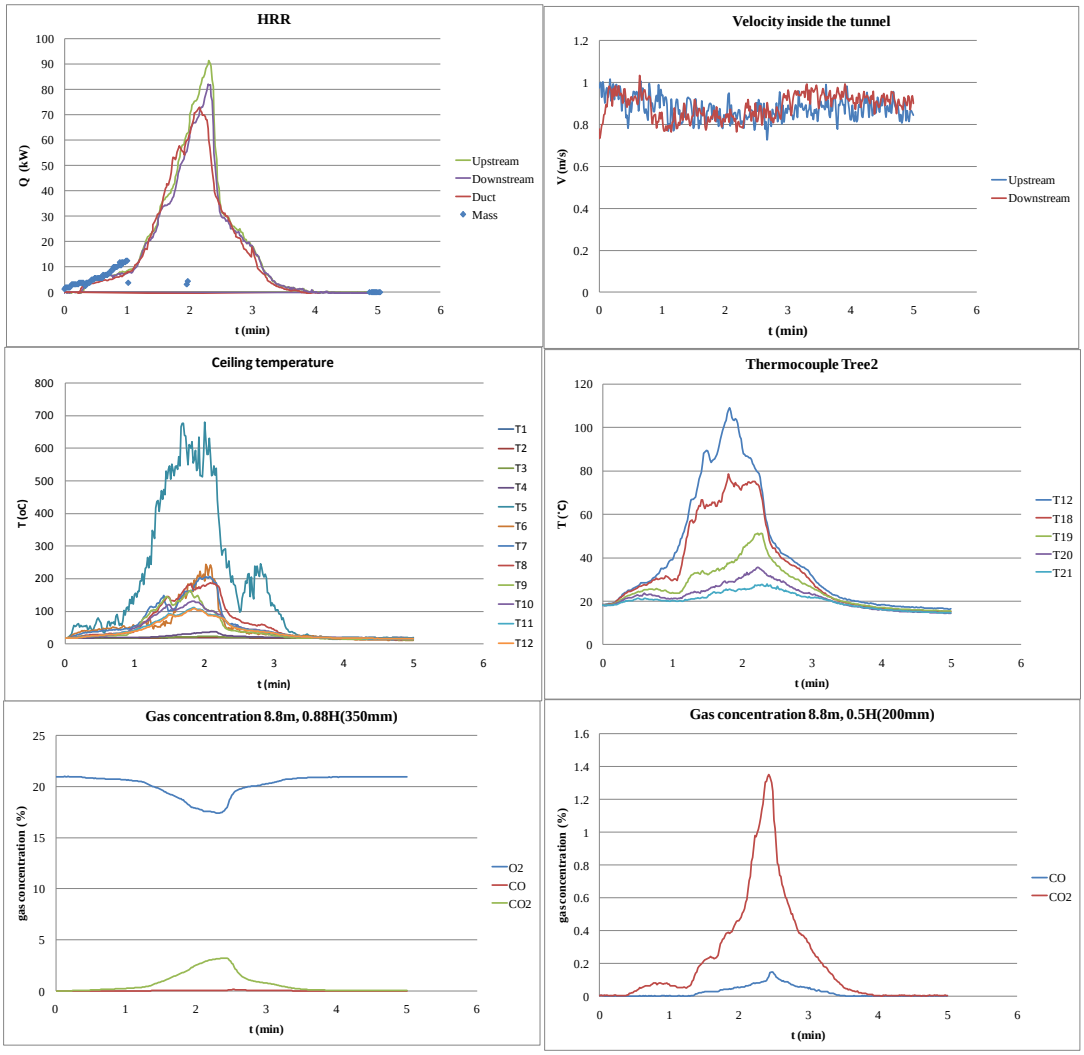

Figure D12 Measured heat release rate, velocity, temperature and gas concentrations in Test 12.

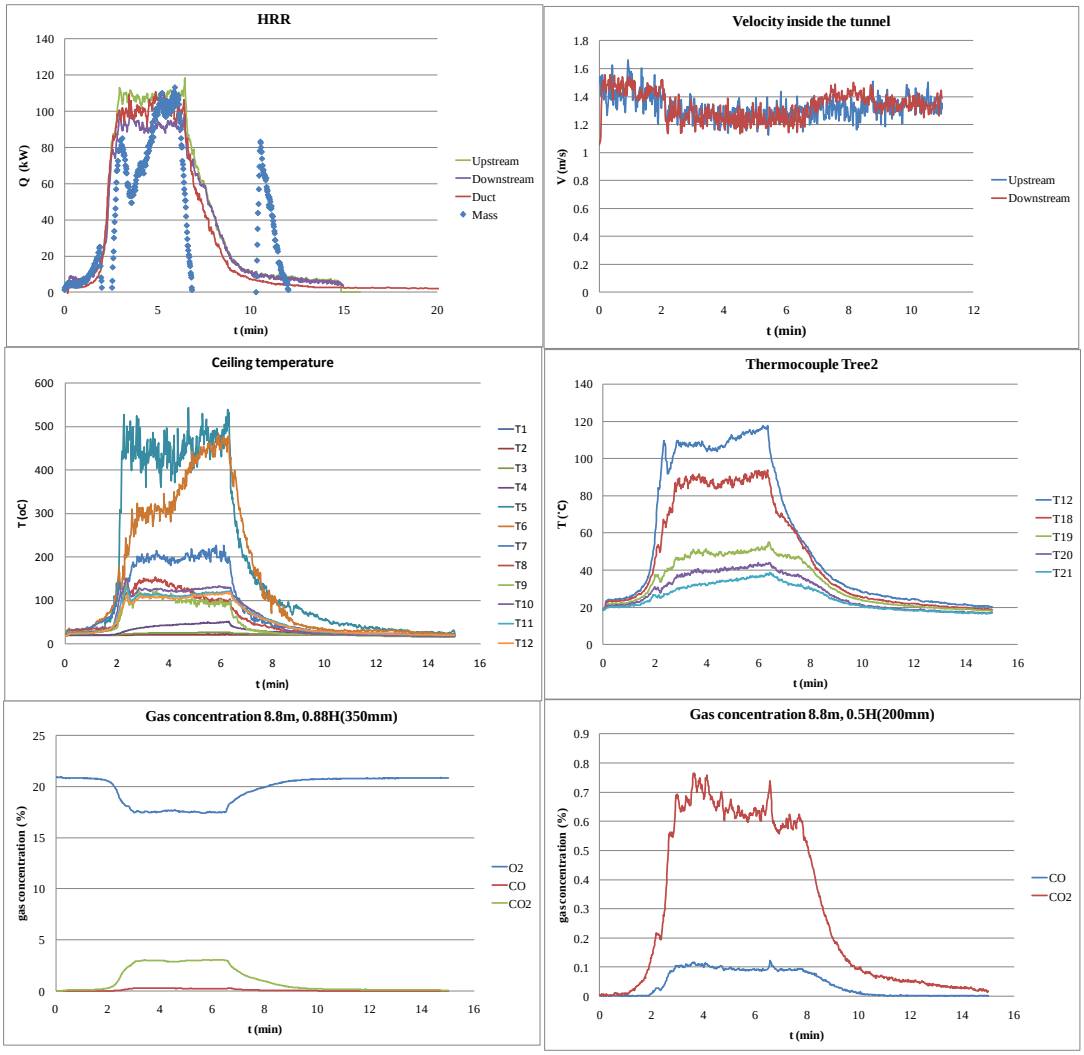

Figure D13 Measured heat release rate, velocity, temperature and gas concentrations in Test 13.

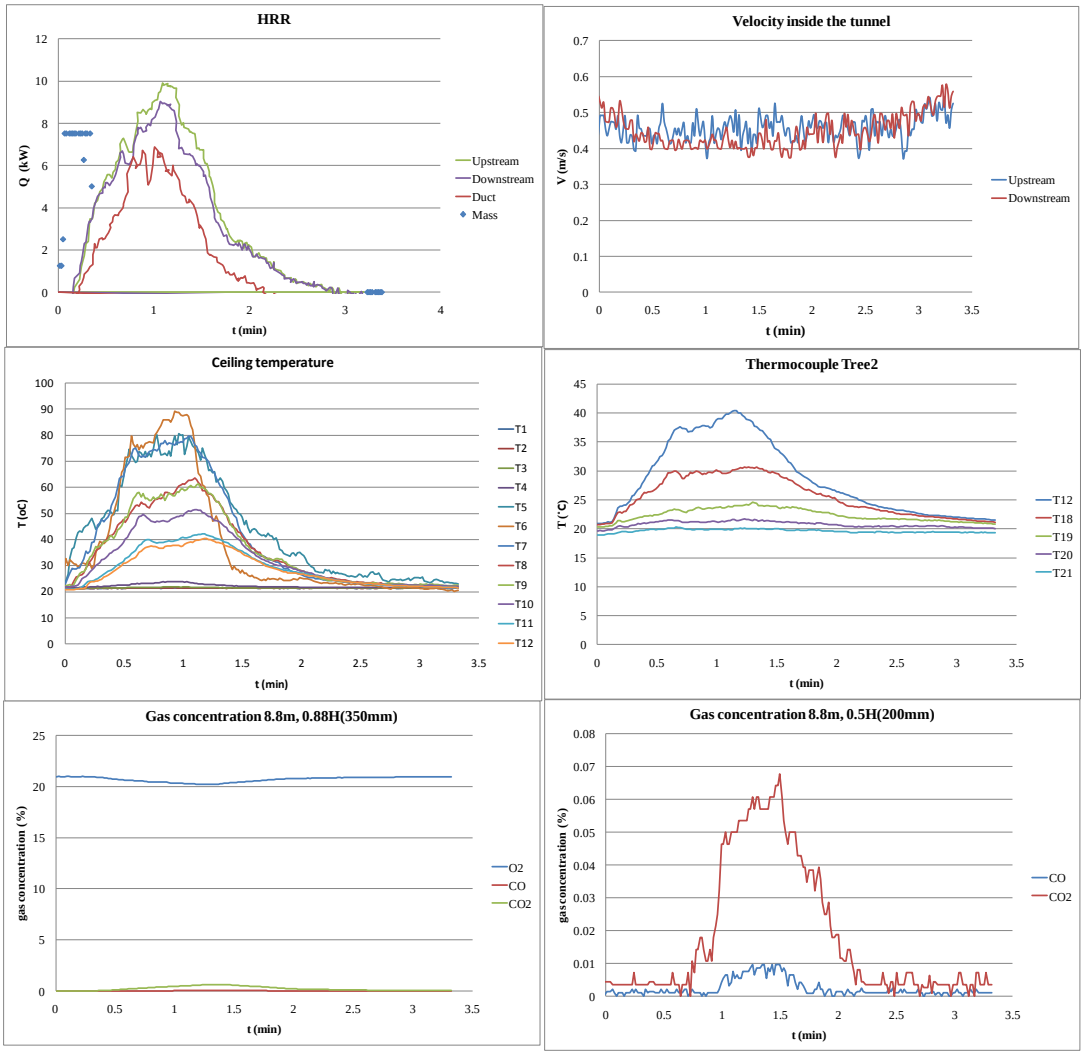

Figure D14 Measured heat release rate, velocity, temperature and gas concentrations in Test 14.

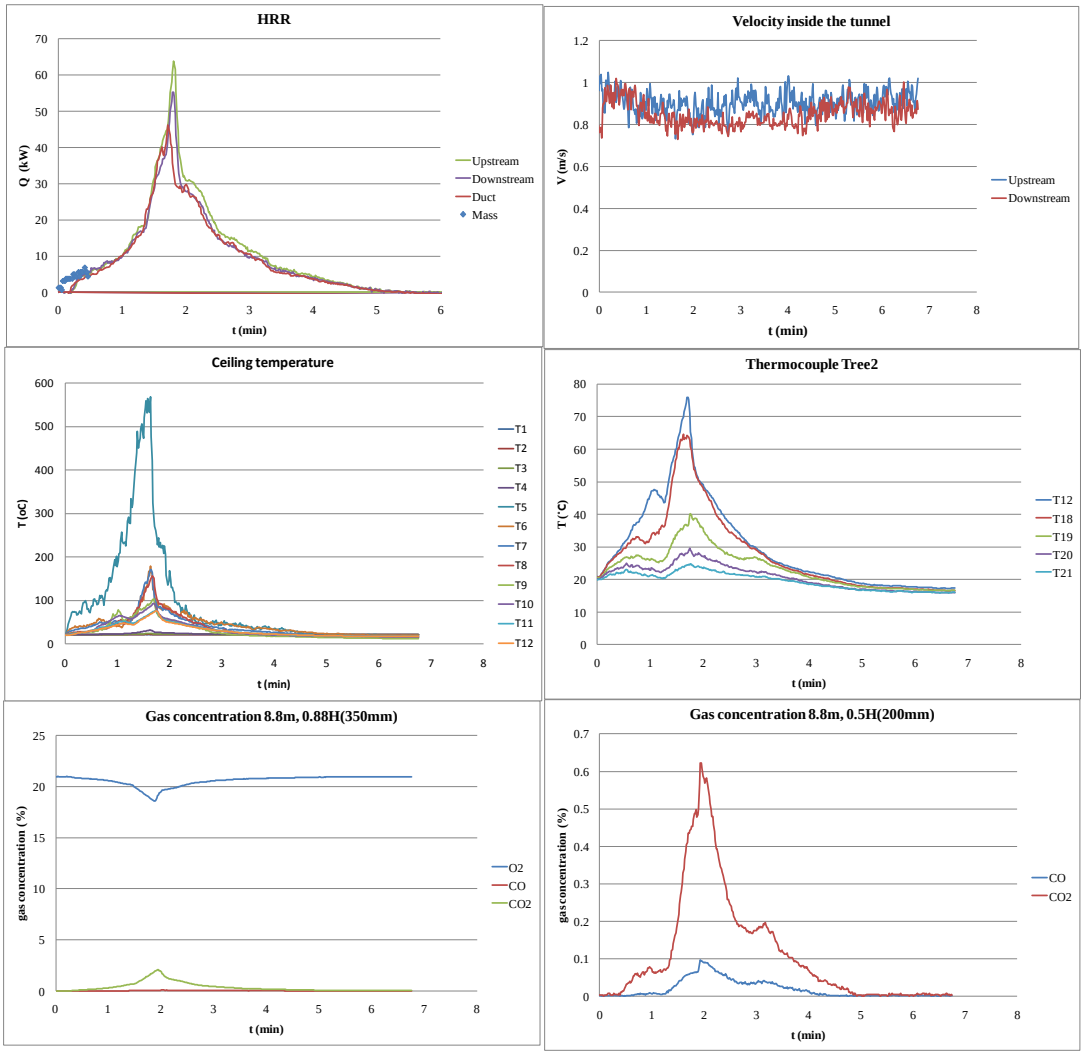

Figure D15 Measured heat release rate, velocity, temperature and gas concentrations in Test 15.

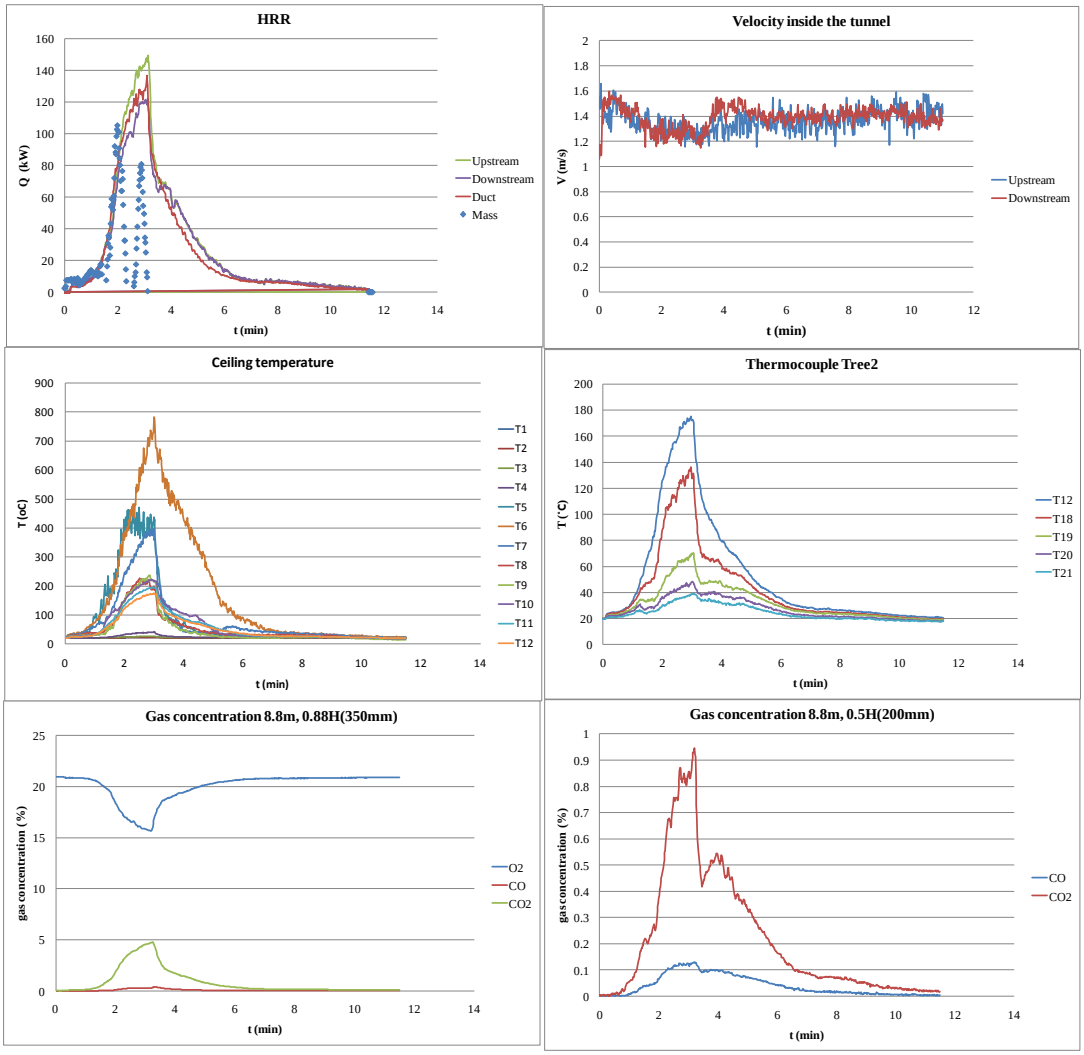

Figure D16 Measured heat release rate, velocity, temperature and gas concentrations in Test 16.

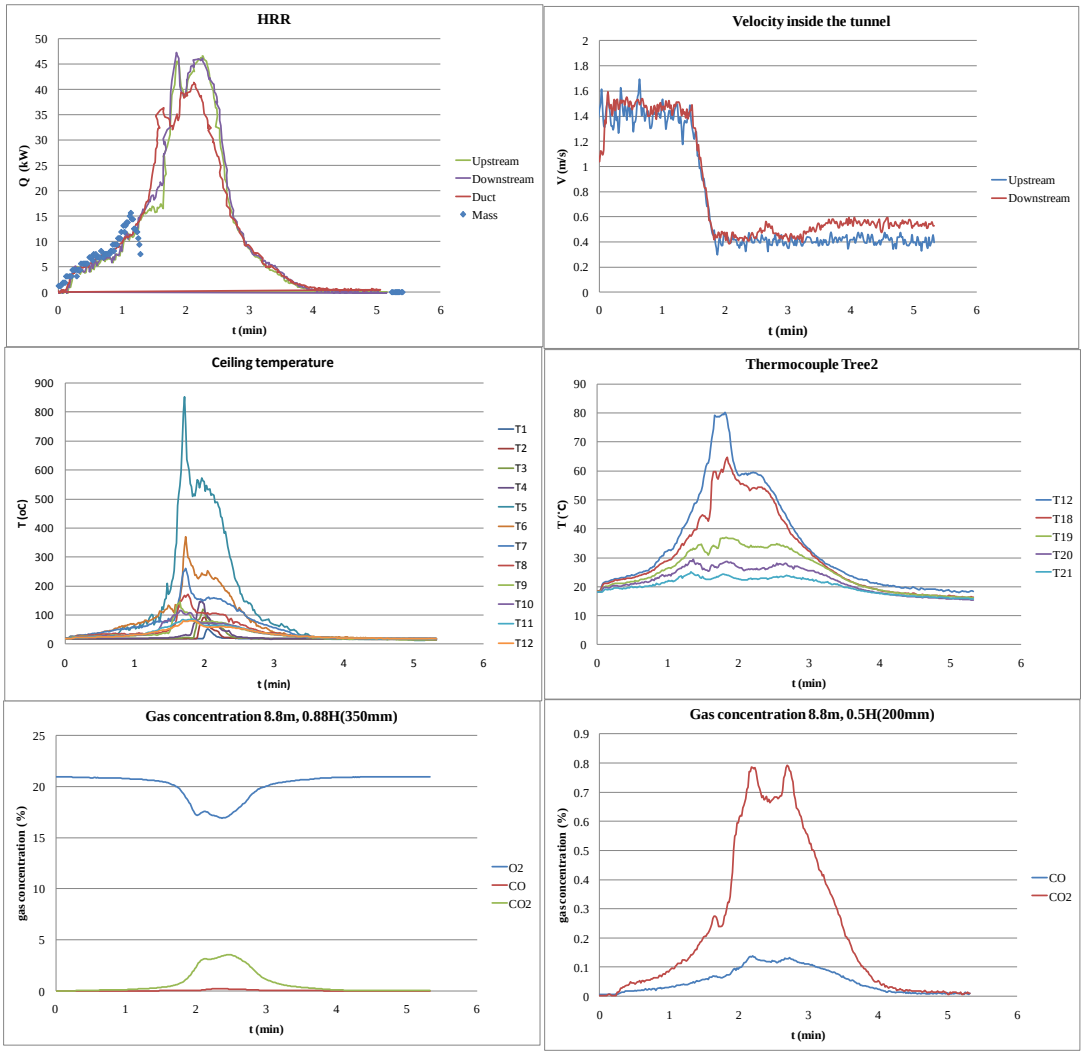

Figure D17 Measured heat release rate, velocity, temperature and gas concentrations in Test 17.

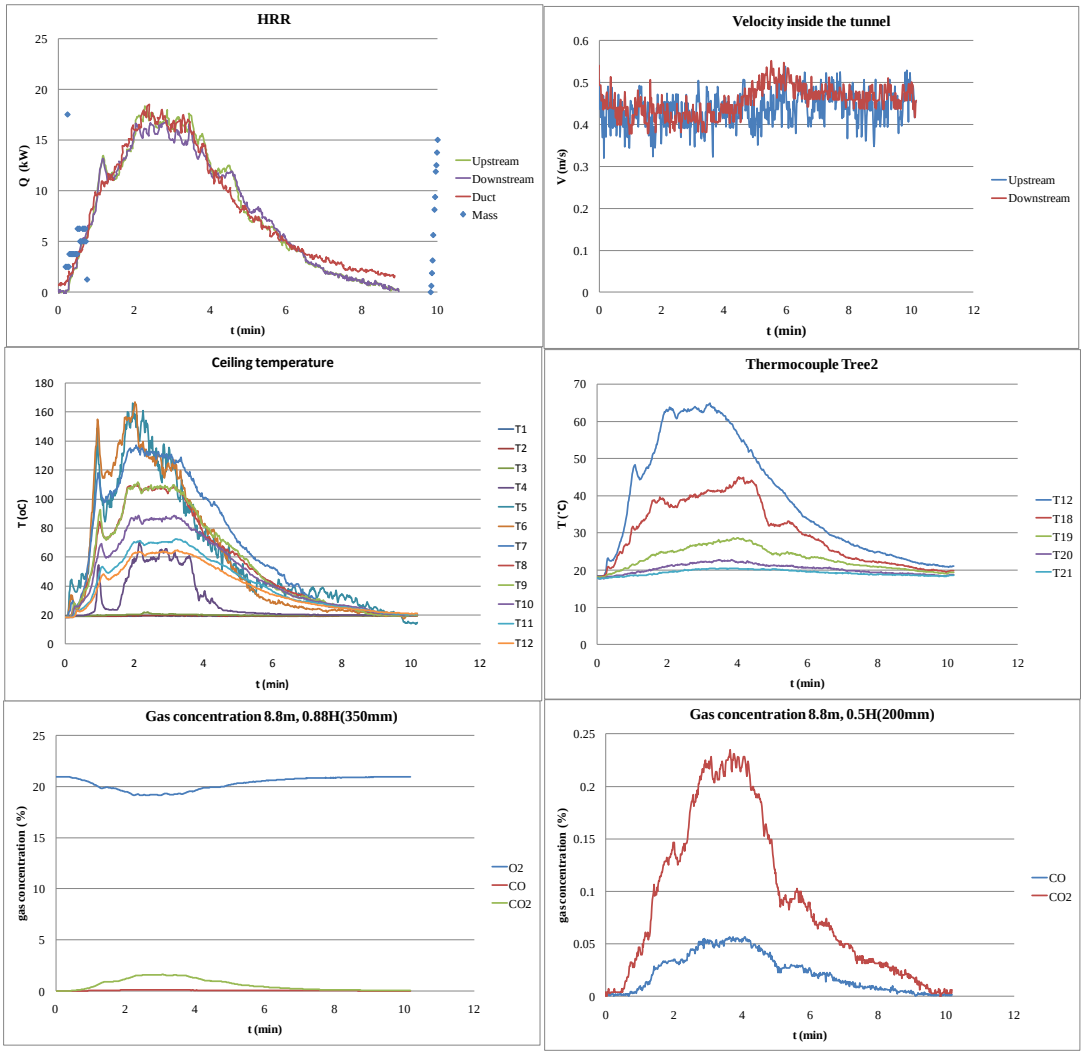

Figure D18 Measured heat release rate, velocity, temperature and gas concentrations in Test 18.

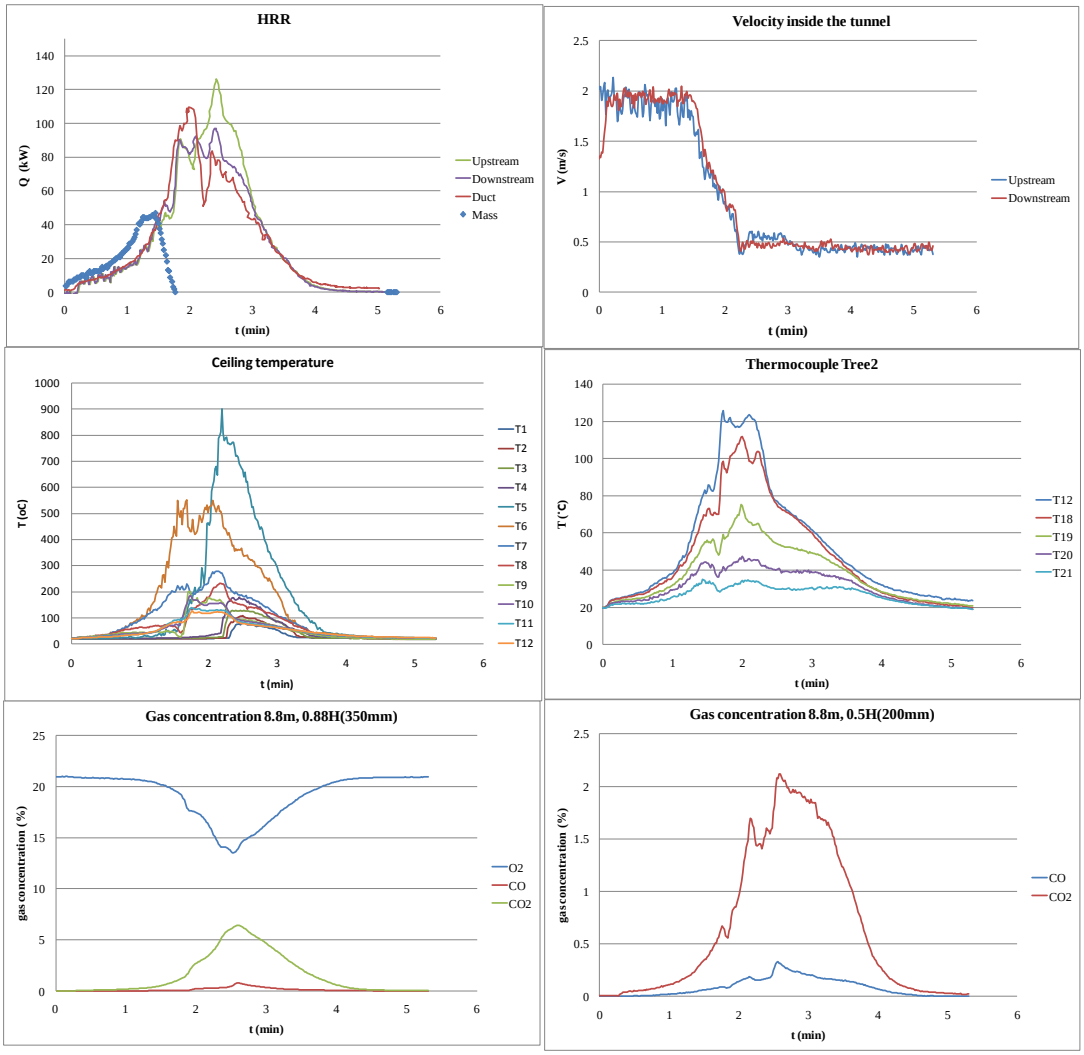

Figure D19 Measured heat release rate, velocity, temperature and gas concentrations in Test 19.

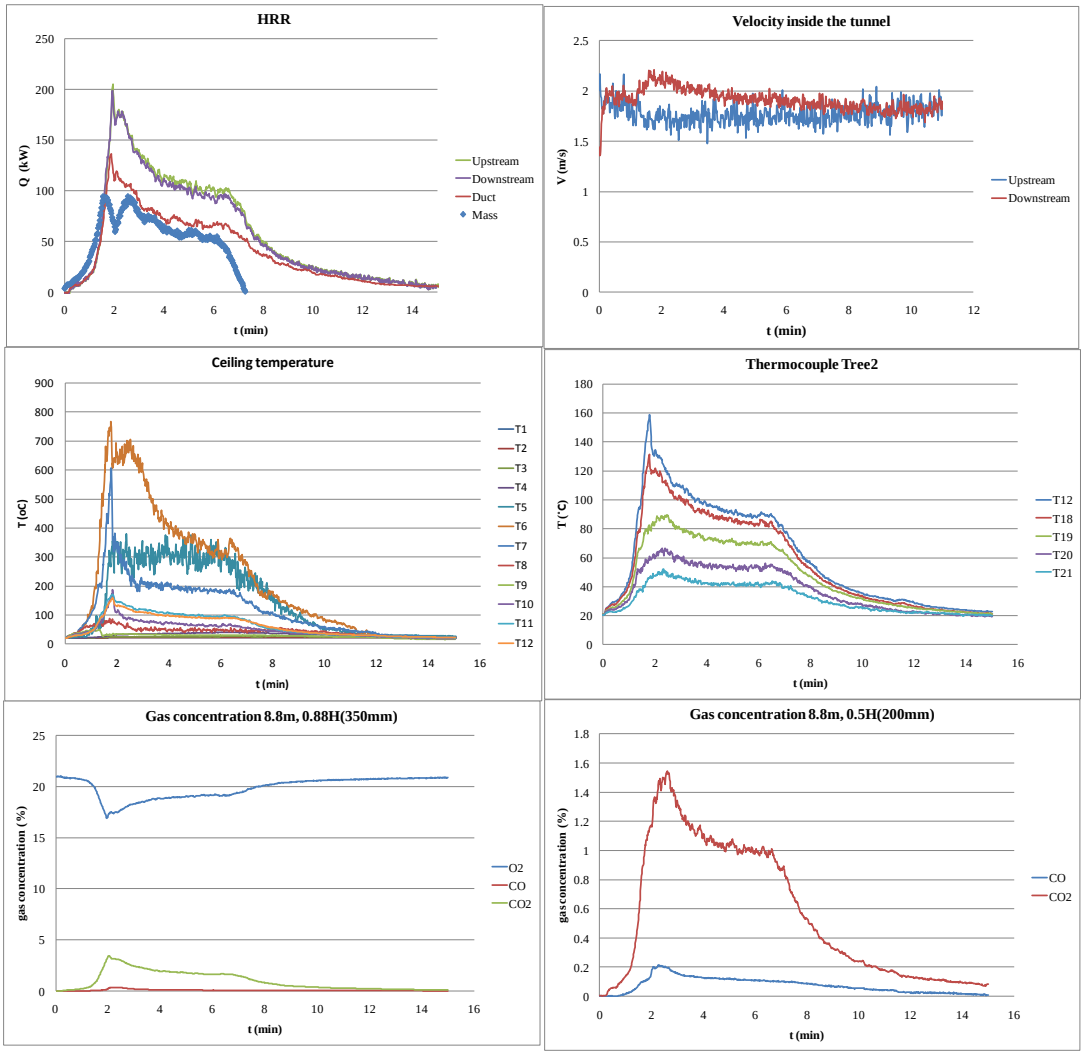

Figure D20 Measured heat release rate, velocity, temperature and gas concentrations in Test 20.

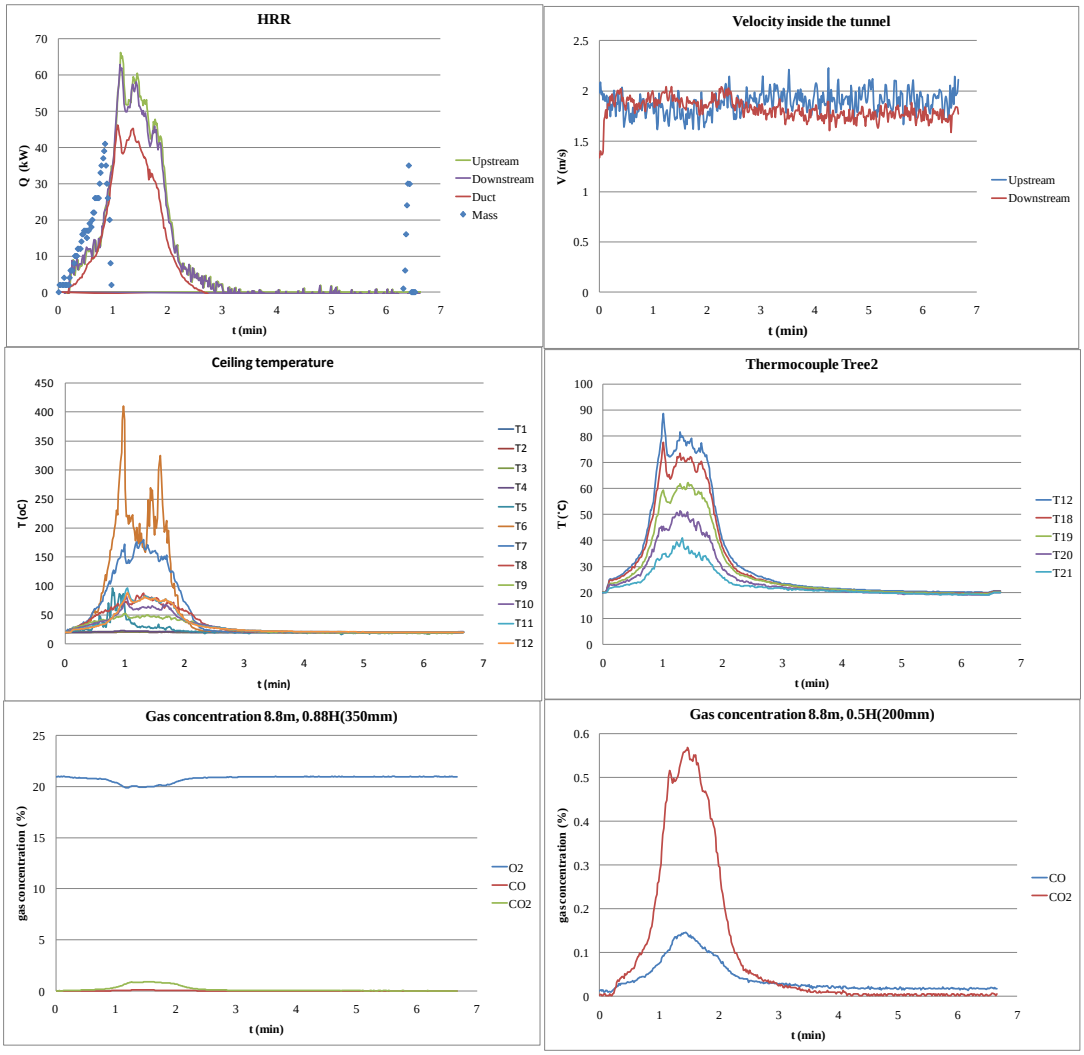

Figure D21 Measured heat release rate, velocity, temperature and gas concentrations in Test 21.

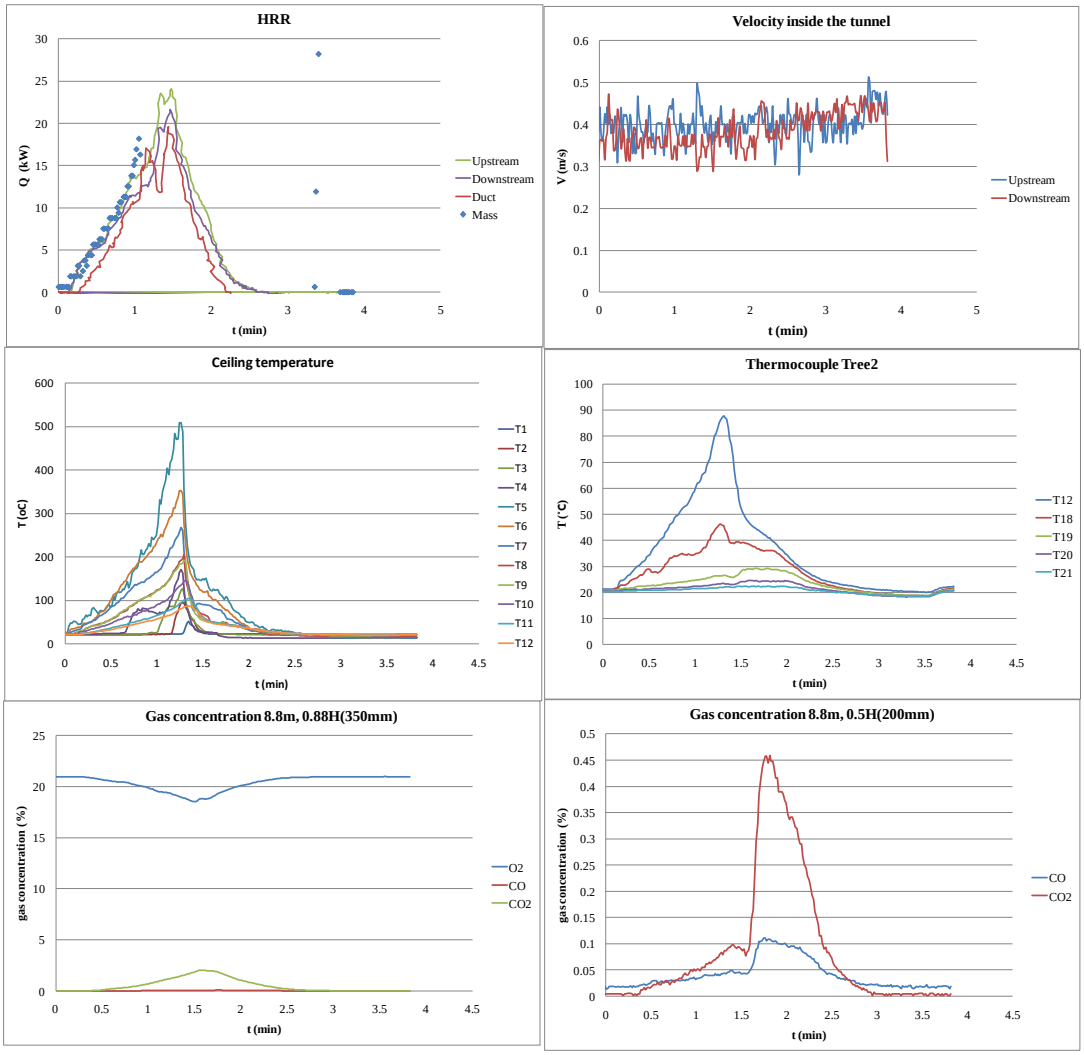

Figure D22 Measured heat release rate, velocity, temperature and gas concentrations in Test 22.

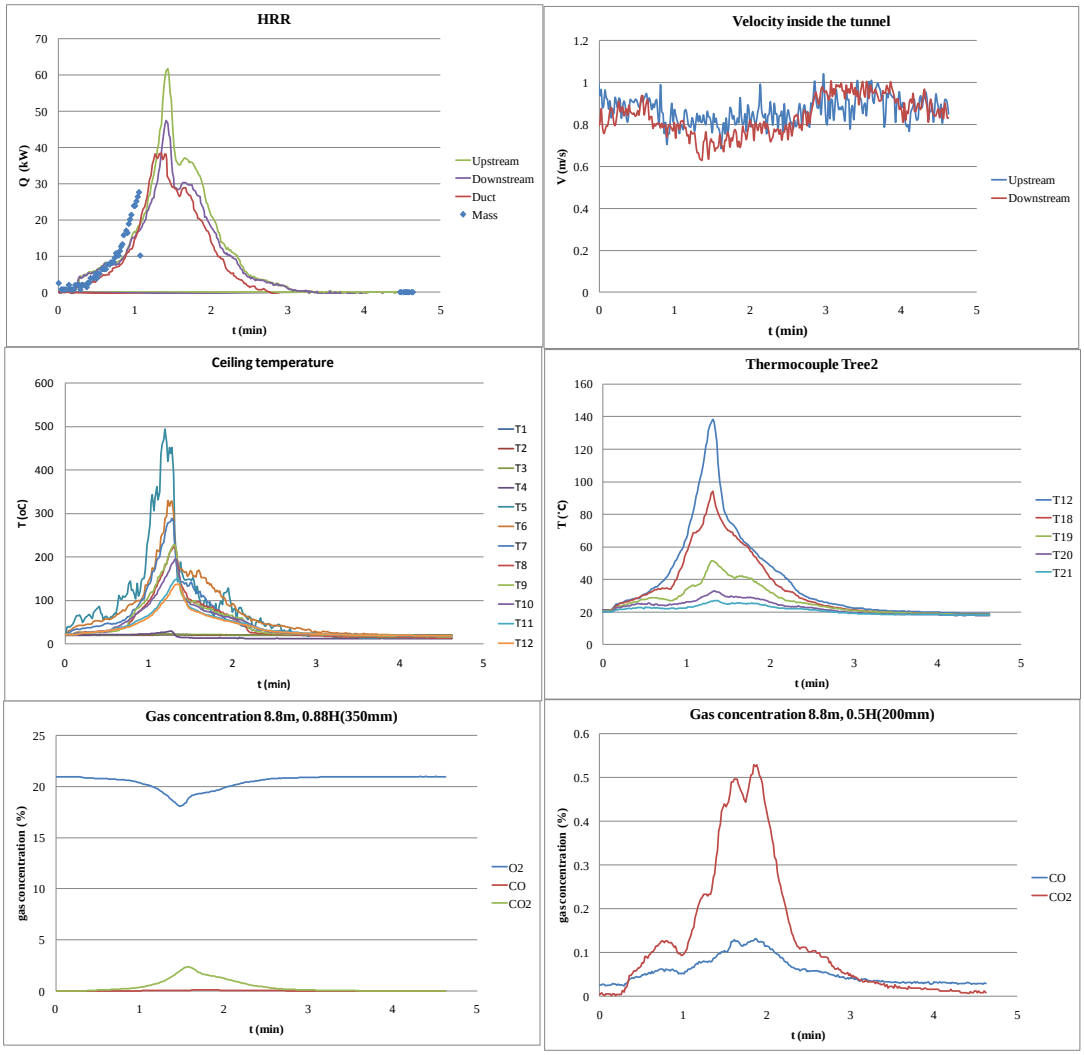

Figure D23 Measured heat release rate, velocity, temperature and gas concentrations in Test 23.

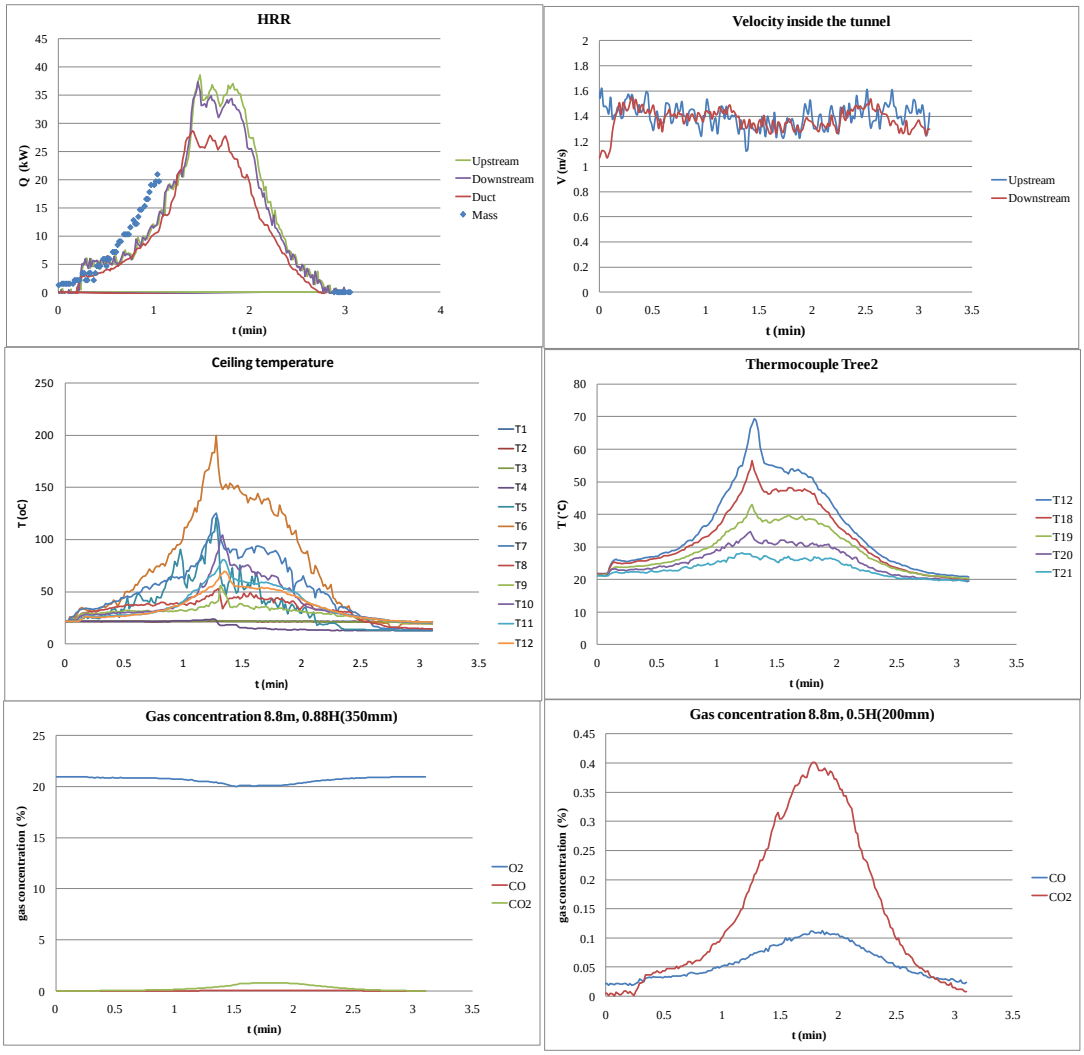

Figure D24 Measured heat release rate, velocity, temperature and gas concentrations in Test 24.

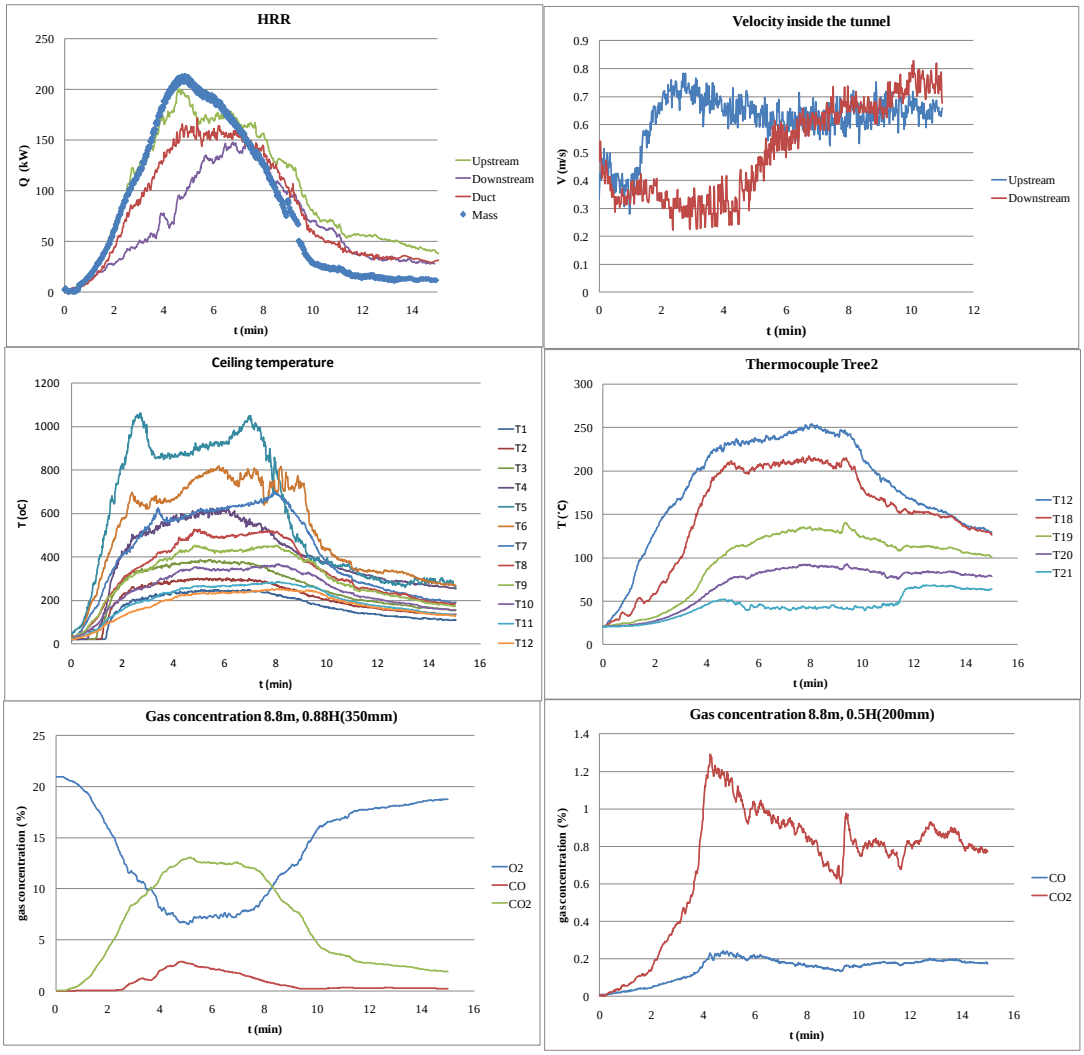

Figure D25 Measured heat release rate, velocity, temperature and gas concentrations in Test 25.

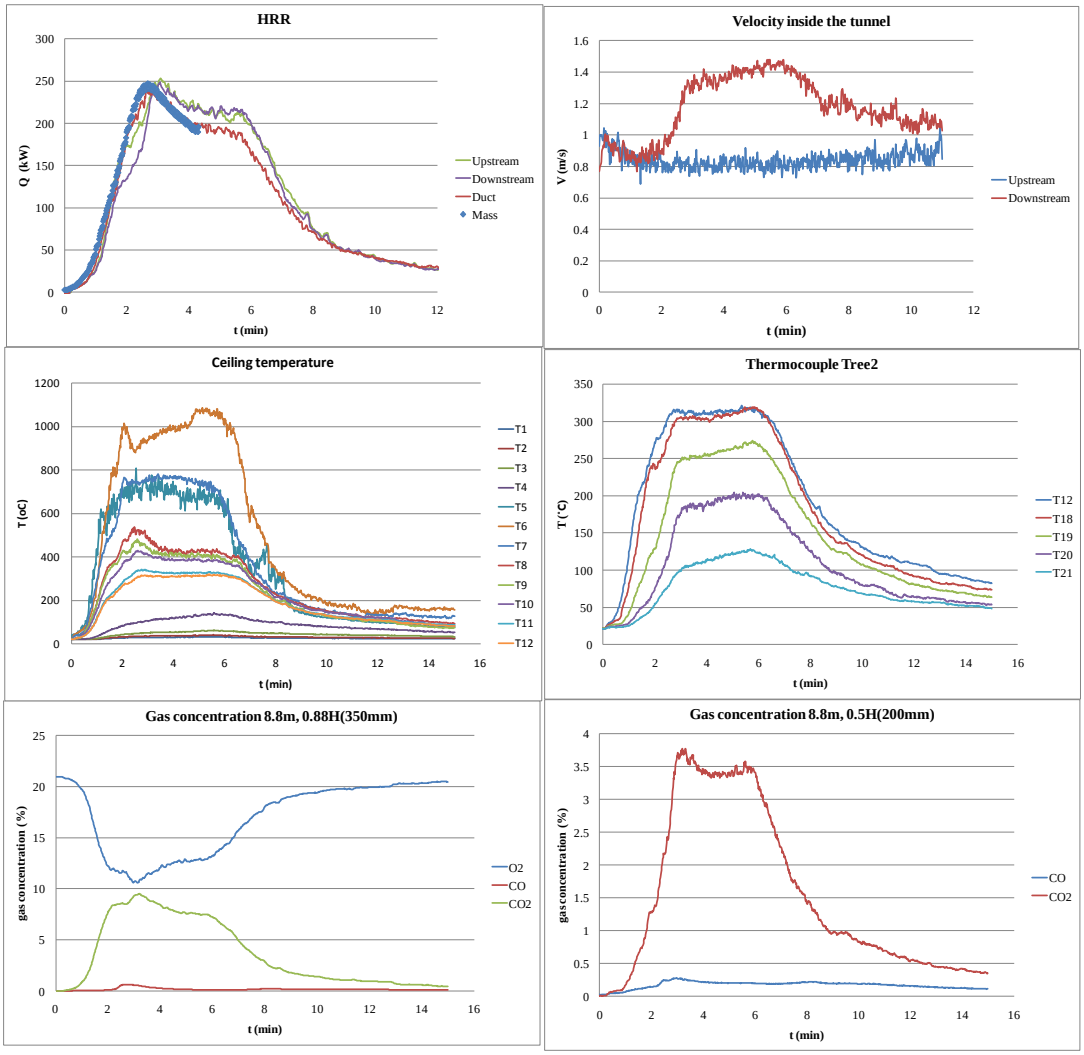

Figure D26 Measured heat release rate, velocity, temperature and gas concentrations in Test 26.

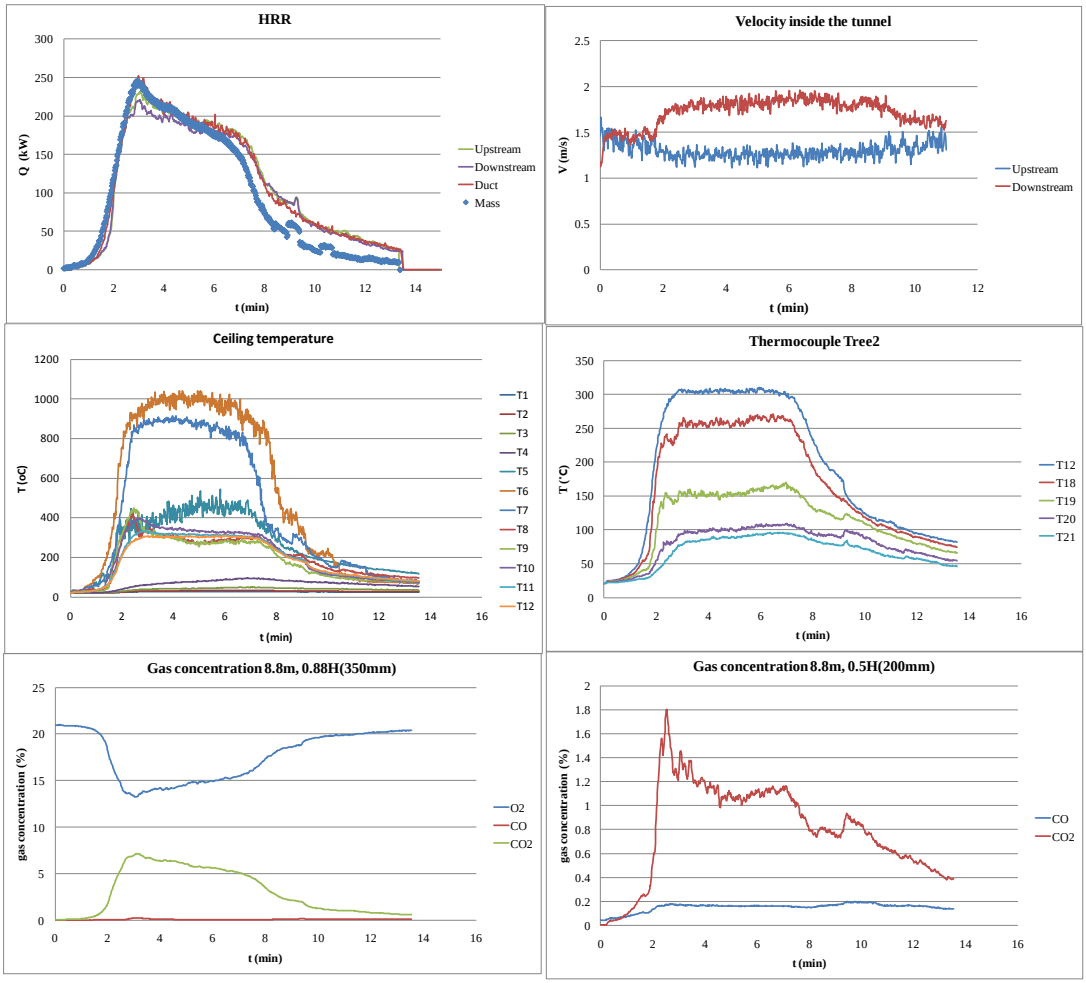

Figure D27 Measured heat release rate, velocity, temperature and gas concentrations in Test 27.

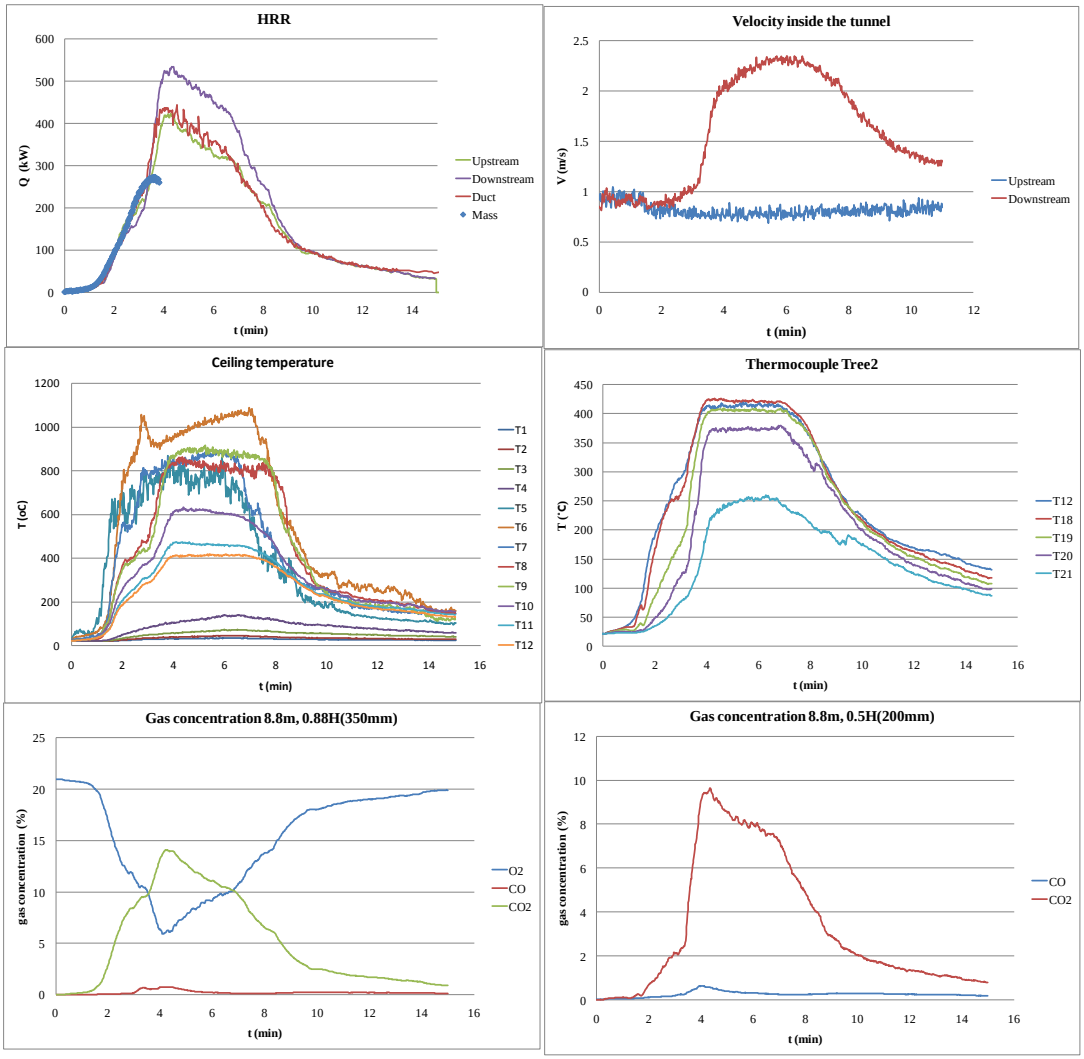

Figure D28 Measured heat release rate, velocity, temperature and gas concentrations in Test 28.

SP Technical Research Institute of Sweden

Our work is concentrated on innovation and the development of value-adding technology. Using Sweden's most extensive and advanced resources for technical evaluation, measurement technology, research and development, we make an important contribution to the competitiveness and sustainable development of industry. Research is carried out in close conjunction with universities and institutes of technology, to the benefit of a customer base of about 9000 organisations, ranging from start-up companies developing new technologies or new ideas to international groups.

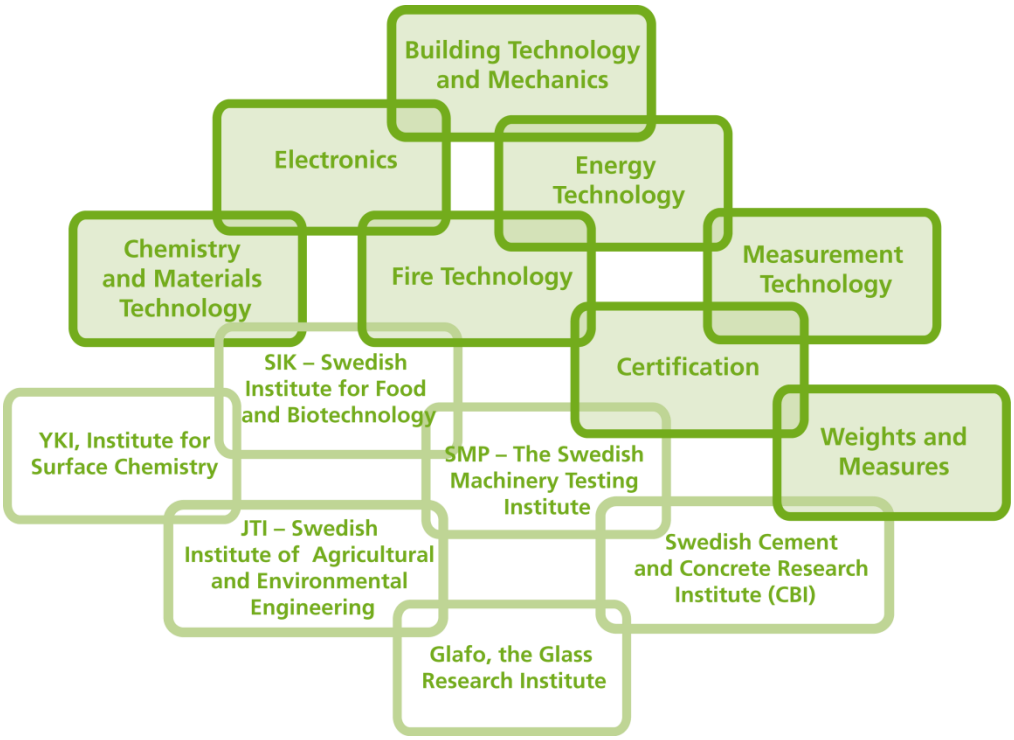

SP Technical Research Institute of Sweden
Box 857, SE-501 15 BORÅS, SWEDEN
Telephone: +46 10 516 50 00, Telefax: +46 33 13 55 02
E-mail: info@sp.se, Internet: www.sp.se
www.sp.se

Fire Technology
SP Report 2011:31
ISBN 978-91-86622-62-6
ISSN 0284-5172

More information about publications published by SP: **www.sp.se/publ**